



NATIONAL TECHNICAL UNIVERSITY OF ATHENS

SCHOOL OF MECHANICAL ENGINEERING

MECHANICAL DESIGN & AUTOMATIC CONTROL | BIOENGINEERING & SYSTEMS BIOLOGY LAB

Identification and Verification of Steatogenic Compounds via Network-Based Pathway Analysis

Diploma Thesis

of

CHALLOTIS ODYSSEAS KONSTANTINOS

Supervisor: Dr. Leonidas Alexopoulos
Associate Professor

Athens, July 2019

ΕΥΧΑΡΙΣΤΙΕΣ

Θα ήθελα να ευχαριστήσω θερμά τον κύριο Λεωνίδα Αλεξόπουλο, αναπληρωτή καθηγητή του ΕΜΠ, για όλη την καθοδήγηση και υποστήριξη, σε ανθρώπινο και επιστημονικό επίπεδο. Θα ήθελα επίσης να τον ευχαριστήσω και για την ευκαιρία να είμαι μέλος του Bioengineering & Systems Biology Lab.

Επίσης θα ήθελα να ευχαριστήσω ιδιαιτέρως τη Δανάη Ζαρείφη, διδακτορική φοιτήτρια, για την υπομονή και την πίστη που μου έδειξε, καθώς και για όλη της την καθοδήγηση. Δε θα μπορούσα να μην ευχαριστήσω και τα υπόλοιπα μέλη του εργαστηρίου ξεχωριστά, για το κλίμα συνεργασίας και αμοιβαίου σεβασμού που δημιούργησαν.

Τέλος, θα ήθελα να ευχαριστήσω τη συνάδελφο Αθανασία Μαντά, για την υποστήριξη που έλαβα καθ' όλη τη διάρκεια των, ομολογουμένως, απαιτητικών σπουδών μου στο ΕΜΠ.

ABSTRACT

Its escalating prevalence in the population (>25% in 2018) establishes NAFLD as the most common cause of chronic liver disease in the US. However, no NAFLD/NASH-specific agent received FDA-approval, despite the advances in its mechanism's decipher and the identification of potential drug targets. NAFLD includes a spectrum of liver diseases ranging from simple hepatic steatosis to Non-Alcoholic Steatohepatitis (NASH), liver cirrhosis, and hepatocellular carcinoma (HCC).

Drug-induced liver injury (DILI) is defined as a liver injury caused by various medications, herbs, or other xenobiotics, leading to abnormalities in liver tests or liver dysfunction with the reasonable exclusion of other etiologies. DILI is one of the leading causes of acute liver failure in the US, while almost 95% of the compounds validated in drug discovery are rejected due to their liver-related side effects. Approximately, 2% of the diagnosed Non-Alcoholic Steatohepatitis (NASH) incidents are attributed to DILI.

Thus, further examination on the compounds that may induce NAFLD-alike liver steatosis needs to be conducted. In that context, a computational platform is developed and, by means of network-based pathway analysis on NAFLD's pathogenesis and known steatogens, yields several potentially hepatotoxic/steatogenic compounds. Among them, three (Pimozide, Clomiphene and Mefloquine) are tested *in-vitro* in order to validate their steatogenic effects on Hep3B and FOCUS hepatocellular lines.

The *in-silico* approach deduces a network similarity, thus identifies compounds inducing liver steatosis *in-vitro*. A high-throughput setup for NAFLD/NASH drug-screening is developed. Further experiments are necessary to decipher the mechanisms identified compounds facilitate and to assess their *in-vivo* effects. Also, additional experiments should be performed in order to classify the tested steatogens in clusters, along with the known NAFLD-inducing compounds, and examine the similarities and differences among them, in terms of the steatogenic mechanisms facilitated and the effects induced.

Keywords: NAFLD, NASH, DILI, liver, steatosis, pathway analysis, networks, drugs, steatogenic compounds, DEGs, genes, systems, biology, systems biology, bioengineering, GLS, GSA

ΠΕΡΙΛΗΨΗ

Η αυξανόμενη επικράτηση της Μη-Αλκοολικής Λιπώδους Νόσου του Ήπατος (NAFLD) στο γενικό πληθυσμό (>25% το 2018) την καθιστά ανάμεσα στις πιο συχνές αιτιολογίες χρόνιας ηπατικής βλάβης στις ΗΠΑ. Παρά το ανησυχητικό αυτό δεδομένο, κανένας φαρμακολογικός παράγοντας δεν έχει λάβει την έγκριση του FDA ως σήμερα και παρά την ολοένα και αυξανόμενη γνώση γύρω από τους μηχανισμούς της παθογένεσης. Η Μη-Αλκοολική Λιπώδης Νόσος του Ήπατος περιλαμβάνει ένα ευρύ φάσμα παθήσεων, το οποίο ξεκινά από απλή στεάτωση και καταλήγει σε Μη-Αλκοολική Στεατοηπατίτιδα (NASH), ηπατική κίρρωση και ηπατοκυτταρικό καρκίνωμα (HCC).

Η Ηπατοπάθεια από Φάρμακα (DILI) ορίζεται από την ηπατική βλάβη, την προκαλούμενη από τη χορήγηση διαφόρων φαρμάκων, βοτάνων και ξеноβιοτικών, που οδηγεί σε ηπατική δυσλειτουργία. Η DILI αποτελεί μία εκ των επικρατέστερων αιτιών οξείας ηπατικής βλάβης στις ΗΠΑ, ενώ περί το 95% των, υπό εξέταση, φαρμακολογικών ουσιών, απορρίπτεται εξαιτίας των ηπατολογικών του επιπτώσεων. Επιπλέον, περί το 2% της Μη-Αλκοολικής Στεατοηπατίτιδας (NASH) δείχνει να οφείλεται στην Ηπατοπάθεια από Φάρμακα (DILI).

Για τους λόγους αυτούς, πρέπει να συνυπολογίζονται οι τάσεις για δημιουργία στεάτωσης -που ομοιάζει προς την NAFLD-στεάτωση- κατά τον έλεγχο νέων, αλλά και ήδη εμπορεύσιμων φαρμάκων. Στο πλαίσιο αυτό, μια υπολογιστική πλατφόρμα, με χρήση της Ανάλυσης Βιολογικών Δικτύων (Network-Based Pathway Analysis) πάνω σε σημαντικά μονοπάτια για την παθογένεση της NAFLD, αλλά και άλλων γνωστών, βιβλιογραφικά, στεατογόνων ενώσεων, δίδει αποτελέσματα για άλλες πιθανές ηπατοτοξικές/στεατογόνες φαρμακολογικές ουσίες. Μεταξύ αυτών, τρεις (Pimozide, Clomiphene, Mefloquine) επιλέγονται προκειμένου να ελεγχθούν και πειραματικά σε Hep3B και FOCUS ηπατικές κυτταροσειρές.

Η *in-silico* προσέγγιση καταλήγει σε δικτυακές επικαλύψεις, από τις οποίες εξάγει πιθανά στεατογόνες ενώσεις. Με χρήση *high-throughput* μεθόδων, γίνεται η *in-vitro* αξιολόγηση των φαρμακολογικών αυτών ουσιών σε σχέση με την τάση τους να προκαλούν ηπατική στεάτωση αντίστοιχη προς της NAFLD. Πρόσθετα πειράματα οφείλουν πραγματοποιηθούν, προκειμένου να αποσαφηνιστούν οι μηχανισμοί της NAFLD παθογένεσης, καθώς και να ομαδοποιηθούν οι υπό-εξέταση φαρμακολογικές ουσίες με τις γνωστές στεατογόνες ενώσεις, προς περαιτέρω αξιολόγησης και των πιθανών στεατογονικών τους τάσεων.

Λέξεις-κλειδιά: NAFLD, NASH, DILI, liver, steatosis, pathway analysis, networks, drugs, steatogenic compounds, DEGs, genes, systems, biology, systems biology, bioengineering, GLS, GSA

CONTENTS

1	Contents	3
2	Introduction.....	5
2.1	Biological Background.....	5
2.1.1	Definitions	5
2.1.2	Epidemiology	7
2.1.3	Natural History of the Disease	8
2.1.4	Molecular mechanisms of Pathogenesis.....	9
2.1.5	Fat metabolism, hepatotoxicity and insulin resistance.....	10
2.1.6	Diagnosis.....	24
2.1.7	Therapy	25
2.1.8	State-of-the-Art: Research Strategies for Non-Alcoholic Fatty Liver Disease	26
2.2	Computational Background	38
2.2.1	Systems Biology.....	38
2.2.2	Biological Networks.....	40
2.2.3	Pathway Analysis.....	44
2.3	Aim of the Project.....	46
3	Materials and Methods.....	47
3.1	Computational Analysis	47
3.1.1	Gene Expression Omnibus (GEO)	47
3.1.2	Volcano Plot.....	47
3.1.3	Gene Level Statistics (GLS).....	49
3.1.4	Gene Set Analysis (GSA).....	51
3.1.5	DrugBank	52
3.1.6	Connectivity Map (cMap).....	53
3.1.7	Methodology.....	54
3.2	<i>In-Vitro</i> Verification.....	56
3.2.1	Cell lines.....	56
3.2.2	Cell Culture.....	59
3.2.3	Steatosis Induction.....	59
4	Results.....	69
4.1	Computational Analysis	69
4.1.1	GEO Microarrays.....	69
4.1.2	Selection of Datasets.....	70
4.1.3	Gene Level Statistics (GLS).....	71

4.1.4	Gene Set Analysis (GSA)	74
4.1.5	Determination of the Drug-triggered Pathways.....	75
4.1.6	Identification of Relative Compounds via cMap.....	77
4.2	In-Vitro Verification.....	81
4.2.1	FBS Threshold Determination Experiment.....	81
4.2.2	FFA Threshold Determination Experiment	82
4.2.3	Bulk Verification of Steatogenic Effects.....	83
4.2.4	IC10 Determination.....	83
4.2.5	Intracellular Lipid Accumulation.....	85
4.2.6	Intracellular ROS Production.....	88
5	Conclusions.....	91
6	References.....	93

I INTRODUCTION

I.1 BIOLOGICAL BACKGROUND

I.1.1 Definitions

I.1.1.1 Non-Alcoholic Fatty Liver Disease (NAFLD)

Non-Alcoholic Fatty Liver Disease (NAFLD) demonstrates escalating paces of circumstance within the general population, mainly attributed to the increasing obesity in both children and adults.

NAFLD accounts for the hepatic component of the metabolic syndrome, while it is officially defined by the excessive, yet non-inflammatory, accumulation of liver fat by causes other than elevated alcohol consumption (<21 in men, <14 in women). [1]

The very term, NAFLD, is referring to a broad spectrum of conditions, commencing from simple steatosis and steatohepatitis (Non-Alcoholic Steatohepatitis; NASH) and potentially leading to liver fibrosis, cirrhosis and hepatocellular carcinoma (HCC), along with their clinical extensions.

NAFLD is tightly linked with insulin resistance, among other obesity-related factors, such as diabetes, central abdominal obesity and dyslipidemia. Found to be an independent risk factor for cardiovascular diseases regardless of age, sex and cholesterol levels, NAFLD is also linked with increased mortality risk of any cause, in which, both liver-related and secondary factors, e.g. malignancies, diabetes and coronary heart disease, contribute. [2]

I.1.1.2 Drug-induced Liver Injury (DILI)

A prevalent, though underestimated cause of liver disease is Drug-induced Liver Injury (DILI). In the United States, DILI is the first cause of acute liver failure and causes 10% of

all cases of acute hepatitis. Interestingly, hepatotoxicity accounts for the first cause of drug withdrawal from global markets and the commercial use.

Several drugs and other xenobiotics may trigger various pathological patterns, involved in the induction of liver damage. Steatosis has been acknowledged to be linked with various steatogenic drugs, such as amiodarone, tamoxifen, irinotecan, methotrexate, valproic acid and glucocorticoids. Although steatogenic pathophysiological pathways are still only partly understood, the primary pathogenic mechanisms by which drugs lead to hepatic steatosis involve the inhibition of mitochondrial β -oxidation, decreased VLDL secretion, insulin resistance and elevated de novo FA synthesis or absorption.

Fatty liver itself is a very prevalent clinical disease, and owing to its underlying metabolic disorder, there is an increasing awareness for NAFLD-induced DILI. Indeed, DILI covers a wide spectrum of liver disorders that ranges from simple steatosis to more severe forms, such as cirrhosis and hepatocellular carcinoma.

The wide epidemiological impact of Fatty Liver Disease and the diagnostic complexity of DILI make the identification of a single molecule, as the origin of drug-induced liver disease, even more difficult. Even if several drugs may be responsible for DILI, few drugs have a proven causative role for steatosis.

1.1.1.3 Drug-induced Steatohepatitis (DISH)

The development of DISH can be considered as the precipitation of pre-existing steatosis or as a de novo liver disease. DISH pathogenesis has not been fully elucidated; however, oxidative stress appears to be a key mechanism.

Mitochondrial dysfunction and inhibition of the mitochondrial respiratory chain induce the increased production of Reactive Oxygen Species (ROS). ROS cause FA peroxidation that, in turn, leads to inflammation and fibrosis, facilitated by the activating Kupffer and Ito cells. ROS and reactive lipid peroxidation can directly damage the mitochondrial

respiratory chain and the mitochondrial DNA, thus creating a vicious cycle of increased ROS production.

1.1.2 Epidemiology

NAFLD's prevalence in individuals of normal weight, lacking metabolic risk factors, is found to approximate 16%. The percentage reaches 43-60% in diabetic patients and rises up to 91% in patients with hyperlipidemia. Its prevalence also rises in accordance with age, as it approximates 20% in ages below 20 to more than 60% in ages above 60. Specifically, age has been proven to be an independent risk factor with regards to steatosis and its potential progression towards fibrosis and cirrhosis. The male sex is found to be independent to the progression of NAFLD towards NASH and fibrosis. [3]

Although some studies suggest that ethnicity influences NAFLD's prevalence, recent data do not back the notion. Interestingly, though, the link between insulin resistance and NASH is significantly different in individuals of Latin origins, when compared to the non-Latin. [4]

Although mortality rates appear increased in patients with steatohepatitis and progressed fibrosis, patients with sole steatosis do not demonstrate significant mortality. A wide-association study on 129 NAFLD patients, diagnosed via liver biopsies, suggested mild mortality rates in NAFLD patients when compared to the increased mortality of NASH patients. While mainly linked with cardiovascular disease, liver-related mortality was found more frequent in patients with NASH cirrhosis. [5] Recent systematic research on 221 biopsy-proven NASH patients revealed age and degree of inflammation to be independent predictors of initial biopsies' progression towards fibrosis. On the other hand, factors such as diabetes, hypertension and obesity were found statistically insignificant as predictors. These findings suggest that the presence of elevated fibrosis is related to the overall increased mortality rates due to cardiovascular disease. [6]

Hamabe et al.'s review suggested smoking as an independent risk factor for NAFLD, regardless of other concurrent metabolic factors. Notably, NAFLD's development rate in

quitters was similar to that of the smokers, most probably due to the consequent weight gain of the former. [7]

Mild alcohol consumption seems not to trigger NAFLD's development, while several studies have shown that it may even limit its occurrence. [8]

1.1.3 Natural History of the Disease

The natural history and pathogenesis of NAFLD is not sufficiently documented. In NAFLD, simple steatosis is defined by the presence of fat in <5% of the hepatic cells, with around 20-25% of the total cases progressing to NASH, from which 20% will develop liver fibrosis and, ultimately, cirrhosis.

The evolutionary mechanisms leading from steatosis to steatohepatitis are complexed and not fully comprehensible, although increased abdominal obesity and insulin resistance in cellular environments of increased FFA release might play a significant role in the transition.

Normally, insulin promotes hepatic and peripheral glucose intake and subdues its production in the liver. In fasting periods, liver becomes the primary organ for glucose production via gluconeogenesis and glycolysis. In insulin-resistant patients, hepatic autoregulation is disturbed and thus, increasing gluconeogenesis and glycolysis lead to hyperglycemia.

The underlining mechanisms of liver failure in NAFLD are thought to be a multiple-hit process that involves insulin resistance, oxidative stress, apoptosis and a deregulation in the levels of adipokines. [9]

1.1.4 Molecular mechanisms of Pathogenesis

1.1.4.1 Two-Hit Hypothesis

The Two-Hit model for NAFLD was first introduced in 1998 by Day et al. The first of the hits addresses the accumulation of Triglycerides (TG) and Free Fatty Acids (FFAs) in hepatocytes, due to insulin resistance, increased dietary lipid intake and elevated hepatic lipogenesis. The second includes lipid peroxidation, mitochondrial dysfunction and inflammation and is leading to cellular damage and fibrosis. Pre-inflammatory pathways, activated by cytokines and pattern-recognition receptors, including toll-like receptors, lead to core signaling pathways: The Nuclear Factor $\kappa\beta$ (NF- $\kappa\beta$) and the C-Jun N-Terminal Kinase (JNK) pathway. NF- $\kappa\beta$'s activation is observed in NASH and may lead to increased transcription of pre-inflammatory genes, while JNK induces insulin resistance via the direct phosphorylation and degradation of IRS1 (Insulin Receptor Substrate 1), therefore limiting the corresponding intracellular signaling processes. Lipid peroxidation may promote the reproduction of Hepatic Stellate Cells (HSCs), thus contributing to fibrosis. Reactive Oxygen Species (ROS) promote cytokine-release that trigger several pathways of the immune system, thus leading to further liver damage. In NASH, hyperinsulinemia, lipid peroxidation and hepatic iron peroxidation amplify oxidative stress, thus causing mitochondrial dysfunction and contributing to the excessive accumulation of triglycerides and, eventually, to cell death. [10]

1.1.4.2 Multiple-Hit Hypothesis

The simplicity of the two-hit hypothesis could not include the complexity of human NAFLD, where multiple concurrent factors act on genetically predisposed individuals and influence the development and progression of the disease. Therefore, a multiple-hit hypothesis was necessary to include dietary habits and environmental and genetic factors that trigger insulin resistance, obesity of reproducing fat cells and changes in the intestinal microbiome. [9]

1.1.5 Fat metabolism, hepatotoxicity and insulin resistance

Fat enters the fatty liver in the form of triglycerides, originating from the esterification of glycerol and free fatty acids (FFA). Upon their synthesis, triglycerides enter the storage and secretory vesicles of the liver.

FFAs originate in the patient's nutrition or the adipose tissue through lipolysis and/or de novo lipogenesis (DNL). In hepatocytes, FFAs form acyl-CoA fatty acids in a process facilitated by acyl-CoA synthetases. Formed acyl-CoA fatty acids undergo esterification or enter β -oxidation.

The influx of triglycerides is not necessarily hepatotoxic. It may represent a homeostatic mechanism of the liver to counterbalance excess FFAs; a notion that is proven in muscle models. Under normal conditions, the synthesis of triglycerides is induced in an effort to reduce FFA overflow. Triglycerides are either stored within the hepatocellular cytoplasm in the form of lipid droplets or secreted in the form of Very-Low-Density Lipoproteins (VLDL). [11]

The inhibited accumulation of triglycerides in novel VLDLs, via the obstruction of the Microsomal-Triglyceride-Transfer Protein (MTP), causes faulty secretion of triglycerides and thus, lipid accumulation without liver injury. The inhibited expression of Diglyceride Acyltransferase 2 (DGAT2) -a key enzyme that is involved in the formation of triglycerides- causes a decrease in the intrahepatic triglycerides and a subsequent rise in FFA oxidation. DGAT2 inhibition has been found to deteriorate steatohepatitis in muscle models. Therefore, the elevated concentration of triglycerides is an epiphenomenon that occurs with the spontaneous production of toxic metabolites, hepatotoxicity and liver injury. [12]

De novo lipogenesis is a metabolic pathway that includes the glycolysis of glucose into acetyl-CoA, the biosynthesis of saturated fats with their subsequent desaturation, and the formation of triglycerides within the liver and the adipose tissue. A deregulation of DNL has been observed in patients with the metabolic syndrome or NAFLD. DNL increases with dietary plans rich in carbohydrates and poor in lipids, that cause an increase in blood's triacylglycerol. The increased synthesis and secretion of VLDL in the liver leads to

hyperglyceridemia and steatosis. Hepatic DNL is induced from the flux of lipids into the liver, due to excessive dietary FFA intake and peripheral insulin resistance. Although the exact mechanism is not fully comprehensible, it is suggested that hepatic insulin resistance may be the or/the effect of liver steatosis. Chronic hyperinsulinemia, as in NAFLD, increased DNL via the positive regulation of lipogenic transcription factors. [13]

Hepatic de novo lipogenesis (DNL) increases subsequently to the activation of several transcription factors, such as the Sterol Regulatory Element-Binding Protein 1 (SREBP-1), the Carbohydrate Response Element-Binding Protein (ChREBP) and the Peroxisome Proliferator-Activated Receptor (PPAR- γ). SREBP-1 is a transcription factor that exists in three isomorphs: (a) the SREBP-1c, activated by insulin, regulates the activation of DNL and the regulatory genes for glucose and FA metabolism, along with those that regulate lipid synthesis, (b) SREBP-2 is involved in cellular homeostasis of cholesterol, thus its deregulation is tightly linked with fat accumulation in the hepatocyte. (c) ChREBP is activated by glucose, increases DNL and provides more substrate for FFA and triglyceride synthesis. [14]

Among the insulin receptors, the Insulin Receptor Substrate 2 (IRS-2) may function, when activated, as a regulator of SREBP1-c, therefore affecting DNL. In cases of insulin resistance, IRS-2 is negatively regulated and thus, SREBP-1 is overexpressed and DNL increases. Additionally, the β -oxidation of FFA is suspended, thus promoting further accumulation of fat within the hepatocytes. [15]

SREBP-1c is also suspended by the Glucose-Regulated Protein 78 (GRP78). GRP78 is a binding protein for immunoglobulin and a substantial regulator of the Endoplasmic Reticulum (ER), thus important for the cell's survival. Research suggests that the levels of Carbomoyl-Phosphate Synthase 1 (CPS1) and GRP78 are gradually decreasing from simple steatosis and towards NASH. [13]

Recent studies on rodents revealed that in obesity, DNL is negatively regulated in White Adipose Tissue (WAT) and that its selective restoration reverses the obesity-induced insulin resistance. Human studies support these findings. The enzymes of DNL are

suppressed within WAT in obese individuals, along with the Glucose Transporter 4 (GLUT4). This suppression is tightly linked with faulty metabolic controls and can be reversed with weight loss via bariatric surgery. This finding suggests that DNL and its corresponding factors, e.g. the monounsaturated fatty acids in WAT, play an important role in regulating systemic insulin resistance and in determining metabolic diseases. Opposite to WAT, hepatic DNL has been found to be positively regulated in obese rodents and humans, where it is believed to induce hepatotoxicity, insulin resistance, atherogenic dyslipidemia and NAFLD. Given this correlation between hepatic DNL and the metabolic syndrome, it is believed that a suppressed DNL may provide a viable approach against several obesity-related diseases. Regardless of the mechanisms facilitated, patients with NAFLD demonstrate increased DNL that is not suppressed through fasting, as well as higher nocturnal levels of FFAs. [13]

Hepatocellular FFAs can injure insulin's signaling pathway, through the activation of kinase-serine, and contribute insulin resistance. Patients with NAFLD demonstrate lowered sensitivity for insulin, in their muscles, liver and adipose tissue. Due to insulin resistance, the adipose tissue becomes resistant to the anti-lipolytic functions of insulin, thus commencing peripheral lipolysis that induces increased FFA influx and guides DNL. Moreover, the lipid overload in beta pancreatic cells leads to a deregulation of insulin secretion and to changes in the expression of the α -receptor, activated by the Peroxisome Proliferator-Activated Receptor α (PPAR- α), the glucokinase, the Glucose Transporter 2 (GLUT2), the Pre-proinsulin and the Pancreatic Duodenal Homeobox 1 (PDX-1), that lead towards insulin resistance as a result of FFA-induced B-cells apoptosis. [9]

The mechanisms of hepatotoxicity, consequent to the ectopic fat accumulation in the liver, have not been sufficiently described. In the case of the energy intake exceeding consumption, an abundance of FFA leads to the ectopic storage of fat in the muscles and the liver. An overload of lipids may be found in other organs, such as the heart, pancreas and the arterial wall. The adipose tissues may store large amounts of FFA excess, but, when their maximum capacity is met, cellular dysfunction and cell death, i.e. hepatotoxicity, occurs. Hepatotoxic mechanisms include apoptosis, increased levels of cardiolipin,

increased permeability of the membranes, cytochrome-release within the mitochondria, NF- κ B activation and oxidative stress. In NAFLD, hepatic fat accumulation is considered a consequence of the imbalance between liver fat intake/production and its subsequent secretion/metabolism. [13]

Other pathways of fat disposal, e.g. the faulty oxidation of fatty acids in the liver or the lowered synthesis and secretion of VLDL, are of minor importance towards determining fat accumulation and hepatotoxicity in NAFLD. Autophagy, which regulates lipid metabolism, lowers the hepatic steatosis and result in a vicious cycle of lipid accumulation and further suppression of the autophagic function. [16]

Insulin resistance is more prevalent in NASH, when compared to simple steatosis. Patients with hepatic steatosis and NASH, but without diabetes type-II, demonstrate lowered sensitivity against insulin. Insulin resistance, as one of the “Multiple Hits” that sets the stage for NAFLD and its progression towards NASH, is of critical importance for hepatotoxicity, oxidative stress and the commencement of the inflammatory signaling cascade.

In patients with NAFLD, both genetic and environmental factors interfere with insulin's signaling pathway and contribute to the conservation and deterioration of insulin resistance: IRS-2 phosphorylation by inflammatory signaling molecules, like JNK1 and IKKb, NF- κ B and SOGS activation are only a portion of the mechanisms facilitated to obstruct the signaling pathway of insulin in NAFLD patients. [17]

1.1.5.1 Dysfunction of the Adipose Tissue

The adipose tissue is not inert, as it was traditionally believed. It has several endocrine functions and secretes hormones (adipokines), like leptin and adiponectin. The adipose tissue is also the primary source of FFAs and is responsible for 60% of the total triglyceride influx.

Lipocytes' hypertrophy, due to lipid overload, is relative to obesity and/or insulin resistance and results adipokine imbalance that can affect not only the tissue but also the liver. The excess lipidic load from the overloaded and malfunctioning adipose tissue may move towards the liver, muscles and other organs, where it is ectopically stored. [13]

The adipose tissue contributes in maintaining low degrees of inflammation, by producing pre-inflammatory cytokines. The levels of IL-6 in the plasma and the expression of TNF- α in adipocytes are increased in obese patients with a tension to lower accordingly to weight loss. In addition, the increased expression of pre-inflammatory genes and the activation of macrophages in the intestinal and subcutaneous adipose tissue of NAFLD patients, is related to the NAFLD's progression towards NASH and fibrosis.

Leptin is a 16kDa anorexigenic hormone with pre-inflammatory action, that defends non-fatty regions against lipid accumulation. In the liver, this is done via a decrease in SREBP-1's expression. However, leptin increases in obese patients as a response against leptin-resistance. Its pre-fibrotic role as been demonstrated in several *in vitro* models and in animal models. Leptin activates the hepatic stellate cells through the Hedgehog and mTOR pathways and stimulates the Kupffer cells. However, in spite of the plethora of data derived from the animal models, leptin's effect and importance in patients with NAFLD or NASH is still undocumented. [9]

Adiponectin improves the hepatic and peripheral insulin resistance and has an anti-inflammatory and hepatoprotective role. This role is accomplished mainly through the increase of sphingolipid deacetylation, performed primarily within the hepatocytes, the cardiac muscle and the pancreatic B-cells. Adiponectin's hepatoprotection addresses the inhibition of hepatic gluconeogenesis and the suppression of lipogenesis, mainly through the activation of the 5'AMP-activated Protein Kinase (AMPK) and the PPAR- α , which both increase fatty acids' oxidation in the liver and the muscles. Moreover, it is negatively correlated to the levels of triglycerides of the plasma, and positively correlated to HDL and LDL-cholesterol levels. [13] Its anti-inflammatory action is performed via the obstruction of NF- κ B's activation, anti-inflammatory cytokine-release and via the inhibition of pre-inflammatory cytokine release, e.g. TNF- α 's and IL-6's. Adiponectin's anti-oxidative

results are regulated by the AdipoR1 receptor, therefore its lowered levels in obese patients may play a causal role in mitochondrial dysfunction and insulin resistance. [9] Patients with NAFLD have lower concentrations of adiponectin than the healthy, in spite of the increased lipolysis and FFA concentrations. Therefore, adiponectin's low levels in NAFLD, increase the influx of FFAs and the lipid oxidation and play an important role in the condition's progression towards NASH. [13] Generally speaking, low levels of adiponectin and increased leptin, in obese patients, may lead to hepatic steatosis, inflammation and fibrosis.

1.1.5.2 Mitochondrial dysfunction

Structural and functional changes within the mitochondria contribute to NAFLD's pathogenesis. The structural changes include mitochondrial-DNA damage as well as morphological changes, while the functional changes involve the respiratory chain and the mitochondrial β -oxidation.

If the mitochondria and the peroxisomes become unable to accommodate the increased lipid influx, the respiratory oxidation may collapse, leading to failing fat-homeostasis and to the production of toxic metabolites, deriving from the lipids and the overproduction of ROS. These molecules activation the inflammatory pathways, thus promoting an inflammation-induced hepatic necrosis and worsening mitochondrial damage. [18]

There is a proven correlation between insulin resistance, obesity, TNF- α and mitochondrial dysfunction. In addition, Reactive Oxygen Species (ROS), along with oxidized Low-Density Lipoproteins (LDL) may activate Kupffer cells and hepatic stellate cells, further inducing inflammation and fibrosis. [19]

However, what remains unknown is whether mitochondrial dysfunction is NAFLD's main pathological event or a consequence of the changes in lipids' metabolism.

1.1.5.3 Stress of the Endoplasmic Reticulum

Increased protein production; the main dysfunction of the ER and ATP deficiency that induces unfolded proteins to accumulate, may activate Unfolded Protein Response (UPR) in response to the reticulum's stressing. UPR's activation involves adaptive mechanisms, like the reduction of protein synthesis, the increased capability of the ER for protein transport, the increased folding and the activation of protein-degradation pathways that ease up a failing folding that would normally lead to apoptosis.

In NAFLD, UPR derives from several factors, including hyperglycemia, ATP-depleting mitochondrial damage, hypercholesterolemia, depletion of phosphatidylcholine and oxidative stress.

UPR results in the activation of JNK, that in turn activates inflammatory pathways or apoptotic pathways, while its activity seems to separate NASH patients from patients with simple steatosis. Moreover, JNK's activity is tightly linked with faulty insulin signaling and diabetes.

Another interesting effect of UPR's is the activation of SREBP-1c's pathways. Through this activation fat accumulation in the liver is sustained, leading to further induction of oxidative stress and UPR. [20]

The X-Box Binding Protein 1 (XBP-1) is the main regulator of UPR that interacts with insulin's P13K signaling pathway. This interaction involves increased nuclear translocation, mainly attributed to insulin. Regulated by the XBP-1-regulated cellular response to ER stress, XBP-1 may be the lost link between steatosis, insulin resistance and inflammation. [21]

1.1.5.4 Inflammation in NAFLD: IL-6 and TNF- α

Elevated FFAs and the subsequent hepatotoxicity, insulin resistance, dysfunction of the peripheral adipose tissue and endotoxins of the intestines that contribute to the activation and maintenance of the pre-inflammatory cytokines' production and release.

NF- κ B is a transcription factor and the main regulator of the inflammatory response, while its IKK2 subunit is the main component required for its activation in acute inflammation. Permanent activation of NF- κ B's pathway is observed in both experimental NAFLD animal models and NASH human patients. IKK2's overexpression, that leads to the permanent activation of NF- κ B's pathway in hepatocytes, causes chronic inflammation and insulin resistance. [22]

The key-role of cytokine production in the liver during hepatic steatosis progressing to NASH, is acknowledged by a plethora of studies conducted on animal models. The liver's exposure to increased levels of pre-inflammatory cytokines leads to histological changes that are regularly observed in NASH, e.g. hepatocellular necrosis and apoptosis, neutrophils' chemotaxis, activation of hepatic stellate cells development of Mallory bodies. Moreover, the plasma and liver-levels of TNF- α are elevated in NASH patients and relative to the histological severity of the liver injury. Finally, the inflammatory response and the activation of NF- κ B may cause carcinogenesis and thus, chronic inflammation in NAFLD. It may also play an important role in the development of Hepatocellular Carcinomas (HCC). [23]

1.1.5.5 Activation of the Inflammasome

Inflammasomes are cytoplasmic poly-proteinic complexes that induce inflammation, consisting of caspases and molecules that derive from several pathogens or injured cells. They act as sensors for endocrine and exocrine pathogens that are related to pathogen-associated molecular patterns (PAMPs) or damage-associated molecular patterns (DAMPs).

The inflammasomes contribute to the immune response against various stimuli, as part of their innate immune system. They regulate the pre-inflammatory cytokine operators by activating of several kinds of Pattern Recognition Receptors (PRPs), like Toll-like Receptors (TLR), NOD-like Receptors (NLRs) and C-type Lectin Receptors (CLRs). DAMP-release

may be induced by various mechanisms, such as cellular necrosis, unremoved apoptotic cells and oxidative stress.

Inflammasome activation -in response to FFAs, oxidative stress and other NAFLD-related pre-inflammatory metabolites- and the subsequent production of Interleukin 1 β (IL-1 β), could play an important role in NASH's progression, through the suppression of PPAR- α and the indirect promotion of the cell-death, via TNF- α . In NASH, the saturated fatty acids positively regulate the inflammasomes and induce danger-signals' release from the hepatocytes in the form of caspase-dependent mechanisms that promote sensitization in IL-1 β 's and Lipopolysaccharide's (LPS) release in hepatocytes. For support, NLRP3-deficient mouse models were protected from nutrition-induced NASH.

Kupffer cells play an important role in inflammasomes' activity: They express large amounts of IL-1 β 's mRNA and their reduction leads to an overall decrease in IL-1 β . Phenotypic regulation of Kupffer cells could become a promising anti-fibrotic strategy.

As a consequence, the expression of proteins that relate to inflammasomes (NLRP3, pro-IL-1 β , pro-IL-18) are significantly elevated in NASH patients when compared to cases of simple steatosis. [9]

1.1.5.6 Cell Death

The hepatocellular apoptosis plays an important role in liver injury and in the development of NASH. The soluble Fas, a membranous death receptor of the TNF family, seems to be a key-point for apoptosis. The flux of FFAs into the hepatocytes causes an increase of the Fas linkers and the activation of Fas receptors that lead to apoptosis. In addition, the reactive caspases (mainly caspase 3) breaks up several substrates inside the cell, including Cytokeratin 18 (CK-18): an important intermediate protein of the liver that leads to apoptosis. Fragments of the CK-18 can be monitored in blood samples, using ELISA, and may become a powerful diagnostic tool in the years to come.

Hedgehog signaling (Hh) is involved in liver tissue repair and is thoroughly studied in NAFLD, in order to verify whether the elongation of the signaling pathway may influence the outcome of the disease. The levels of Hh activity seem to be proportionate to the extent and severity of the liver injury, both in rodents and in humans. The macrophage infiltration has been also observed in NASH patients, where the Monocyte Chemoattractant Protein 1 (MCP-1) is considered another important factor that might regulate the progression of the disease, by causing chronic inflammation as a result of leukocytes' infiltration into the liver. [13]

1.1.5.7 Genetic Factors

Genetic factors, mainly in the form of Single Nucleotide Polymorphisms (SNPs), affect the flux of FFA, the oxidative stress, the reaction against endotoxins and the production and activity of cytokines.

Comparative genomic studies have verified the role of several SNPs on the Patatin-like Phospholipase 3 (PNPLA3) with regards to the development and progression of NAFLD and, particularly, the I148M (rs738409 C/G) polymorphism. This single mutation replaces cytosine (C) with guanine (G), that, in turn, changes codon 148 from isoleucine to methionine. PNPLA3 encodes adiponutrin; a protein that demonstrates considerable homology to the enzymes involved in lipid metabolism and may promote lipolytic activity in triglycerides. In humans, this protein is expressed, primarily, in regions of the intracellular membrane of hepatocytes, and its activity is promoted either during insulin resistance or after food consumption. The G-allele seems to be linked with elevated influx of triglycerides into the liver, and thus, with NAFLD. The wild-type phenotype is expressed by the CC allele, whereas in NAFLD, the expression of alternative CG and GG alleles is tightly linked with the progression of the disease towards fibrosis and cirrhosis. [13] The PNPLA3 148M allele (CG) is related to decreased DNL and expression of SREBP-1c, despite the seeming increase in lipidic load. In contrast, hepatic β -oxidation is not influenced by the lipogenic factor.

Additionally, fat accumulation on PNPLA3 148M carriers is linked with lowered secretion of triglyceride-rich lipoproteins from the liver. [9]

Following the discovery of PNPLA3's mutation, and its potential correlation with steatosis and steatohepatitis, several SNPs have been observed in NAFLD/NASH patients. Genomic studies on Non-Hispanic, Caucasian women, diagnosed with NAFLD via liver biopsies, suggested that non-alcoholic steatosis is significantly correlated with mutation rs264524 of chromosome 8, on the gene encoding Farnesyl Diphosphate Farnesyl Transferase-1 (FDFT-1); the main regulator of cholesterol's biosynthesis. The same study revealed a strong correlation between the degree of fibrosis and SNP rs343062 of chromosome 7, although its function remains unknown. Another three SNPs have been linked with the inflammation of the hepatic lobes: (a) rs1227756 of chromosome 10, on gene $\alpha 1$ of collagen XIII (COL13A1), (b) rs6591182 of chromosome 11, and (c) rs887304 of chromosome 4, on the gene of the Calcium-Binding Domain 4B, EFCAB4B [13].

A polymorphism on the gene of the Transmembrane 6 Superfamily Member 2 (TM6SF2) is probably implicated in NAFLD's pathogenesis. TM6SF2 causes the secretion of VLDL, while the polymorphism rs58542926, through a loss-of-function, is related to hepatic steatosis, lower plasma levels of VLDL and higher levels of ATP. Interestingly, although the polymorphic carriers are more likely to develop NASH, they remain protected against cardiovascular diseases, due to the lower levels of VLDL. [9]

Another alteration of the gene, that has been thoroughly studied, is that of the Glucokinase Regulatory Protein (GCKR). GCKR regulates the glucokinase, a phosphorylating enzyme that is responsible for the hepatic metabolism of glucose and the activation of hepatic lipogenesis. Polymorphisms on this gene, e.g. rs780094 and rs1260326, appear related to an increased risk for diabetes type-II, especially in Asian populations. [13]

1.1.5.8 Epigenetic Factors

Epigenetic variations are constant changes at the transcriptional level, such as DNA methylation, histone modifications, and activity of microRNAs (miRNAs) that do not alter the basic DNA sequence and contribute to cellular homeostasis with a high degree of developmental and environmental plasticity. It is assumed that the distribution of this equilibrium can determine increased susceptibility to NAFLD. In a study of mouse models that induced NASH via diet, a correlation was observed between NASH development and epigenetic modifications, and, more specifically, cytosine methylations.

Methylation of DNA is considered an important factor in the progression of simple steatosis to NASH. It is primarily influenced by dietary deficiencies in methyl vectors, such as betaine and choline.

Modifications to histone acetylation, via histone deacetylases (HDACs) and histone acetyltransferases (HATs), are the most comprehensible of epigenetic modifications. Silent information regulator-2-family (SIRT) includes proteins with deacetylating activity, among which, SIRT1 is related to the regulation of glucose homogenate proteins, oxidative stress, fat solubility and inflammation response. The relationship between NAFLD and the lowered expression of SIRT1 is observed in both animal models and humans.

In studies of obese patients of all NAFLD stages and healthy controls, differences in the expression and methylation levels were observed in 9 genes, encoding key-enzymes for the mediated metabolism and the signaling pathway of insulin. Interestingly, these differences were partially reversed after bariatric surgery.

Finally, non-coding RNAs regulate the mechanisms of NASH's epigenetic gene expression. Research on these non-coding regions of RNA are limited to miRNAs, the small endogenous monoclonal RNA molecules that regulate various cellular mechanisms by affecting the transcriptional and post-transcriptional gene expression. Changes in the expression of miRNAs have been linked to the pathogenesis of NAFLD/NASH. mir-122, the most abundant hepatic miRNA, leads to decreased levels of cholesterol when suspended. It also leads to differential expression of the hepatic genes, mainly associated

with cholesterol and FA metabolism. 113 miRNAs were found to be differentially expressed in the abdominal adipose tissue of NASH patients, when compared to patients with simple steatosis. Among these, 7 miRNAs, involved in gene regulation of several metabolic pathways, were significantly correlated with NASH, while two (mir-97, mir-99) were found associated with the extent of hepatic fibrosis. [9]

1.1.5.9 Dietary Factors

Several dietary factors, with regards to both quality (specific ingredients), quantity and calorie consumption, are related to the development of NAFLD and NASH. In a study that involved 18 healthy individuals, the normal calorie consumption was doubled with fast-food meals. This caloric excess led to an increase in the serum's ALT and induced steatosis in less than 4 weeks.

Fructose is a lipogenic, pro-inflammatory agent that causes oxidative stress and elevated expression of TNF- α . Special insulin-independent kinases cleave fructose to fructose 1-phosphate, that in turn transforms into triose-phosphate and enters the glucose pathway, where it produces DNL substrates. In muscle models of fructose-induced NAFLD, fructose intake -of industrial origin- was found associated with increased fibrosis.

Mono-unsaturated FAs, commonly met in the Mediterranean diet, seem to have a protective role against NAFLD. A Japanese study of 5.000 individuals, suggested moderate alcohol consumption to also have protective effects against NAFLD. In a meta-analysis of over 40.000 people, moderate alcohol consumption was associated with a decrease in the incidence of NAFLD and in its progression to NASH. [9]

1.1.5.10 Influence on the microflora: the gut-liver axis

Intestinal microflora is involved in the pathogenesis and the progression of NAFLD, via the so-called gut-liver axis. More than 50% of the visceral blood-volume passes through the liver. Thus, the liver is the organ with the greatest exposure to intestinal toxins and, as

such, the first line of defense against bacterial products. The host-microflora communication is of profound importance for the development and homeostasis of the host's adaptive immunity. Lipopolysaccharides (LPS) are one of the major bacterial toxins. They act, when bound to the CD14 co-receptor, as a ligand for TLR resulting in the activation of an inflammatory cascade that includes stress-activated kinase pathways: the JNK, Insulin-3 Regulating Agent and the JB transcription factor. These pathways are involved in the development of insulin resistance, obesity and liver fat accumulation, as well as in the development of progression of NASH. Specific patterns of the microflora can increase intestinal permeability and cause lipo-polysaccharidemia. Patients with NAFLD demonstrate increased intestinal permeability and elevated bacterial microflora when compared to the healthy controls. The significant correlation between elevated bacterial microflora and NASH is observed in cases even lacking increased intestinal permeability.

The intestinal microflora affects the energy balance of the host, by kneading resistant starchy and non-starchy polysaccharides into short-chain fatty acids (SCFAs) that become absorbable from the intestinal epithelium. Additionally, the bacteria suppress the synthesis of the Fasting-Induced Adipocyte Factor (FIAP) leading to increased lipoprotein lipase activity and triglyceride accumulation. They may also produce enzymes that catalyze the conversion of dietary choline into toxic products (mainly methylamines). When taken in by the liver, these amines convert into trimethylamine-N-oxides and cause inflammation and liver injury. Recent studies have shown that a dysbiosis with the microflora can cause NASH by either lowering choline levels or increasing methylamine levels. Another mechanism through which NAFLD is induced, involved a change in the metabolism of bile that affects several functions, such as hepatic DNL and VLDL secretion.

Apart from these, the intestinal microflora is an important source of endogenous alcohol production. Several obesity-related abnormalities are associated with elevated levels of alcohol-breath. Research on the identification of potential differences between the intestinal microflorae of NASH, obese and healthy children revealed an abundance of alcohol-producing bacteria in NASH, along with a consequent increase in blood's alcohol

levels; a hypothesis that explains the similarities in histological and genetic characteristics of Alcoholic and Non-Alcoholic Fatty Liver Disease.

Finally, failing NALP3 inflammasomes are associated with low levels of various intestinal cytokines, including IL-18, that regulate the intestinal microflora. As a result, an increased flux of TLR4- and TLR5-antagonists into the portal circulation leads to more acute NASH phenotypes. [9]

1.1.6 Diagnosis

Non-Alcoholic Fatty Liver Disease is basically a non-symptomatic condition and, as such, its diagnosis is often incidental. Clinicians ought to consider the likelihood of NAFLD's occurrence in patients with abnormal liver markers and/or metabolic risk-factors, as the likelihood of occurrence increases proportionally to the number of metabolic-syndrome factors.

Although the levels of Aspartate Transaminase (AST) and Alanine Transaminase (ALT) are significantly different in NAFLD patients, the traditional thresholds may address them as "Normal". Several studies have shown that ALT is not a good biomarker for predicting fibrosis in patients with NAFLD.

Ultrasounds is a good diagnostic tool for cases with at least 30% hepatic steatosis (64% sensitivity & 85% specificity). Other diagnostic tools include Magnetic Resonance Spectroscopy (MRS) and FibroScan's Control Attenuation Parameter (CAP), which are more sensitive and offer quantitative liver analysis.

For non-invasive diagnosis, there are various scoring systems that help in the classification of patients with minor or significant liver fibrosis. Several of those systems use AST, ALT, age and decreased glucose tolerance as input variables. Alternative tests include the European Liver Fatigue Table, which combines three biomarkers of the blood's serum (hyaluronic acid, pre-collagen-III peptide and metalloproteinase 3-specific inhibitor) and FibroTest. Transient elastography, such as Fibroscan, has been tested for the diagnosis of

NAFLD and is usually used in complementary non-invasive tests. However, up until today, liver biopsy remains the most reliable and widespread means for NAFLD/NASH diagnosis and evaluation, and the primary endpoint for clinical trials. [24]

1.1.7 Therapy

1.1.7.1 Weight Loss

A change in lifestyle and dietary habits still remains the primary treatment method for NAFLD, as there are no approved therapeutic agents. Although lifestyle changes are effective, they can be difficult to implement, and, thus, a gradual weight loss over a 6- to 12-month period seems reasonable. A calorie deficit down to 500-1000 kcal per day is usually suggested to NAFLD patients, the progress of which is consistently monitored by a clinical dietitian.

Simple carbohydrates, such as fructose, have been linked to NAFLD. Carbohydrate consumption affects glucose homeostasis and FFA metabolism by the liver, therefore low-carb diets have been thoroughly studied. Several studies have shown that a 7-10% weight loss is associated with reduced liver inflammation. Although exercise alone has not been proven effective, when combined with dietary changes, light exercise, e.g. 30- to 40 minutes of daily walking, seems to improve NAFLD's histological and biochemical factors.

Considerable weight loss can be achieved with pharmacological agents. Orlistat leads to moderate weight loss via a 30% reduction in fat absorption through lipase inhibition. However, recent studies revealed moderate results, limited only to patients that achieved a 9% weight loss attributed to lifestyle changes. Sibutramine is a serotonin- and noradrenaline-inhibitor that increases satiety and may lead to moderate weight loss. In a study on NASH patients receiving Sibutramine over a 6-month period, a 10% weight loss improved insulin resistance and achieved lower transaminase levels. However, its use was withdrawn due to the risk of fatal heart disease. Finally, Rimonabant, a cannabinoid receptor-antagonist, has been a promising therapeutic agent due to the fact that non only

did it led to substantial weight loss, but also to improved insulin resistance and lipid-adiponectin levels in the serum. However, it was withdrawn from commercial use in 2008, due to severe psychiatric side-effects. [25]

Bariatric surgery, which is widely used for weight loss, reduces most of the histological characteristics of NAFLD and diabetes type-II, which is associated to obesity and insulin resistance. Up until today, bariatric surgery is not considered necessary for NAFLD patients, as the surgery increases the insulin sensitivity in viruses, muscle and adipose tissue, due to weight loss, and thus improves overall metabolic health. The mechanisms facilitated for the improvement of insulin sensitivity remains unknown. [26]

1.1.7.2 Liver Transplant

For the end-stage NAFLD patients, liver transplantation is the only alternative. However, NASH recurrence is a frequent phenomenon, mainly due to the ongoing metabolic risk factors and the use of immunosuppressants, such as corticosteroids. [27]

1.1.8 State-of-the-Art: Research Strategies for Non-Alcoholic Fatty Liver Disease

1.1.8.1 Dietary Free Fatty Acids

Among the many factors associated with the pathogenesis of NAFLD, the role of FFAs is the most direct. The notion has been demonstrated *in-vivo*, by the tight relationship between FFA-bearing adipocytes and target cells, such as hepatocytes. [28]

The main sources of FFAs are the following:

- a) Dietary Fatty Acids, mainly in the form of chylomicrons absorbed in the intestines;
- b) Increased lipolysis of WAT's peripheral fat, that flows in the form of non-esterified Fatty Acids toward the liver;
- c) Newly synthesized intrahepatic Fatty Acids via DNL [28]

The most direct way to validate FFA's effect on hepatocytes is by their exposure to elevated concentrations of FFAs that will generate intracellular lipid droplets, associated with changes in the cell's oxidative state.

Hepatocytes exposed to 0.1% triglycerides revealed an increase in intracellular ROS production levels that led to cell death and lipo-apoptosis. The use of a special flavoprotein-inhibitor, such as oxidase and NADPH (Nicotinamide Adenine Dinucleotide Phosphate) limits the ROS increase, indicating that this increase is flavoprotein-dependent and derives from Mitochondrial Complex I or from NADPH's oxidase. [29]

In addition to oxidative stress, cytotoxicity, due to FFA-exposure, occurs via caspase-dependent apoptosis, with JNK triggering mitochondrial apoptosis by activating Bim-dependent Bax. Interestingly, it has been suggested that the use of unsaturated fatty acids can mimic the "two-stroke hypothesis" *in-vitro*. The exposure to FFAs has made hepatocytes more vulnerable to apoptosis, through low concentrations of glycogone deoxycholic acid. This phenomenon is associated with significant transcription of IL-8 and IL-22 pro-inflammatory cytokines, but only in the stem cells. [30]

Oleic acid is a monounsaturated fatty acid and one of the most common fatty acids of human nutrition. It is necessary for the formation of the plasma membrane and acts as an energy source. Palmitic acid is a saturated fatty acid with similar function and the most prevalent in fatty hepatocytes.

The effect of FFA differs among the various kinds of fatty acids, or, in descending likelihood for apoptosis: Stearic Acid > Palmitic Acid > Palmitoleic Acid > Oleic Acid. In accordance with this observation, a differential effect of oleic and palmitic acid on hepatic cell viability, activation of caspases and DNA breakage, has been identified. This observation underlines the importance of saturated-unsaturated ratio, especially in experimental design. [31]

Additionally, different fatty acids bind to the cell membrane and are facilitated from the cell in different manners. In high concentrations, diffusion is the most important transport mechanism, while protein-assisted transport takes place at lower concentrations.

Due to their lipophilicity, fatty acids bind to serum's albumin. Thus, only the unbound free fatty acids can enter the cell. CD36 / fatty acid translocase, caveolins and the fatty-acid-transport protein are the major plasma membrane FFA-transporters. As binding differences have been monitored between humans and rodents, the source of albumin and the type of the used FA are important components for the *in-vitro* study. For example, the binding of oleic acid to human serum albumin resembles that of the palmitic acid to bovine serum albumin, and vice versa. With regards to the other forms of fatty acids, the correlation coefficients differ depending on the albumin binding site. All these results underline the need for a meticulous calculation of albumin's concentration, ligand molarity (FFA) and albumin/FFA ratio under each of the experimental conditions. [28]

1.1.8.2 Exogenous administration of steatogenic compounds

Several drugs induce steatosis or steatohepatitis that bear pathological resemblances to NAFLD. Drug-induced steatosis falls into different categories that are based on the predominant characteristic of the steatosis they induce. These categories could be:

- 1) Macro-vesicular steatosis is described by the presence of small or large lipid droplets in the hepatocellular cytoplasm along with profound nuclear displacement. This type of liver injury is usually reversible, but, over time, it may progress towards steatohepatitis and cirrhosis. In general, it is associated with increased hepatocellular exposure to alcohol, glucocorticoid therapy, total parenteral nutrition, Methotrexate (MTX) and Amiodarone (AMI). Also, this type of steatosis may be induced by chemotherapeutic drugs like Tamoxifen (TMX), Irinotecan (IRI) and Asparaginase.
- 2) Steatohepatitis is characterized by steatosis, necroinflammation and hepatocellular "bloating" with or without Mallory bodies. In some cases, fibrosis may also occur. Drugs that are found to induce steatohepatitis are Amiodarone (AMI), Tamoxifen (TMX), Methotrexate (MTX) and Irinotecan (IRI).

- 3) Micro-vesicular steatosis is demonstrated by the accumulation of numerous small lipid droplets within the hepatocellular cytoplasm but lacking nuclear translocation. Micro-vesicular steatosis is the most severe form of liver injury, characterized by mitochondrial dysfunction, and can be lethal, when extensive or prolonged. Associated drugs include Valproic Acid (VPA), Tetracyclines (TET), Aspirin, Glucocorticoids and various non-steroidal anti-inflammatory compounds. [32]

1.1.8.3 Valproic Acid (VPA)

Valproic acid (VPA), along with its corresponding sodium salt form, sodium valproate, is the most widely used antiepileptic drug and a chemical analogue of linoleic acid. Daily administrations are estimated to exceed one million patients. Recently, VPA has been characterized as a histone-deacetylase inhibitor. VPA is effective against various types of epileptic seizures, including bipolar disorder, when administered alone or in the context of a wider treatment. Its antispasmodic properties were discovered in 1963 and commercialized in 1966 (France) and in 1978 (US). VPA has a wide range of action against general and partial epilepsy in both children and adults. Thus, it usually is the first compound to be considered against newly diagnosed epilepsies. Recently, its administration was proposed for other medical conditions, such as neuropathic pains, migraines and headaches. Also, it was suggested as an alternative mood stabilizer for various psychiatric conditions, while it may rarely be administered to patients with dementia or within a treatment for spinal muscular atrophy.

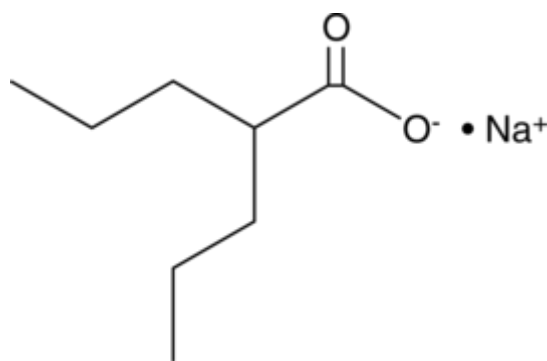


Figure 1.1.8.3.1: Valproic Acid's chemical structure

In 1978, a number of clinical studies revealed some biochemical abnormalities of the liver associated with VPA. VPA-induced hepatotoxicity may be manifested in one of the following ways:

- 1) Hyperammonemia: a single biochemical finding that can be observed with a simple blood test. Hyperammonemia may be a complicating condition of increasing loss of consciousness and orientation with subsequent gastro-intestinal symptoms, such as nausea, vomiting, anorexia and diarrhea. These symptoms fade out within, approximately, three days of medical discontinuation.
- 2) Hepatitis-like syndrome: characterized by a dose-dependent increase in serum aminotransferases. The majority of patients are asymptomatic, although some might develop anorexia and lethargy. Biochemical abnormalities and clinical symptoms are usually stabilized after medical discontinuation.
- 3) Reye's-like syndrome: a risky, rare and idiosyncratic syndrome. Patients usually experience acute cases of high fever, lethargy, anorexia, vomiting, loss of consciousness and cerebral edema.
- 4) Non-alcoholic Fatty Liver Disease: the steatogenic side-effects of VPA have been detected in the 1980s. The notion is backed from histological findings on liver tissue, extracted from patients thought to have died due to VPA-induced hepatotoxicity, as well as by experimental studies on animals. [33, 34]

VPA causes NAFLD by inducing weight gain, hyperinsulinemia and insulin resistance. The association between VPA and weight gain was first observed in 1981, but even today, the underlying pathological mechanisms are not fully comprehensible. It is regulated, both centrally and peripherally, by various neuropeptides and cytokines. These regulatory substances include resistin, the Fasting-Induced Adipose Factor (FIAF), adiponectin, leptin, ghrelin and visphatin. [35] VPA can increase appetite by amplifying the signal of the γ -aminobutyric acid (GABA) in the hypothalamic pathways. It can also alter the gene expression of several adipokines, such as resistin and FIAF. This can lead to insulin- and leptin- resistance and, eventually, to obesity. These mechanisms have been observed in patients that received VPA for several years. As mentioned, adiponectin is a protein of the

adipokine family that plays an important role in lipid metabolism and insulin sensitivity and, thus, in body-weight regulation. VPA has been shown to negatively regulate adiponectin's gene expression in adipocytes and to increase the expression of its corresponding receptor (adipoR1) in hepatocytes. The latter contributes to the deregulation of FA oxidation. Leptin is another adipokine that suppresses hunger and increases FA metabolism in the adipocytes. Its serum and mRNA levels in adipocytes are directly correlated to insulin deficiency and obesity. Leptin levels and leptin resistance may not be related to VPA but may result from its abundance in adipose tissue. Ghrelin is an appetite-generating hormone that acts to increase appetite. Plasma levels increase before meals and decrease afterwards. In addition, it regulates leptin- and insulin- secretion and selectively utilizes carbohydrates over lipids. An increase in ghrelin's levels have been observed in the initial period of VPA administration. [42]

Hyperinsulinemia has been extensively recorded during VPA treatments and is known to be related to obesity, dyslipidemia and insulin resistance. Interestingly, some scientists regard insulin resistance as a consequence of weight gain, but as its driving force. [36] The notion is supported by several observations that related VPA-induced obesity to an increase in insulin levels and a decrease in glucose levels. Hyperinsulinemia can stimulate appetite and therefore lead to obesity and to the hypothesis that VPA can induce insulin resistance. [35] Various assumptions on the role of VPA in hyperinsulinemia and insulin resistance have been formulated:

- 1) VPA is a GABA agonist and can directly increase insulin levels by stimulating GABA receptors in β -pancreatic cells. [37]
- 2) VPA and its metabolites can increase oxidative stress and dysfunction of pancreatic β -cells. [38]
- 3) VPA may affect the sympathetic response to the glucose load. [39]
- 4) VPA metabolism may antagonize mitochondrial FA oxidation and therefore increase the levels of FFAs in the plasma, leading to an increase in glucose secretion by pancreatic β -cells. [40]

- 5) VPA may destruct insulin's signaling pathway, by inhibiting the expression of GLUT-1 mRNA, a transmembrane carrier protein associated with the aforementioned pathway. [41, 42]

With regards to the clinical image of the liver, VPA causes micro-vesicular steatosis. This type of steatosis is caused by the failing β -oxidation of the mitochondria. Following its conjugation with co-enzyme A (CoA) and the formation of valproyl-CoA, VPA enters the mitochondria. This leads to the inhibition of the mitochondrial FA oxidation, as VPA is oxidized into various products antagonizing the endogenous lipids for the oxidative enzymes. [43, 44] The first step in VPA's activation pathway involves its dehydrogenation by cytochrome P450 (CYP) 2C9 and CYP2A6 and the subsequent formation of 4-ene-valproate. This process activates an additional inhibitory mechanism for β -oxidation. *In-vivo* and *in-vitro* studies have shown that 4-ene-valproate is more steatogenic and cytotoxic than the parent drug. Following its formation, 4-ene-valproate is transformed into 2,4-dienylproyl-CoA, that can inactivate β -oxidation enzymes. [45, 46] VPA may also act as an anionic decongestant by transferring protons to the mitochondrial matrix. This may result in the inhibition of mitochondrial respiration and in the opening of the mitochondrial duct and thus, assisting an alternative VPA-induced cell death. [47] Only recently, a new mechanism that facilitates VPA-induced hepatic steatosis was proposed. In this mechanism, VPA-CoAs inhibit the action of Palmitoyl Carnitine Transferase 1, which carries FFAs into the mitochondria, resulting in a reduction of mitochondrial FFA uptake and a subsequent increase of the triglyceride input. [48]

In summary and regardless of the involved mechanism, VPA significantly increases body weight and hence, the likelihood for obesity, insulin resistance and the metabolic syndrome to occur. These account for NAFLD's main risk-factors, as well as for cardiovascular disease, dyslipidemia and diabetes.

1.1.8.4 Amiodarone (AMI)

Amiodarone (AMI) is a large amphiphilic, di-ionized derivative of benzofuran, a third-class antiarrhythmic drug that is used to treat abdominal and atrial arrhythmias. Long-term treatment with AMI is limited, due to a variety of extracardiac side-effects, such as pulmonary toxicity, cutaneous hyperpigmentation, thyroid dysfunction and liver failure due

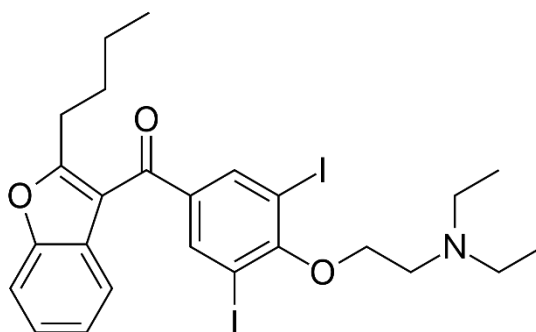


Figure 1.1.8.4.1: Amiodarone's chemical structure

to the inhibition of mitochondrial β -oxidation. Hepatic steatosis is usually induced in mice, at a dose of 150 mg per kg per day, over a period of 4 to 7 days. [49]

In its protonated form, AMI can easily migrate through the external mitochondrial membrane. Following its protonation, AMI diffuses through the internal mitochondrial membrane. Within the -relatively alkaline- mitochondrial matrix, AMI renounces its protonated state and causes a decrease to the membrane potential. Apart from this, AMI inhibits the Microsomal Triglyceride Transport Protein; the protein that carries triglycerides and assembles them into VLDLs and chylomicrons. [50]

In chronic treatment, asymptomatic elevations of transaminase levels, by up to three times the normal range, have been observed in 50% of patients, although recent studies conclude to a relatively reduced rate. The latency period varies from a few weeks to several years, while in more than 90% of the patients, it exceeds 90 days. Although liver injury is usually reversible, the levels of the hepatic enzymes take months to re-stabilize. Symptomatic liver impairment is reported in 1-3% of the patients receiving amiodarone. In these cases, both macro- and micro-vesicular steatosis comprise the most frequent pathological features. Steatohepatitis, cell "bloating", Mallory bodies and cirrhosis are also

common. Cases of micro-vesicular steatosis and hepatocellular necrosis that resemble the symptoms of Reye's syndrome have been observed. Approximately 18% of patients proceed to drug discontinuation due to the development of AMI-induced NAFLD or NASH. [49]

A number of mechanisms have been proposed to facilitate AMI-induced liver injury. Amiodarone, and its lipophilic metabolite, des-ethyl-amiodarone, are in high concentrations in the liver, associated more to the administered dose than to AMI's concentration in the plasma. The intrahepatic storage of Amiodarone may cause phospho-lipidation due to the increased influx of phospholipids. This process appears to be a systemic symptom for the cationic, amphiphilic substances, regardless of the presence of liver injury or steatohepatitis, and the result of phospholipase inhibition. [49]

In animal models, AMI-induced liver injury appears to be dose-dependent and proportional to the increased production of cholesterol, as well as to the accumulation of hepatocellular triglycerides. Research on mice revealed increased expression of several genes, with the androgen receptor and HNF4 α among them. This overexpression results in a rise of intrahepatic lipids. Furthermore, both PPAR- α and PPAR- γ appear to rise up, suggesting a sustained antagonism between the elevated lipid synthesis and the subsequent increase in FA oxidation. [51] An *in-vitro* exposure of HepRG hepatocytes to AMI, induced vesicular steatosis with a distinct accumulation of triglycerides, along with a concurrent overexpression of the lipogenic genes (SREBP1, FAS and ACL) and the formation of lipid droplets. [52]

Another important mechanism deriving from micro-vesicular liver injury is mitochondrial dysfunction. Amiodarone and its metabolite accumulate in the hepatic mitochondria and obstruct the Electron Transport Chain and Oxidative Phosphorylation. In animal models, AMI induces reduced mitochondrial β -oxidation leading to elevated ROS production. Hence, a reasonable explanation for liver injury could involve mitochondrial FA β -oxidation and the subsequent induction of micro-vesicular steatosis, apoptosis and necrosis. [53] Dronedarone, an amiodarone-like anti-arrhythmic drug, was proposed as an alternative for the treatment of atrial fibrillation and was alleged to be less hepatotoxic.

Nevertheless, Dronedarone seems to have the same inhibitory potential as AMI. Interestingly, dronedarone-treated mice inhibited mitochondrial β -oxidation, resulting from the reduced activity of Carnitine Palmitoyl Transferase I (CPT1), without affecting the respiratory chain, *ex-vivo*. [54]

1.1.8.5 Tetracyclines (TET)

Tetracyclines (TETs) are broad-spectrum antibiotics used to treat infections in humans and animals. Their efficiency lies in their activity against gram-positive and gram-negative bacteria, but also mycoplasma and chlamydia. Tetracyclines were among the first drugs found to induce micro-vesicular steatosis, that typically occurred within 4-10 days after high doses of intravenous administration. [55]

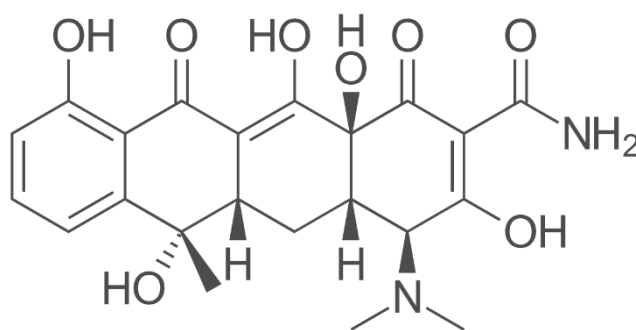


Figure 1.1.8.5.1: The chemical structure of Tetracyclines

Micro-vesicular steatosis has been observed in parenchymal hepatocytes, following the administration of tetracyclines, both in humans and rodents.

Although chemically induced steatosis is usually reversible, some dangerous forms may be lethal. The “Fatty Liver” was first described in 1951 on patients receiving high doses of tetracyclines, via intravenous or oral administration. [56]

TETs' cellular effects were initially monitored via liver biopsies or via the *in-vivo* exposure of isolated livers. Interestingly, the first findings regarding hepatic steatosis were extracted from TET-treated models. These models allowed for the investigation of key molecular pathways, with regards to lipid accumulation. For instance, the correlation between the intracellular overload of triglycerides and the limitation of mitochondrial β -oxidation was

examined by use of TET-models. [57] Since then, various *in-vitro* models have been used to decipher the biochemical basis of abnormal lipid accumulation. Today, the underlying mechanisms that result in the Fatty Liver are well documented. These mechanisms mainly concern the inhibition of FA oxidation and the secretion of lipoproteins. The fatty liver has also been attributed to the association between triglycerides and apoproteins, towards lipoprotein formation. [58]

Recent genomic studies have shown that many genes are involved in FA transport and the esterification of triglycerides. In the same context, an association between these genes and the induction of steatosis was established. Among them, the Fatty Acid Translocase (FAT) CD36 and the Diacyl-Glycerol Acyltransferase 2 (DGAT2) appeared to be the most important. Interestingly, their expression increased after the *in-vitro* exposure of HepG2 hepatocytes to TET solutions. In addition, TET negatively regulated the phosphorylation of the Extracellular Signal-Regulated Kinase (ERK) that, in turn, reduced DGAT2. [59]

1.1.8.6 Tamoxifen (TMX)

Tamoxifen is a selective estrogen receptor (SERM) and a golden standard for treating estrogen-related breast cancer. It acts both agonistically and antagonistically and executes both beneficial and harmful processes. In the breast tissue, it prevents the signaling of estrogen and thus, reduces the death rate of breast cancer.

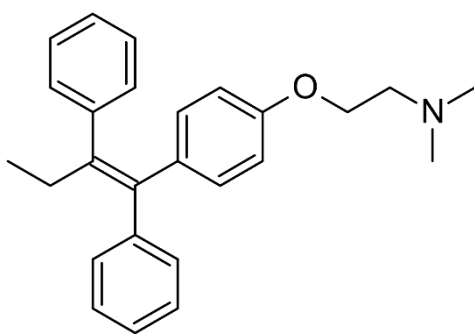


Figure 1.1.8.6.1: Tamoxifen's chemical structure

Another known side-effect of TMX is the induction of hepatic steatosis. It occurs as an increase in hepatic enzymes, observed in approximately 43% of the patients, and normalizes within 6 months after withdrawal. The most frequent findings include mild steatohepatitis, micro-vesicular steatosis and, in rare cases, cirrhosis. Factors associated with TMX-induced liver injury, include NAFLD's main risk factors plus glucose resistance, diabetes, hyperlipidemia and hypertension. [51]

Like AMI, TMX is an amphiphilic drug that becomes protonated inside the transmembrane space and deprotonates into the mitochondrial matrix, in order to move through the inner mitochondrial membrane. This loss of protons decouples during oxidative phosphorylation. TMX disrupts the Electron Transport Chain and limits the regeneration of important co-factors, such as NAD (Nicotinamide Adenine Dinucleotide) and FAD (Flavin Adenine Dinucleotide). [60]

The *in-vitro* exposure of HepG2 hepatocytes to TMX revealed significant hepatic steatosis and increased triglyceride accumulation in the cytoplasm. Assumptions on the underlying mechanism included an increase of FA biosynthesis, due to the positive regulation of SREBP-1c and the lipogenic genes. Additionally, the accumulating triglycerides increased the expression of the Microsomal Triglyceride Transfer Protein (MTP), which is associated with the assembly and secretion of VLDLs. Several *in-vivo* models back the aforementioned notion and suggest that de-novo FA biosynthesis is the main event leading to liver steatosis. [61]

The role of mitochondria is still in question. Studies on rodents have shown that TMX accumulates within the mitochondria, where it inhibits β -oxidation and cellular respiration, via the inhibition of CPT I -the enzyme that regulates the rate of β -oxidation- and topoisomerases, that both lead to the destruction of the mitochondrial DNA. [62] However, *in-vitro* studies on HepG2 hepatocytes revealed no association between CPT I and TMX. [61]. Likewise, other rodent models have shown that TMX does not influence tri-glycerol secretion or FA oxidation. [63] Oxidative stress seems to play a key role. In studies where TMX was administered to rat populations, exhaustion of hepatic glutathione

and accumulating oxidized glutathione, lipid peroxidation and inhibited hepatic activity of glutathione reductase (GR), superoxide dismutase (SOD) and CAT were observed. [64]

1.1.8.7 Methotrexate (MTX)

Methotrexate is used to treat rheumatoid arthritis, psoriasis, psoriatic arthritis, inflammatory bowel disease and Crohn's disease. It works by inhibiting the production of folic acid, a major regulator involved in RNA and DNA synthesis.

MTX enters the cell via the organic anion-transporting polypeptide (1B1) and inhibits the respiratory chain. Patients with obesity and diabetes are more likely to demonstrate hepatotoxicity with histological features that resemble NASH's. [65]

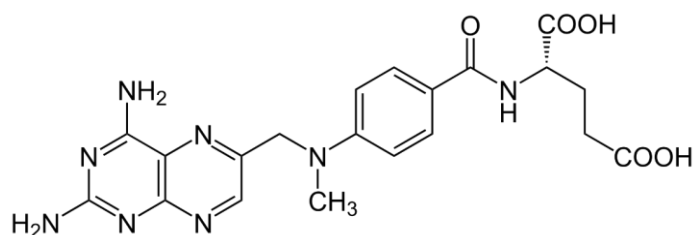


Figure 1.1.8.7.1: Methotrexate's chemical structure

1.2 COMPUTATIONAL BACKGROUND

1.2.1 Systems Biology

Systems Biology is a constantly developing branch of Biology that implements the idea of addressing the various biological phenomena based on Systems Theory. Systems Theory is used in many sciences and has a strong mathematical background. Thus, the collaboration between scientists of different fields and backgrounds, such as biology, physics, mathematics and computer science facilitate mathematical modeling towards the analysis of ecosystems, organisms and cells. In this context, the different approaches, deriving from the interdisciplinarity of each scientific sector, can be combined to create a new way of deciphering the complex functions of biological systems.

In the past few years, high-throughput technologies have been developed, which, unlike their predecessors, allow the measurement of multiple targets extracted from multiple samples; in a process characterized by high speed, performance, accuracy and sensitivity. Systems Biology can utilize these measurements via the use of mathematical theories and models. Thus, in an effort to provide substantial explanations to the function of each system of interest, new hypotheses may be formulated, and new theories may be discovered. [136]

The key concept implemented in Systems Theory includes the notion that each system consists not only of its interdependent parts, but also of the relationships involved between them. A typical example is that of gene expression. The independent study of a few genes may not provide substantial data on the condition of the organism, whereas the cumulative study over a large set of interdependent genes, along with the physiology of the organism, may lead to more secure conclusions. For example, the immune system of an organism cannot be adequately described by the concentration or activity of independent immunoglobulins, as its function cannot be considered the result of single underlying mechanisms or genes. According to Systems Biology, the immune system involves a set of complex interactions between numerous genes, protein complexes, metabolic mechanisms and external factors, the orchestration of which aims at dealing with various pathological conditions, including several diseases and infections. Thus, critical information for an adequate and representative prediction of an organism's response against the various pathogens and/or pathological factors may lie within the genome, or among the abundant intra- and extracellular proteins, or within the fusion of the aforementioned sources. [137]

Therefore, Systems Biology models biological entities, along with their interdependent functions, in networks, the structure and dynamics of which define the accuracy and validity of their resulting predictions. Thus, via selecting the appropriate inputs into the appropriate models, a prediction of the system's time-response can result. Systems Biology finds several applications, i.e. the development of disease-specific biomarkers for the prediction of the patients' response to various drugs.

1.2.2 Biological Networks

Biological Networks are networks associated with and a superset of various networking communities, formulated either between different organisms or between different functions facilitated by the organisms. [139] Biological Networks are met in all scales of life; from the “largest” macroscopic, such as ecosystems, to the “smallest” microscopic. Systems at the molecular level are particularly complex, due to the plethora of interactions involved. Even the simplest of organisms needs to regulate thousands of biochemical processes in order to express the appropriate genes, on time, to synthesize its vital metabolic products and to extract the energy that is necessary to sustain its existence and efficiently respond to stimuli. This vast array of cross-linked processes creates dense and complex networks.

In the pages to come, a summary of the major Biological Networks will be made. Their sharing feature is their composition, which, in all cases, involves molecules, genes, proteins and metabolites along with the interdependent interactions.

1.2.2.1 Regulatory Networks

Regulatory Networks are used to define the grid of functional transgenic interactions for the proper regulation of gene expression. These networks consist of genes or their corresponding post-translational proteins and their interactions, that represent their interdependent regulation [140]. In accordance to the Central Dogma of Biology, the extent of a gene’s expression is regulated by various transcription factors that are, in turn, regulated by the levels of protein transcription. Each transcription factor has the ability to identify and bind onto factor-specific, short DNA sequences, in order to positively or negatively regulate the transcription levels of the corresponding genes. Noteworthy, a transcription factor is able to regulate more than one gene, whereas a single gene can undergo the regulation of more than one transcription factors (gene expression). The Regulatory Networks consist of nodes and edges. Each of the nodes represents a gene or a transcription factor, while the internodal edges represent the interactions between the

nodes of interest. They may be directional, in the sense that they may also provide information on the type of the examined regulation, that is either inductive or repressive. In addition, Regulatory Networks may account the extent at which the regulation of interest defines an element's expression.

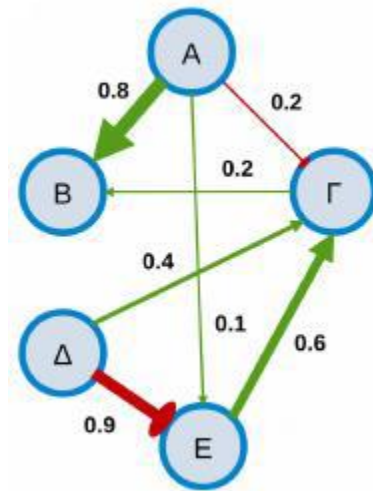


Figure 1.2.2.1.1: Example of Regulatory Network

In summary, Regulatory Networks are of crucial importance, as they depict the level of cellular function, that provides the framework for key cellular processes, such as cellular specialization, growth and response to environmental stimuli. Given these, the Regulatory Networks are dynamically transformable, that is altering the type of internodal interactions or the interaction altogether. Last but not least, Regulatory Networks are tightly linked with other types of Biological Networks, as they comprise a superset of the elements involved in them.

1.2.2.2 Metabolic Networks

Metabolic Networks are networks that consist of metabolic pathways or the sequences of biochemical reactions, associated to the cell's energy management. Their elements may lie within two discrete categories, the so-called bipartite. They consist of metabolites, namely the substrates and the products of the biochemical reactions, along with the corresponding catalytic enzymes. Thus, in Metabolic Networks, the nodes represent the

metabolites and enzymes, while the edges represent their relationship. [141] In *Figure 1.2.2.1*, each of the red nodes represent a metabolite, while each of the green nodes represent an enzyme. Thus, enzyme E1 acts on substrate S and induces the production of metabolite P. Directional networks are usually used, in order to distinguish the substrates from their products. In some cases, Metabolic Networks may be formed in a way that the depicted nodes correspond only the metabolites, thus a connection between them indicates the presence of a shared enzyme. This method is used only to simplify the network and to reduce the number of nodes.

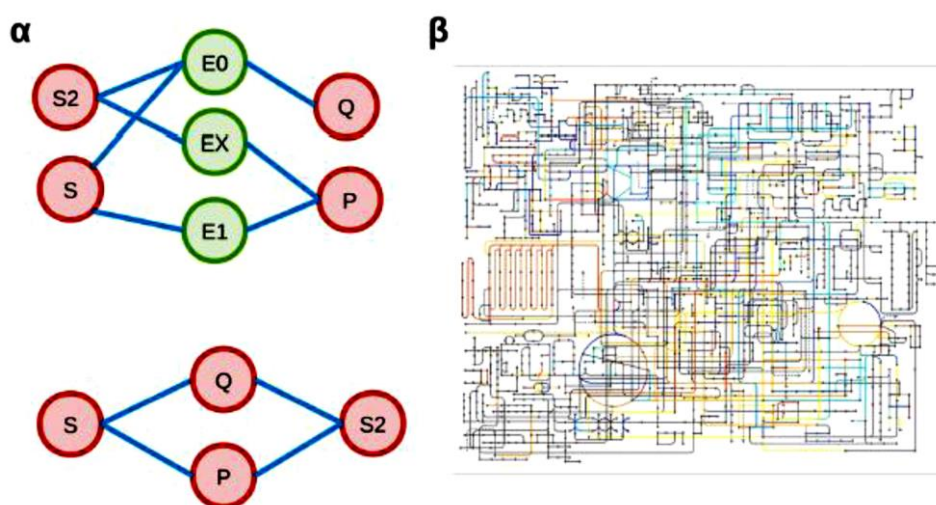


Figure 1.2.2.1: (a) Example of a Metabolic Network, (b) Portion of a human's metabolic reactions

1.2.2.3 Signaling Networks

Signaling Networks consist of the signaling pathways, facilitated in cellular signal transduction, and of the cellular signaling processes that are involved in either the activation or the suppression of proteins and enzymes. Their elements are -almost exclusively- proteins, whereas the internodal edges depict the relationships between them, corresponding to either inductive or repressive reactions that comprise the stages of signal transduction. Complex networks may be created, as each of the elements can simultaneously transmit information on multiple pathways. Each pathway typically uses an environmental stimulus -of the extracellular matrix to the corresponding ligand- as input, that in turn activates the appropriate transmembrane protein-receptors. Binding is followed by a chain of molecules and signaling reactions inside the cytoplasm that reaches

the corresponding nuclear transcription factors. [142] This induces a change in the intracellular concentrations of several signaling molecules, such as calcium or cyclic nucleotides. [143]

Although Signaling and Metabolic Networks bear significant resemblances, they are different in the type of information they provide and in the purpose they serve. The Signaling Networks are associated with data transduction via molecular signals, are extremely dynamic and their response times vary from milliseconds to several minutes or so. Furthermore, and despite a difficulty in comprehension, Signaling Pathways are crucial, especially in fields like molecular immunology. [144] On the other hand, Metabolic Networks are static and associated with the cell's energy management, that is energy production and consumption mechanisms. [145]

1.2.2.4 Networks of Protein Interactions

Strictly speaking, all of the aforementioned networks are networks that involve protein interactions. Thus, the term may describe networks difficult to define or comprehend, either regarding the nature or the variety of interactions. These are “mixed” networks of many different functional relationships interlinking the nodal proteins. [146]

However, the term may also refer to networks where the nature of interactions is clearly defined. These networks regard molecularly interlinked proteins that bind to create autonomous functional units, the protein complexes. Experimental identification of these links is profoundly demanding; therefore, it is not uncommon for these networks to involve heterogenous information. Their edges are non-directional, in spite of the interactions being transient in the sense of a complex altering a protein that in turn affects neighboring interactions. These kinds of interactions comprise the dynamic portion of the network. [143]

1.2.3 Pathway Analysis

Typically, genomic analyses involve the study of gene expression, that is the determination of differentially expressed genes (DEGs). DEGs may be over-expressed or under-expressed within the study condition (pathological samples) and when compared to the control (healthy samples). However, the identification of individual DEGs does not provide sufficient information about the underlying mechanism that is altered between the study and control conditions.

According to Systems Theory, genes do not act independently, but interact as parts of a network. Pathways are biological networks associated with a particular process of a cell or organism. For example, cellular endocytosis involves several pathways. The transition from the differential expression of genes to the differential expression of pathways is the key to adequately comprehend the phenomena that distinguish the study from the control. As the study condition usually reflects a disease, this kind of analysis offers an in-depth understanding of the pathology, in the sense that can identify the cellular processes that are associated with the condition. [147]

Furthermore, several diseases are associated with slight changes in gene expression that are difficult to identify, especially in the case of individual genes. However, when studying the pathway expression, several slightly over-expressed genes can cumulatively lead to the false perception of a pathway as differentially expressed. For example, in diabetes type II, no individual DEGs are identified. However, a gene set -involved in oxidative phosphorylation- exhibited coordinated reduction in diabetic patients. [148]

There are three different ways for the analysis of pathways, presented in *Figure 1.2.3.1*. The first, Over-Representation Analysis (ORA), uses DEGs and their belonging pathways as input. After calculating the amount of under- and over-expressed genes that belong to a certain pathway, pathways that exhibit the largest amounts of DEGs are given as the method's output. Nevertheless, ORA has several limitations. The method uses only a portion of the genes involved (only DEGs), while it does not count in the levels of differential expression. It also considers genes and pathways to act independently of each other.

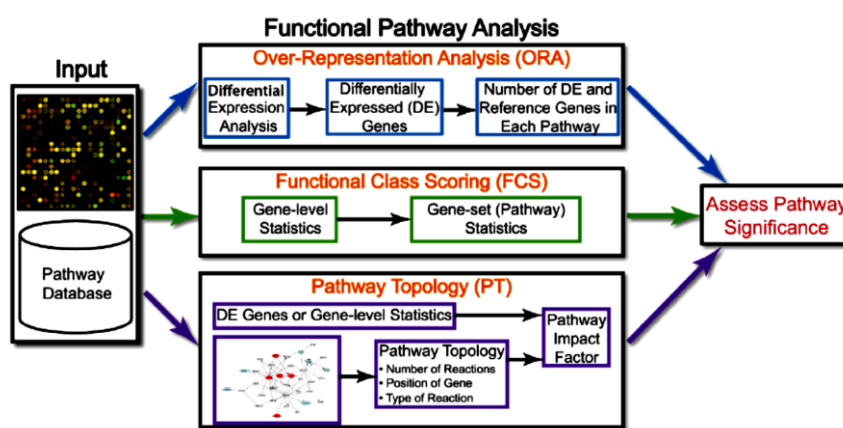


Figure 1.2.2.4.1: Methods of Pathway Analysis (Khatri et al.,2012)

The second method is the so-called Functional Class Scoring (FCS). This method uses gene-level analysis as input, in the sense that it takes in all the genes and their corresponding expression levels. A statistical analysis of the pathways is then performed. This analysis counts in the pathways' area and the transgenic correlations. FCS gives each of the pathways examined, a value, which corresponds to their statistical significance. However, FCS excludes the possibility of a gene being involved in more than one pathway and therefore, if a significant pathway contains a gene that is involved in also other, it is likely that these other pathways will be falsely named as statistically significant. Another limitation of FCS is that the method neglects the values of expression levels, except for the initial classification, thus resulting in significantly over- and under-expressed genes not being given the appropriate gravity. Fortunately, the latter may be tackled through the efficient selection of additional statistical analyses.

The third way involves Pathway Topology-Based Analysis (PT). PT follows the exact steps of FCS but counts in the pathways' topology, i.e. the ways their genes interact in changing conditions. PT's main limitations regard the actual topology of the pathways which is dependent on the cell type. In the vast majority of cases, this information is not adequately provided. The generalization and integration of this kind of information into databanks, are challenging for the current means of bioinformatics.

1.3 AIM OF THE PROJECT

Drug-induced liver injury (DILI) is defined as a liver injury caused by various medications, herbs, or other xenobiotics, leading to abnormalities in liver tests or liver dysfunction, with the reasonable exclusion of other etiologies.

Non-Alcoholic Fatty Liver Disease (NAFLD) is recognized as a leading cause of liver disease in the western world. It includes a spectrum of liver disorders that range from simple hepatic steatosis to Non-Alcoholic Steatohepatitis (NASH), liver cirrhosis and hepatocellular carcinoma (HCC).

The present project aims to the identification of potential steatogenic compounds, via network-based pathway analysis on NAFLD, and to the subsequent *in-vitro* verification of their steatogenic and hepatotoxic effects, in an effort to validate candidate DILI-inducing compounds.

2 MATERIALS AND METHODS

2.1 COMPUTATIONAL ANALYSIS

2.1.1 Gene Expression Omnibus (GEO)

GEO is a public functional genomics data repository, provided by the National Center for Biotechnology Information (NCBI). The majority of data derives from genomic analyses over various biological concepts, including disease, evolution, immunology, toxicology and metabolism. Each study provides its resulting data in the form of microarrays. [160]

At the initial stages of analysis, a selection of the data to be processed must be made. These data are extracted by means of search within the GEO repository. This search is performed by use of the term “NAFLD” and returns 628 corresponding datasets.

Information including the set’s title, summary, organization, references, author and sample number are extracted out of each dataset. Given these clues and based on the organization and summary of each resulting set, datasets of the Homo Sapiens species are selected. These datasets include both healthy individuals, that will be used as control, and patients with NAFLD.

2.1.2 Volcano Plot

For each sample, the dataset provides values of assayed concentrations that quantify intracellular gene expression. Subsequent calculations aim to determine the total number of DEGs. The measure that describes how much of a gene’s expression changes between the control and study conditions, is given as the logarithm of the study-over-control ratio:

$$\log_2[\text{FC}(g)] = \frac{E(g)_{\text{test}}}{E(g)_{\text{control}}}$$

Thus, zero is the relation’s neutral point, while positive ratios correspond to over-expression of the examined gene and negative ratios to under-expression. Interestingly,

when $\log_2FC=1$, in the study condition, a gene demonstrates two-times the expression of the control, whereas, when $\log_2FC=-1$, it demonstrates half the control's expression.

In order to evaluate the significance of these values and neglect apparently significant that occurred due to random variation, the dataset should undergo statistical testing. Therefore, a comparison between a pair of distributions -instead of values- must be made for each gene. Thus, each expression experiment should be conducted for at least three times [161] In this case, statistical testing is performed by use of Student's t-test. The null hypothesis regards the case of the distributions' mean values to be identical and attributes a corresponding t-value. The t-value in turn corresponds to the p-value. The smaller the p-value, the stronger the indication that the null hypothesis does not stand, i.e. the mean values of the two distributions are significantly different, meaning that the difference observed is of statistical significance and thus, the gene examined is differentially expressed.

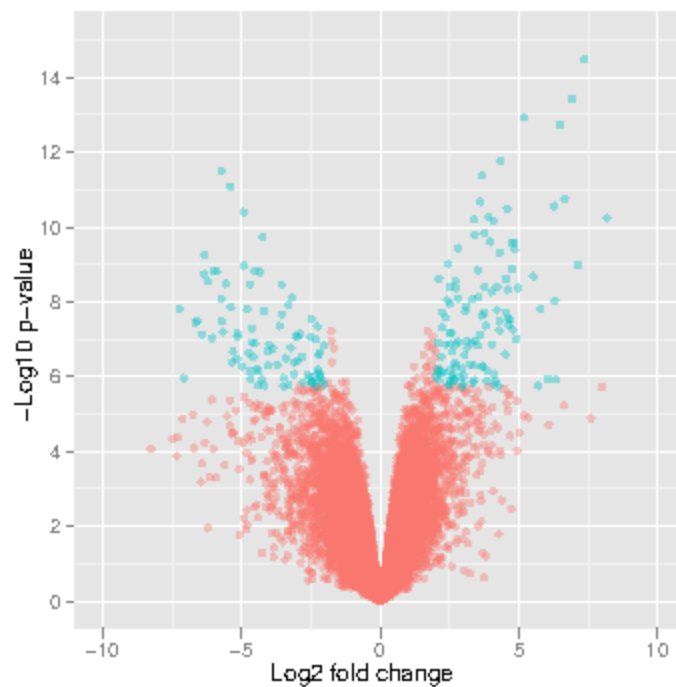


Figure 1.2.2.4.1: Example of a volcano plot

A volcano plot depicts the relation between these two values. Each point of the diagram corresponds to a specific gene. The x-axis attributes the value of \log_2FC , while the y-axis attributes the negative decimal logarithm of the p-value. Given these, the higher a gene stands with regards to the vertical axis, the more significant its differential expression may

be considered. Also, the more distant a DEG is from x-axis' zero point, the greater its intensity. Statistically significant differential expression is considered by use of the following thresholds: $|\log_2FC|>1$ and $p\text{-value}<0.05$.

2.1.3 Gene Level Statistics (GLS)

GLS is performed by use of a dedicated package of R-Bioconductor, named "Linear Models for Microarray and RNA-Seq Data" or Limma. [163]

For each gene a linear model is created by means of the following formula:

$$y_g = \beta_{g,0} + \beta_{g,1} \cdot x_{g,1} + \dots + \beta_{g,n} \cdot x_{g,n} + \epsilon_g$$

where:

y_g is the value of g-gene's expression; $\beta_{g,0}$ is the control's g-gene's expression; $\beta_{g,1}, \dots, \beta_{g,n}$ is the difference between g-gene's expression from samples (1, ..., 1-n) that is subtracted from the control's; $x_{g,1}, \dots, x_{g,n}$ are binary variables that determine whether the comparison includes the n-sample; ϵ_g is the calculation error

By eliminating ϵ_g , y_g is approximated by \hat{y}_g , while β -parameters are approximated by $\hat{\beta}_{g,1}, \dots, \hat{\beta}_{g,n}$ accordingly. The null hypothesis, H_0 , regards the case when the difference between the n-sample's g-gene's expression to the control's is zero, or $\hat{\beta}_{g,n} = 0$. As known from Linear Algebra, this vector can be calculated via the following formula:

$$\hat{\beta}_{g,n} = (X^T X)^{-1} X^T Y$$

where:

X is the array of $x_{g,0}, \dots, x_{g,n}$ variables, where each of its rows correspond to a gene and each of its columns correspond to a sample; Y is the vector of gene expressions

The standard error that derives from this calculation is determined as $se(\hat{\beta}_{g,n}) = \sqrt{s_g^2 \cdot (X^T X)^{-1}}$, where s_g^2 accounts for g-gene's variation and its corresponding significance test, from which the t-value is calculated for each of the genes, as of: $t = \hat{\beta}_{g,n} / se(\hat{\beta}_{g,n})$.

The aforementioned methodology involves one major issue. When the standard error reaches sufficiently small values, the method may deliver several false positives (FPs). This issue is tackled by use of hierarchical models that describe the changing β -coefficients and the variation s_g^2 as functions of the examined genes.

Specifically, initial categorization of the patients leads to the formation of three distinct groups: the Healthy, the NASH-patients and the Steatosis-patients. Then, by use of the aforementioned methodology, a linear model is created for each of the genes. However, only $x_{g,1}$ and $x_{g,2}$ terms receive a value, as instead of n single samples, the method uses the three formed groups of patients. Then, two contrasts are performed: one between Healthy and NASH-patients and one between Healthy and Steatosis-patients (Figure 2.1.3.1).

Levels	Contrasts	
	NASHvHealthy	stvHealthy
Healthy	-1	-1
NASH	1	0
Steatosis	0	1

Figure 1.2.2.4.1: Yielded contrasts between Healthy, NASH-patients and Steatosis-patients

Finally, empirical Bayes method attributes the necessary hyperparameters and the B-value, while a moderated t-test is also conducted. The analysis results in the parameters shown in Figure 2.1.3.2, demonstrated for each contrast and gene.

	LogFC	AveExpr	t	P.Value	adj.P.Val	B	TF
1	-3.979716	11.02524	-12.821248	3.202044e-19	2.222112e-15	33.23330	FOSB
2	-2.857281	10.13552	-8.021568	3.259439e-11	4.712379e-09	15.33726	IL6
3	-2.768875	12.93391	-10.355020	3.134180e-15	2.104854e-12	24.34196	FOS
4	2.706911	12.30086	8.700111	2.134833e-12	5.108631e-10	17.99350	CYP7A1
5	-2.687602	11.97376	-13.629670	1.856159e-20	1.932169e-16	35.97085	MYC
6	-2.632605	11.47382	-12.073915	4.796385e-18	1.426513e-14	30.62267	JUNB

Figure 1.2.2.4.2: Example of yielded results

2.1.4 Gene Set Analysis (GSA)

The analysis of pathways (Gene Set Analysis; GSA) is performed by use of another dedicated package of R-Bioconductor, named “Platform for Integrative Analysis of Omics Data” or Piano. [164] By using gene-sets, derived from the “Molecular Signatures Database” (MSigDB), and the GLS results, GSA is performed by means of nine distinct statistical methods:

- Fisher: The basic form of Fisher’s test evaluates the independency between two variables by calculating p-values for 2x2 affinity matrices. [166]
- Stouffer: Stouffer’s method is based on p-values and allows for the use of weight coefficients. [167]
- Reporter: The algorithm maps gene analysis into metabolic gene networks, via the identification of adjacent DEGs. It is based on Patil & Nielsen’s “Reporter Metabolites Algorithm” [168]
- Tail Strength: Assuming a null hypothesis that considers p_i p-values to be independent and identically distributed within the interval [0,1] and their comparative relations to be $p_1 \leq p_2 \leq \dots \leq p_m$, the Tail Strength test calculates a p-value’s deviation from its expected value and attributes it to a TS value. Positive TS values suggest that H_0 does not stand, meaning that small p-values were more than expected. TS attributes weight towards the smaller p-values and thus it is more sensitive to tail deviations. [169]
- Page: For each gene-set, this method (Parametric Analysis of Gene Enrichment Page) calculates Z-scores from the FoldChange (FC) values and, by means of the normal distribution, it attributes statistically significant gene-sets. [170]
- MaxMean: In this method, a mean value for the positively and negatively expressed genes is calculated. This calculation is performed in each gene of each gene-set and is followed by a selection of the gene-sets that return the greatest absolute expression value. [171]

- o Sum, Mean, Median: These methods calculate the Sum, Mean and Median values of each gene-set. Sum uses the t-value, while Mean and Median use the FoldChange (FC).

As none of these methods can be considered to be much better than the rest, a combination of outcomes, resulting from each of the nine aforementioned analyses, is performed in order for the prevailing trend to dominate (*Figure 2.1.4.1*). Thus, the statistical analysis of genes progresses into the statistical analysis of pathways. These pathways are classified into five discrete categories, according to their p-value:

- o Distinct Up: Over-expressed and under-expressed genes are mutually excluded, leading to a prevailing over-expression of the pathway.
- o Mixed Up: Over-expressed genes prevail by neglect of the under-expressed.
- o Non-Directional: The absolute value of the differential expression is used, meaning that its direction is not considered.
- o Mixed Down: Under-expressed genes prevail by neglect of the over-expressed.
- o Distinct Down: Over-expressed and under-expressed genes are mutually excluded, leading to a prevailing under-expression of the pathway.

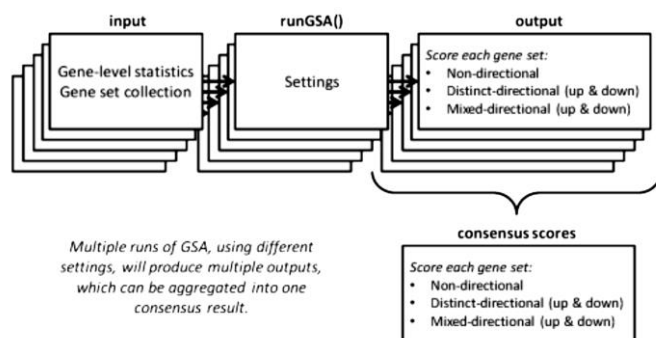


Figure 1.2.2.4.1: Consensus among different GSA methods

2.1.5 DrugBank

DrugBank is an online database for bioinformatics and chemoinformatics that combines detailed data of every pharmacological agent along with its molecular and genetic interactions. DrugBank's latest version contains 10,500 drugs, among which 1,737 approved small drug molecules, 870 food supplements and over 5,023 experimental drugs. In addition, DrugBank provides data on 4,772 drug-associated proteins, such as drug-

targets, enzymes, transporter and carrier complexes. For each drug, 50% of the provided information is dedicated to chemical data and another 50% to the drug targets [172].

2.1.6 Connectivity Map (cMap)

Connectivity Map (cMap) is an online bioinformatics tool and the product of Harvard university's collaboration with MIT. It contains a database of gene-signatures of several drugs, along with a dedicated tool for the identification of intra-signature similarities. The database consists of gene expression elements that are obtained by *in-situ* Oligonucleotide Microarrays technology. 1.309 bioactive molecules and drugs have been administered on 5 cancer cell-lines at different concentrations and in different durations. These cancer cell-lines are: leukemic cells (HL60), breast cancer cells (MCF7, ssMCF7), prostate cancer cells (PC3) and melanoma cells (SKMEL5). The treating concentrations are proximal to those successfully used in experimental *in-vitro* applications. In cases where prior knowledge on the treating concentrations is limited or insufficient, 10 μ M are used instead. Each treatment lasts for 6 and/or 12 hours in an effort to monitor the drugs' direct mechanisms of action. The bioactive molecules are called perturbagens, as their administration disrupts the normal cellular function and leads to the differential expression of several genes. A wide variety of substances may be considered as perturbagens, ranging from antibiotics to chemotherapeutic drugs and plant extracts. In each of the experiments, some of the cell microarrays are treated (treatment), while others are pseudo-treated (vehicle) and used as control. Thus, pairs of treatment-control are formulated. By use of a probe set, DEGs in treatment over control are listed. The list has over-expressed genes in its upper rows and under-expressed genes in its latter rows. Each experiment yields treatment instances that total 6.100 in number. Each of the instances is assigned an identification number and is characterized by its original experiment in terms of the used cell line, the name and the treating concentration of the drug and the scanning number of the microarrays, both treatment and control. As a result, a gene profile (gene signature) is created for each drug.

The intra-signature similarities are identified by cMap's dedicated tool that operates by means of a signature-question. This question, provided by the user, may be the gene signature of any disease or the gene signature of another drug. Contrasts are made via the Kolmogorov-Smirnov (K-S) statistical test, i.e. a non-parametric method that determines whether the distributions of two samples are statistically different. [173] In practice, the test is performed between the signature-question and similar/opposite gene signatures of the registered drugs. Each gene bears a signal at the signature-question that indicates whether it is over- or under-expressed. The comparison between the signature-question and the registered drugs is performed in the following way: if the question's over-expressed/under-expressed genes coincide with the upper/latter rows of a drug profile, the two substances share a similar gene signature; if the over-expressed genes coincide with the profile's latter rows (and vice versa), the two substance share an opposite gene signature. During this procedure, a value called the Enrichment Score (ES) is calculated. ES lies within the [-1,1] interval. ES's positive values correspond to a similar gene signature, while the negative ones correspond to an opposite gene signature. For each signature-question asked, a table of bioactive substances is produced (Figure 2.1.5.1).




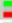

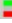
rank	cmap name	mean	n	enrichment	p	specificity	% non-null	
1	cefamandole	-0.633	4	-0.930	0.00002	0.0000	100	
2	glycopyrronium bromide	-0.608	5	-0.883	0.00006	0.0000	100	
3	cefoperazone	-0.589	3	-0.943	0.00028	0.0000	100	
4	meclocycline	-0.623	4	-0.872	0.00056	0.0000	100	
5	amiodarone	0.753	5	0.800	0.00078	0.0069	80	
6	sulfamethizole	-0.560	4	-0.833	0.00145	0.0000	100	

Figure 1.2.2.4.1: Table of bioactive compounds, yielded from cMap's dedicated tool

2.1.7 Methodology

As mentioned, datasets extracted from human samples (Homo Sapiens) are first selected from GEO repository. These datasets include three groups of samples: Healthy, NASH-patients and Steatosis-patients. Following the construction of the corresponding volcano plots, a second screening is made, based on the number of DEGs, as the greater the number the more adequate the information extracted.

The next step is to analyze the selected datasets. Following the bulk calculation of the number of DEGs, provided by the volcano plots, the goal of this step is to determine the

statistically significant pathways that are involved in the pathogenesis of NAFLD. Firstly, GLS is performed and followed by GSA. Note that for each dataset, this analysis is carried out separately.

Initially, raw data are extracted from the selected datasets and RMA normalization is performed. This method yields comparable distributions in cases where the original data do not follow the normal distributions. It is essentially based on the comparison of value ratings and thus, it is independent of moments, such as the mean value, the dispersion etc. [138] Raw data are organized in a single measurement per sample, for each transcription factor that corresponds to the gene of interest. Often are the cases where the exact same transcription factor corresponds to several genes or several transcription factors correspond to the same gene. The former factors are excluded from further analysis, whereas the latter are classified into mean-dependent groups. GLS is performed in the manner previously discussed and yields data for each contrast of each gene.

Then, GSA is performed for each dataset and contrast, with datasets being classified in five groups: Distinct up/down, Mixed up/down and Non-Directional. The twelve top-rated pathways are selected from each group. These pathways have the most significant NAFLD-associated differential expression and comprise Group 1.

The study is preceded by the creation of NAFLD-induction models of primary human hepatocytes and hepatocellular lines by means of five different pharmacological substances. These substances were carefully selected in order to relate to various induction mechanisms of the disease. What is crucial at this stage is to determine those pathways triggered by the steatogenic NAFLD-inducers.

Research over these steatogenic compounds in DrugBank yields relevant drug targets and drug-related carrier- and transport-protein-encoding genes. Then, via MSigDB, the corresponding pathways are listed for each of the yielded genes. These pathways comprise Group 2.

Then, by use of cMap's dedicated tool, similarities in the drugs' gene signatures are extracted. Known NAFLD-inducers -steatogenic compounds- are used as the signature-question. Each compound is inputted separately, along with the names of three cell lines (HL60, MCF7 and PC3) and the concentration that is most proximal to the experimental. From the yielded results, bioactive compounds that demonstrate significantly (p -value <0.05) similar ($ES>0$) or opposite ($ES<0$) expression are selected. Each of these yielded compounds are then searched on DrugBank and MSigDB in order to conclude on the pathways that they significantly affect. These pathways comprise Group 3.

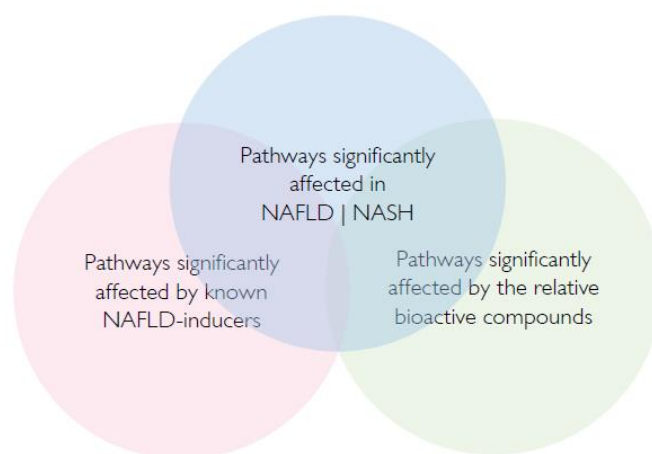


Figure 1.2.2.4.1: The intersection of the three groups contains potential steatogens

Since candidate NAFLD-inducing steatogenic compounds need to be sharing common pathways with the disease, they are extracted from the super-intersection of Groups 1, 2 and 3 (Figure 2.1.7.1). Out of these, three compounds (Pimozide, Clomiphene and Mefloquine) are selected for *in-vitro* verification.

2.2 IN-VITRO VERIFICATION

2.2.1 Cell lines

HepG2 is an immortalized cell line consisting of human liver carcinoma cells, derived from the liver tissue of a 15-year-old Caucasian male who had a well-differentiated hepatocellular carcinoma. Hepatocellular carcinoma is the fifth most-common cancer worldwide. The morphology of HepG2 cells is epithelial and contains 55 chromosome pairs. HepG2 cells can be grown successfully at a large scale, and secrete many plasma

proteins, such as transferrin, fibrinogen, plasminogen and albumin. They can be stimulated with human growth hormone. HepG2 cells are adherent, epithelial-like cells growing as monolayers and in small aggregates.

Originally thought to be a hepatocellular carcinoma cell line but shown to be from an hepatoblastoma (PubMed=19751877).

- Doubling time: ~50-60 hours (DSMZ)
- Disease: Hepatoblastoma (NCIt: C3728)
- Species of origin: Homo sapiens (Human)
- Sex: Male
- Category: Cancer cell line

The human hepatocellular carcinoma cell line (FOCUS—Friendship of China and United States) was derived from a patient with primary hepatocellular carcinoma. This cell line has been in continuous culture over an 18-mo period. The morphological and ultrastructural features of FOCUS are consistent with its neoplastic hepatocellular origin. FOCUS cells contain aspartate aminotransferase and glucose-6-phosphatase activity. In addition, α 1-antitrypsin, fibrinogen, alpha fetoprotein, and carcinoembryonic antigens were detectable in the cytoplasm of the cultured cells, by immunochemical staining techniques. The karyotype of the FOCUS cell is human in origin and it contains human DNA sequences as detected by molecular hybridization analysis. The FOCUS cells do not show evidence of density-dependent inhibition of growth under confluent conditions. Repeated growth curves over an 18-mo period were identical, revealing a doubling time of 42 to 48 h. The malignant potential of FOCUS cells was further demonstrated by their ability to lead to gross tumor formation after subcutaneous infection into nude mice. From one of the solid tumors grown in nude mice, re-cultured cell lines have been established and found to have properties identical to the original FOCUS cell line. This FOCUS cell line represents an additional model for further investigation of tumor specific antigens and the relationship between hepatitis B virus (HBV) and hepatocellular carcinoma. Preliminary

molecular characterization has indicated the existence of integrated HBV sequences within the FOCUS genome.

- Doubling time: 42-48 hours (PubMed=6086498)
- Disease: Hepatocellular carcinoma (NCIt: C3099)
- Species of origin: Homo sapiens (Human)
- Sex: Male
- Category: Cancer cell line

HUH7 is a well differentiated hepatocyte-derived cellular carcinoma cell line that was originally taken from a liver tumor in a 57-year-old Japanese male in 1982. The line was established by Nakabayshi, H. and Sato, J. The HUH7 cell line is an immortal cell line of epithelial-like, tumorigenic cells. These cells are adherent to the surface of flasks or plates and typically grow as 2D monolayers. Although containing many mutations and INDELS, it is worthy to note the HUH7 cells have a point mutation in the p53 gene.

- Doubling time: 24 hours
- Disease: Hepatocellular carcinoma (NCIt: C3099)
- Species of origin: Homo sapiens (Human)
- Sex: Male
- Category: Cancer cell line

Hep3B is hepatocellular carcinoma cell line, derived from an 8-year-old male. Cells contain integrated Hepatitis B virus genome. However, there is currently no evidence that this cell line produces infectious Hepatitis B virus. The cells should be handled under laboratory containment level 2. Ethnicity: Black. P53 null.

- Doubling time: ~40-50 hours (DSMZ).
- Disease: Hepatocellular carcinoma (NCIt: C3099)
- Species of origin: Homo sapiens (Human)
- Sex of cell: Male

- Category: Cancer cell line

2.2.2 Cell Culture

All hepatic cell lines are cultured in Dulbecco's Modified Eagles Medium (DMEM) High Glucose, with the addition of 10% v/v Fetal Bovine Serum (FBS; FB-1001/500) and 1% v/v of Penicillin/Streptomycin, provided by BIOSERA, France. The cultures are incubated at 37°C, 5.0% CO₂ and 90% humidity.

Upon sufficient confluency, all cell lines are seeded on 96-well plates, (Corning® Costar®, 3599) at corresponding densities:

- HuH7: 15000 cells per 100µl of medium per well
- Hep3B: 15000 cells per 100µl of medium per well
- HepG2: 20000 cells per 100µl of medium per well
- FOCUS: 15000 cells per 100µl of medium per well

2.2.3 Steatosis Induction

2.2.3.1 Serum Concentration or Determining the Healthy Hepatocyte

Numerous studies have now documented significant elevations in fasting lipogenesis, especially in cases of obesity, insulin resistance and diabetes. However, in order to determine the steatogenic effects of candidate NAFLD-inducing compounds, a prior health condition of the hepatocytes should be assured. Short-term fasting hepatocytes tend to over-express the lipogenic pathways, thus leading to a seemingly fatty phenotype even prior to the administration of steatogenic compounds. In this context, the *in-vitro* verification of candidate steatogens cannot be conclusive, as the prior health condition is violated. On the other hand, cells growing in serum exhibit the issue of the administered drug binding to the serum proteins, instead of the cellular. In order to eliminate this possibility, serum-free cultures should be the case, while dosing solutions should be made in the absence of serum.

Therefore, a consensus in the serum's concentrations should be reached in order to accommodate both these limitations: on one hand, as little serum to not interfere with the drugs administered, and on the other hand, as much to suppress DNL and maintain the prior health condition of the hepatocytes.

Hepatocellular fasting and the medium's proteinic component -that may interfere with the drugs' binding- is attributed mainly to the addition of Fetal Bovine Serum (FBS). Given this, the aforementioned consensus eventually regards the FBS concentrations in the culture medium. Thus, an FBS-concentration threshold that satisfies both the restrictions should be determined.

In order to do so, HUH7 cell line is introduced to medium of different FBS concentrations (0% v/v, 1% v/v, 2% v/v, 4% v/v, 5% v/v, 6% v/v, 7% v/v, 8% v/v, 9% v/v and 10% v/v). Fat levels are reviewed within 24h of treatment.

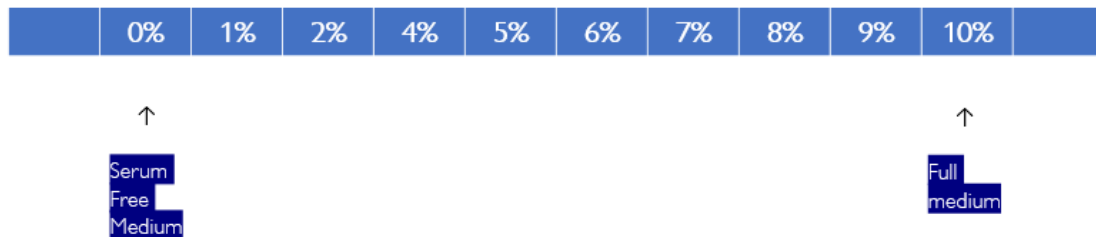


Figure 2.2.3.1.1: FBS experimental design

2.2.3.2 NAFLD induction

NAFLD induction is performed by exposing the cells to treatments of known NAFLD-inducing compounds. These are:

- Oleic & Palmitic Acid (Cayman Chemicals; 90260, 10006627)
- Tamoxifen Citrate (Cayman Chemicals; 11629)
- Amiodarone Citrate (Cayman Chemicals; 15213)
- Tetracycline Hydrochloride (Cayman Chemicals; 14328)
- Valproic Acid Sodium Salt (Cayman Chemicals; 13033)

The fatty acids, approximated by a mixture of oleic and palmitic acid in a molar ratio of 1:2 palmitic: oleic, are dissolved in 100% ethanol at 90°C and in accordance to the manufacturer's instructions.

The pharmacological NAFLD-inducers (TMX, AMI and TET) are diluted in DMSO according to the manufacturer's instructions. Valproic Acid is diluted in 100% ethanol at 90°C and in accordance to the manufacturer's instructions.

The cells are exposed to the following concentrations for 24h, in 0.1% v/v DMSO and 1.0% v/v etOH to the medium: TMX 8µM, AMI 20µM, TET 150µM, VPA 6mM.

2.2.3.3 FFA-induced Steatosis or Defining the Fatty Hepatocyte

With the healthy hepatocyte being determined, the fatty phenotype should be concluded. Normally, hepatocytes have a capacity to accommodate the excessive amounts of extracellular FFAs, either by facilitating them in β -oxidation or by regulating triglyceride biosynthesis. Above a threshold though, hepatocytes are unable to accommodate the excess and thus, fat, in the form of extracellular FFAs, accumulates.

This threshold may be determined by the exposure of FOCUS hepatocytes to various increasing FFA concentrations (100µM, 200µM, 400µM, 500µM, 600µM, 700µM, 800µM and 1000µM). The fatty acids, approximated by a mixture of oleic and palmitic acid in a molar ratio of 1:2 palmitic: oleic, are dissolved in 100% ethanol at 90°C and in accordance to the manufacturer's instructions. Fat levels are reviewed within 24h and 48h of treatment. A bulk determination of FFAs threshold concentration is then made.



Figure 2.2.3.3.1: FFA steatosis-induction experimental design

2.2.3.4 Resazurin Viability Assay

For the computationally yielded candidate steatogens, the *in-vitro* verification must be performed at appropriate dosing concentrations. These concentrations should assure that 90% of the treated hepatocytes should remain alive and are named EC90 or IC10.

For the IC10 determination, dose-response curves should be constructed for each agent and cell line. The data from which the curves originate, are determined by means of the Resazurin Viability Assay.

Resazurin is a cell-permeable redox cell marker that is used to measure the number of viable cells. It can be dissolved in physiological solvents (e.g. PBS) to form a dark blue solution that is added directly to the cell cultures in a homogeneous manner. Living cells with active metabolism can reduce resazurin into the pink and fluorescent resorufin (Figure 2.2.3.4.1).

The addition of an intermediate electron-donor is not necessary to for the reaction to occur, but it could accelerate its pace. The amount of resorufin produced is proportional to the number of viable cells and quantitated by fluorescence measurement at a 560nm excitation wavelength and an emission wavelength of 590nm. Quantification may also be performed by means of the optical absorption measurement, but at a much less sensitivity.

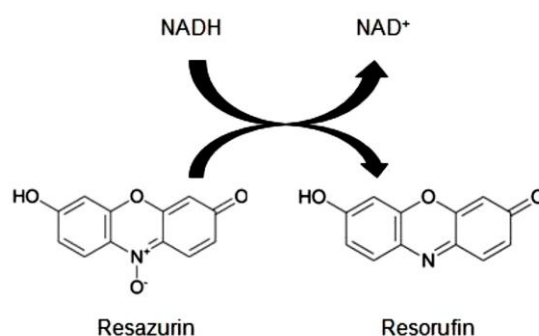


Figure 2.2.3.4.1: Resazurin is reduced to Resorufin according to the cell's metabolic activity

The incubation time required to produce a sufficient fluorescent signal is usually 1-4 hours and depends on the metabolic activity of each cell type, cell density and culture conditions, such as the culture medium. The incubation time should therefore be

experimentally determined and be small enough to avoid reagent toxicity but large enough to be sufficient for the sensitivity of the method. Also, further reduction of resorufin leads to formation of hydro-resorufin, which is colorless and non-fluorescent, and can therefore lead to erroneous results (Figure 2.2.3.4.2).

In the present study, Resazurin sodium salt (SIGMA; R7017) is first dissolved in Dulbecco's Phosphate Buffered Saline, pH 7.4, (Biosera; PM-B2092), and further diluted into fresh medium prior to each experiment. After the 24-hour exposure of the cells to the inducing substances, the medium is replaced and Resazurin is added at 60 μ g/mL concentration. After a 2-hour incubation at 37°C, 5.0% CO₂ and 90% humidity conditions, Resazurin's fluorescence at Ex560nm/Em590nm wavelengths is measured by use of VarioSkan™ LUX multimode microplate reader (Thermo Scientific™). Cell viability is expressed as the percentage of the cells exposed to the NAFLD-inducers to the non-exposed. [135] This method is used to construct a dose-survival curve for the NAFLD-inducing substances, in order to determine the dosing concentrations that do not reduce viability below 90%.

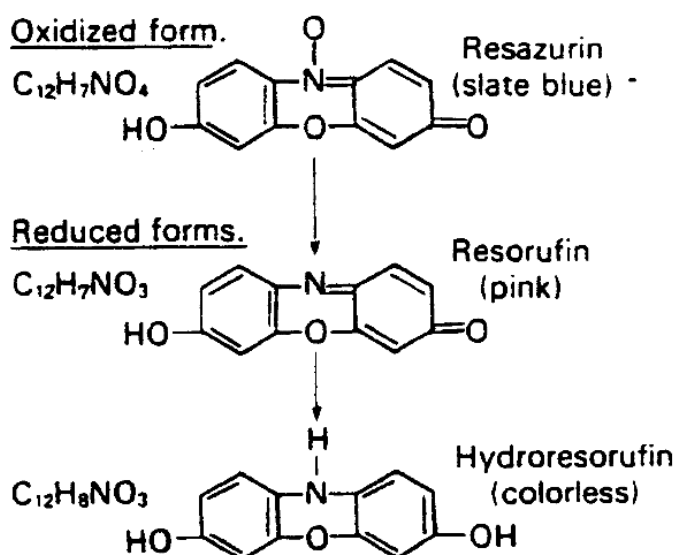


Figure 2.2.3.4.2: Further reduction of resorufin leads to formation of hydro-resorufin

2.2.3.5 Reactive-Oxygen Species (ROS) Production Measurement

Intracellular production of Reactive Oxygen Species (ROS) is measured by means of the cell-permeable, fluorescent CM-H₂DCFDA substrate (ThermoFisher Scientific; C6827). CM-H₂DCFDA is passively transported inside the cells, where acetate groups are cleaved by intracellular esterases. Thio-active chloromethyl groups react with the intracellular glutathione and other thiols. Subsequent oxidation generates the fluorescent 2', 7'-dichlorofluorescein (DCF) product that is trapped inside the cell (Figure 2.2.3.5.1). DCFDA's fluorescence can be measured at an excitation wavelength of 492-495nm and an emission wavelength of 517-527nm.

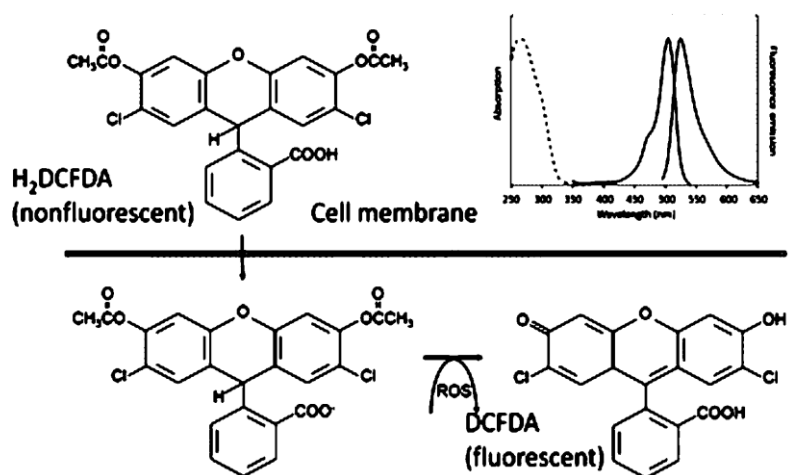


Figure 2.2.3.5.1: Overview of CM-H₂DCFDA intracellular reactions

Following the 24-hour exposure of the cells to the inducing compounds, the medium is removed, and the cells are washed with PBS. The cells are then exposed to 10 μ M of PBS-dissolved CM-H₂DCFDA and incubated for 15 minutes at 37°C, 5.0% CO₂ and 90% humidity conditions. Fluorescence is then measured at Ex494nm/Em520nm by use of VarioSkan™ LUX multimode microplate reader (Thermo Scientific™). Fluorescence needs to be normalized by the total protein concentration of the sample, that is determined via the BCA method and expressed in RFU/ μ g protein.

Considering the antioxidant role of albumin, albumin levels are maintained in all samples. Cells exposed to 400 μ M of H₂O₂ for 30 minutes comprised the experiments positive controls for ROS production. The optimal concentration of H₂O₂ was determined through

dose-viability curves, where a concentration, that did not affect the cells' viability, was selected.

2.2.3.6 High Content Screening of Lipid Droplets

Intracellular fat load is determined by fluorescent microscopy. Lipid droplets are stained with Nile Red (Thermo Fisher Scientific; N1142), a red fluorescent dye, while the counterstaining of the cells' nuclei is performed by use of Hoechst 33342 (Thermo Fisher Scientific; H3570) blue fluorescent probe.

Nile Red is used to identify and quantify lipids, and intracellular neutral lipid droplets in particular. It is almost non-fluorescent in water and other polar solvents, but it fluoresces in non-polar environments at an 552nm excitation wavelength and an emission wavelength of 636nm (Figure 2.2.3.6.1).

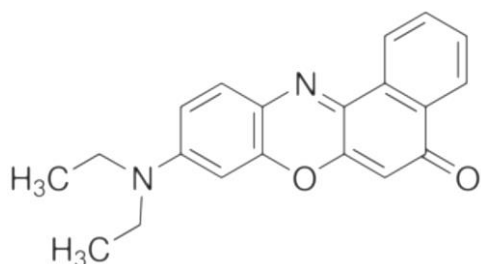


Figure 2.2.3.6.1: Nile Red's chemical structure

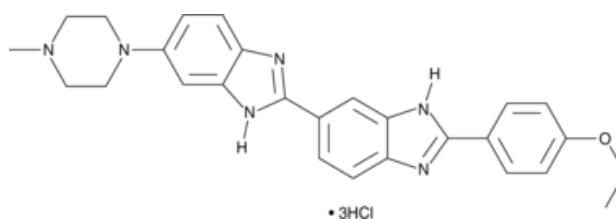


Figure 2.2.3.6.2: Hoechst's chemical structure

Hoechst 33342 is a cell-permeable pigment that emits blue fluorescence when bound to dsDNA Ex392nm/Em440nm (Figure 2.2.3.6.2).

Following the 24-hour exposure of the cells to the inducing compounds, the medium is removed, and the cells are washed with PBS. The cells are then exposed to a staining solution, consisting of Nile Red 2µg/mL and Hoechst 33342 5µg mL and dissolved in fresh medium. After incubated for 45 minutes at 37°C, 5.0% CO₂ and 90% humidity conditions, the stained medium is again removed, the cells are washed with PBS and fresh medium is added. Automatic image acquisition is then performed by using the JuLI™ Stage Real-Time ChR (NanoEnTek), in 20x magnification of channels DAPI (Excitation 390/40, Emission 452/45) and RFP (Excitation 525/50, Emission 580).

RFP (corresponding to Nile Red) and DAPI (corresponding to Hoechst 33342) intensities are quantified through a procedure similar to the Viability Assay's, and by use of VarioSkan™ LUX multimode microplate reader (Thermo Scientific™).

Finally, the ratio RFP Intensity / DAPI Intensity is calculated for each of the samples. Statistical processing is then performed by use of the GraphPad Prism 6.0 software.

2.2.3.7 Cell Lysis – Protein Isolation

Cell lysis often refers to the breakdown of the cellular membrane, performed primarily by viruses, enzymes or osmotic mechanisms. In the present study, cell lysis is achieved by means of a detergent solution, the Lysis Buffer (ProtaVio Ltd). Proteins are the product of cell lysis. In order to protect proteins from the intracellular proteases, protease inhibitors (PIs) are introduced to the buffer, along with the Phenyl-methane-sulfonyl fluoride (PMSF; SIGMA; P4626) serine-protease-inhibitor.

Following the 24-hour exposure of the cells to the inducing compounds, the medium is removed, and the cells are washed with PBS. Lysis buffer, PMSF and PIs are then added to the cells which are then incubated at -80°C for 1 hour. After incubation, the samples are sonicated and centrifuged in order to isolate the protein-containing supernatant. Low temperature and ultrasound treatment contribute to the effective breakdown of the cellular membranes.

2.2.3.8 BCA Method for measuring Total Protein Concentration

The Bicinchonic Acid or BCA method is a biochemical method for measuring the total protein concentration in a solution and is similar to the Lowry and Bradford methods. The principle relies on the use of BCA as a Cu^+ detection reagent, formed when Cu^{2+} is reduced by the proteins of an alkaline environment (biuret reaction). The purple product of this reaction is produced by the chelation of two BCA molecules with a copper Cu^+ ion (Figure 2.2.3.8.1).

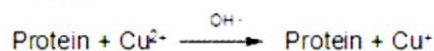
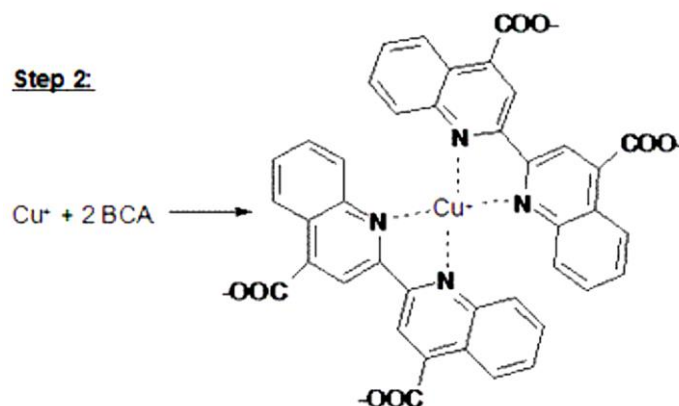
Step 1:**Step 2:**

Figure 2.2.3.8.1: The purple product of this reaction is produced by the chelation of two BCA molecules with a copper Cu^+ ion

This chromogenic compound exhibits high optical absorbance at a wavelength of 562nm, which in turn exhibits linearity with increasing protein concentrations ranging between 20 and 2000 $\mu\text{g/mL}$. The color generated is due to the macromolecular structure of the protein, the number of peptide bonds and the presence of four specific amino acids (cysteine, cystine, tryptophan, tyrosine). In the BCA method, the reaction does not reach an end point, i.e. the color continues to develop. However, after a specific incubation time, the pace of color-generation slows substantially, therefore not allowing the concurrent determination for several samples.

Total protein concentration is determined on the basis of a commonly known standard protein, such as Bovine Serum Albumin (BSA), of known concentration. A series of dilutions of a known protein concentration is prepared and placed in the unknown concentration that can now be determined by means of a standard curve.

An alternative method to BCA, is the Micro BCA that exhibits greater sensitivity (it has the ability to detect lower concentrations) but has a smaller dynamic range. In particular, Micro BCA is optimized to detect protein concentrations in the range of 0.5-20 $\mu\text{g/mL}$.

For the purposes of the present study, the Pierce TM BCA Protein Assay Kit (Thermo Fisher Scientific; 23225) and the Micro BCA TM Protein Assay Kit (Thermo Fisher Scientific; 23235) are used.

2.2.3.9 Methodology

Day 0: Cell seeding on 96-well plates

- HuH7: 15000 cells/100µl medium/well
- Hep3B: 15000 cells/100µl medium/well
- HepG2: 20000 cells/100µl medium/well
- FOCUS: 15000 cells/100µl medium/well

Day 1: Compound Treatment

- Positive Control: Free Fatty Acid (FFA) mix of Oleic Acid : Palmitic Acid (2:1 molar ratio) diluted in etOH absolute
- Final Concentration: 200uM; 1% v/v
- Valproic acid (VPA), diluted in etOH absolute; 1% v/v
- Amiodarone (AMI), Tamoxifen (TMX), Tetracycline (TET) diluted in DMSO at 0.1% v/v
- Steatogenic compounds: Mefloquine (MEF), Clomifene (CLO), Pimozide (PIM) in DMSO at 0.1% v/v
- Negative Control: DMEM, etOH at 1% v/v, DMSO at 0.1% v/v

Day 2: Additional Experiments

1. Verification of lipid droplet formation using high content screening. Nile Red for staining lipids, Hoechst 33342 for counterstaining nuclei, JuLiStage
2. Resazurin cell viability assay – Construction of IC curves
3. ROS Production using fluorescent probe CM-H2DCFDA

3 RESULTS

3.1 COMPUTATIONAL ANALYSIS

3.1.1 GEO Microarrays

GEO yields several microarrays, from which four are selected. This selection is made on the basis of two major criteria. Firstly, the microarray should concern data extracted from human samples (*Homo Sapiens* sp.) and secondly, each microarray should contain data from both healthy and NAFLD-patients. The main features of the selected microarrays are shown in the following table (*Table 3.1.1.1*):

# GEO	Author	Healthy Samples	Patients Samples	Type of Sample	NAFLD Stage
GSE48452	Jochen, H. et al.	14	59	Liver Biopsy	Healthy obese, NASH, Steatosis
GSE63067	Frades, I.	8	11	Liver Biopsy	NASH, Steatosis
GSE72756	Chuanzheng, S. et al.	5	5	Liver Biopsy	NAFLD
GSE89632	Allard, JP. et al.	24	39	Liver Biopsy	NASH, Steatosis

Table 3.1.1.1: Datasets extracted from GEO

3.1.2 Selection of Datasets

Each dataset extracted, yields a corresponding Volcano Plot that is shown below:

GSE48452

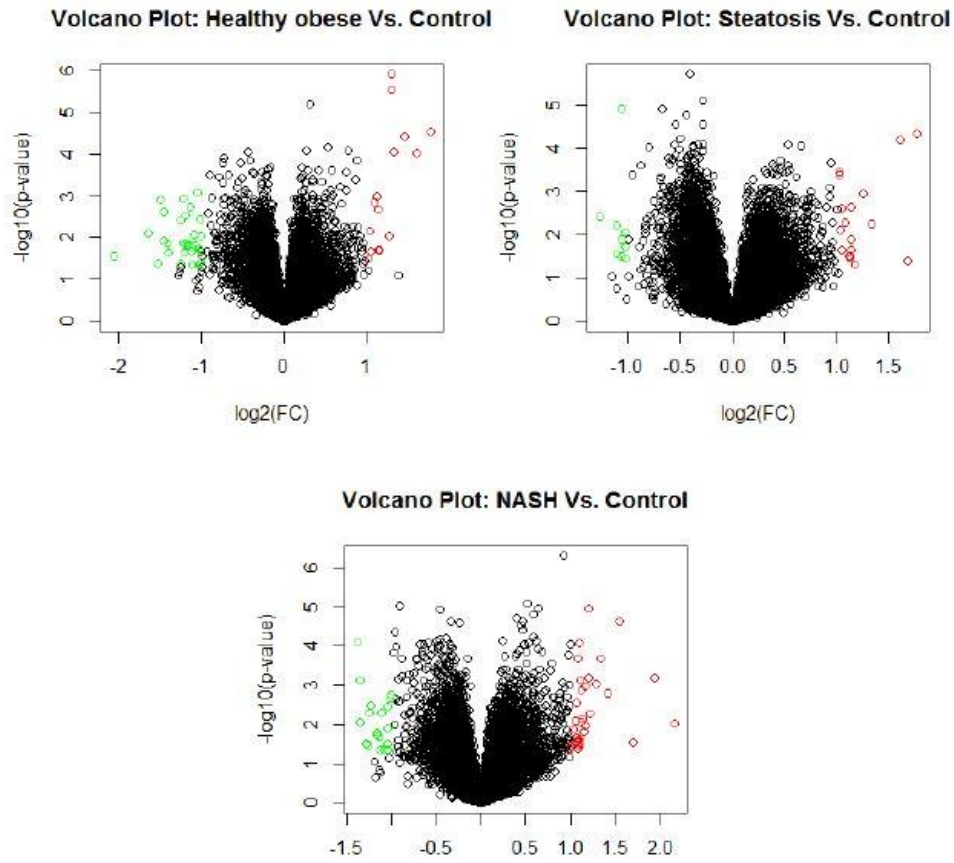


Figure 3.1.2.1: Volcano Plots extracted from GSE48452 dataset; Contrasts between Healthy Obese, Steatosis and NASH

GSE63067

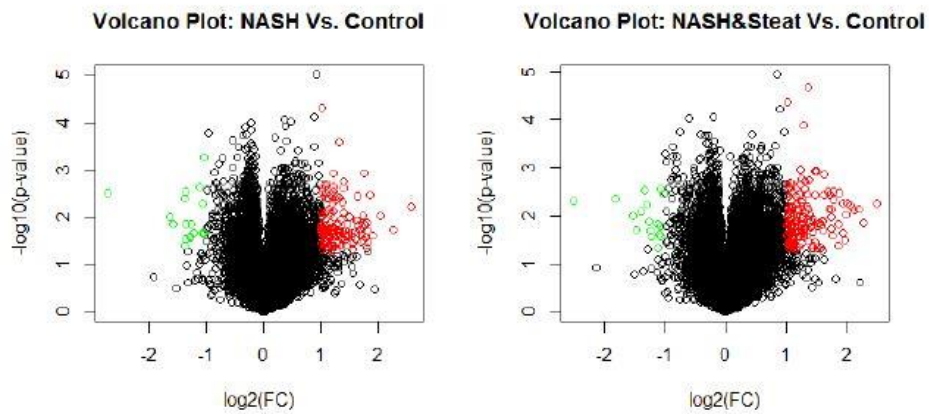


Figure 3.1.2.2: Volcano Plots extracted from GSE63067

GSE72756

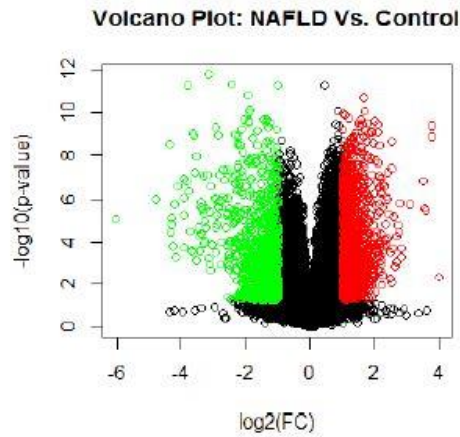


Figure 3.1.2.3: Volcano Plot extracted from GSE72756

GSE89632

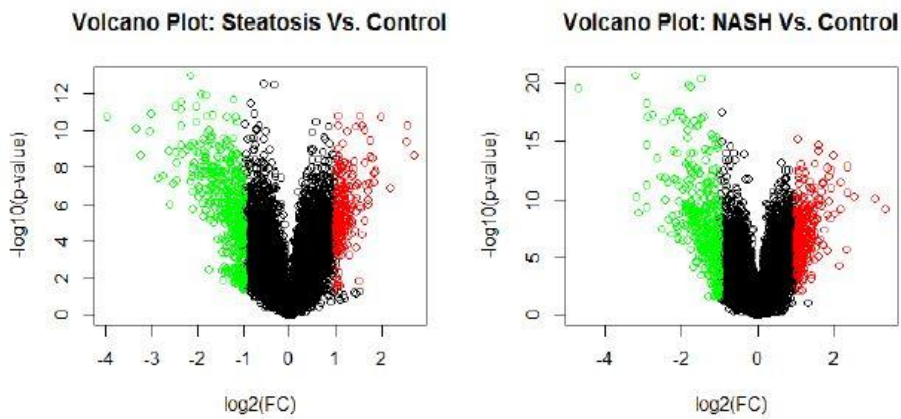


Figure 3.1.2.4: Volcano Plots extracted from GSE89632

From these, GSE63067 and GSE89632 are selected, mainly due to the greater sample number and also due to the amount of DEGs discovered.

GSE48542 and GSE72756 do not possess either the appropriate number of samples, for the results to be adequately reliable, or a sufficient number of differentially expressed genes.

3.1.3 Gene Level Statistics (GLS)

Following GLS analysis, the yielded results regarding the DEGs of each of the selected datasets, are shown in the Volcano Plots that follow:

GSE63067

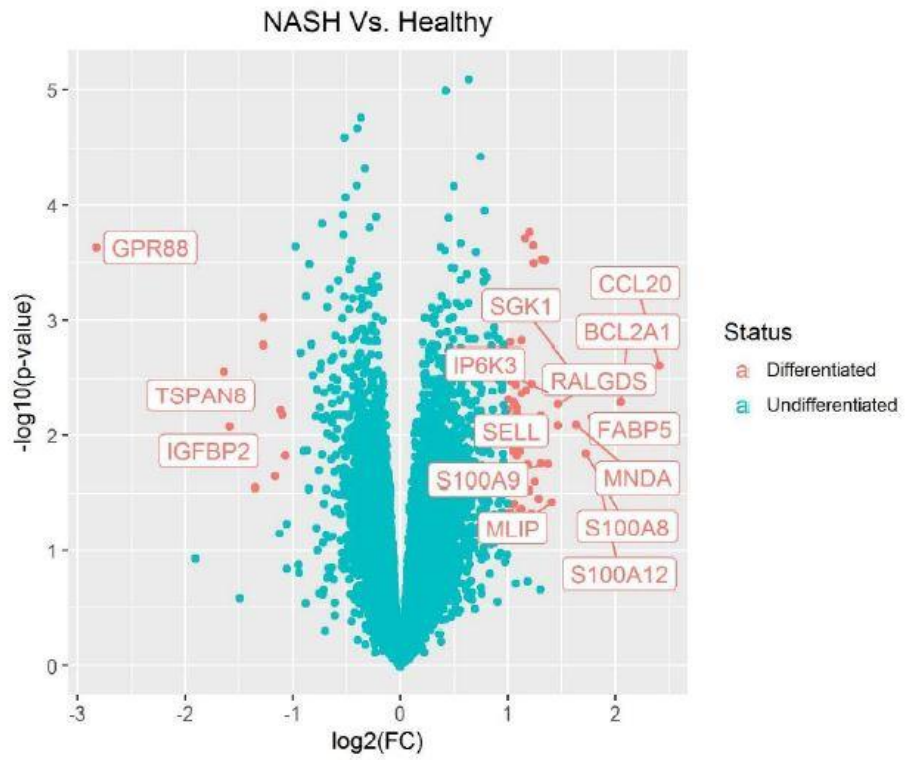


Figure 2.2.3.9.1: NASH vs Healthy | Volcano Plot with marked DEGs, extracted from GSE63067

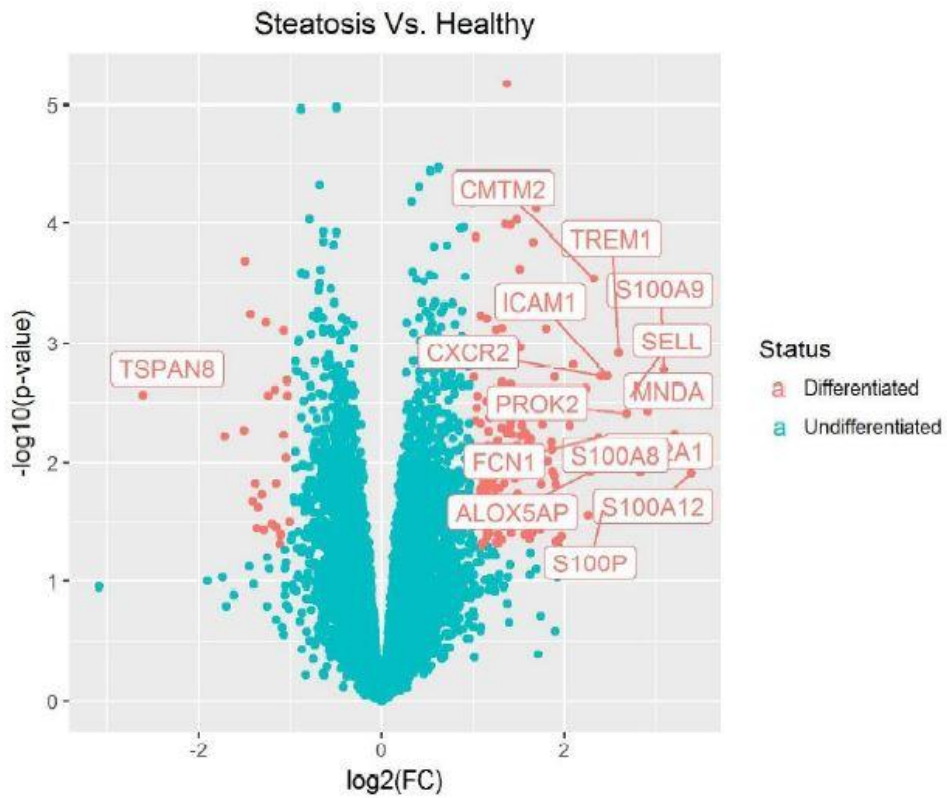


Figure 3.1.3.2: Steatosis vs Healthy | Volcano Plot with marked DEGs, extracted from GSE63067

GSE89632

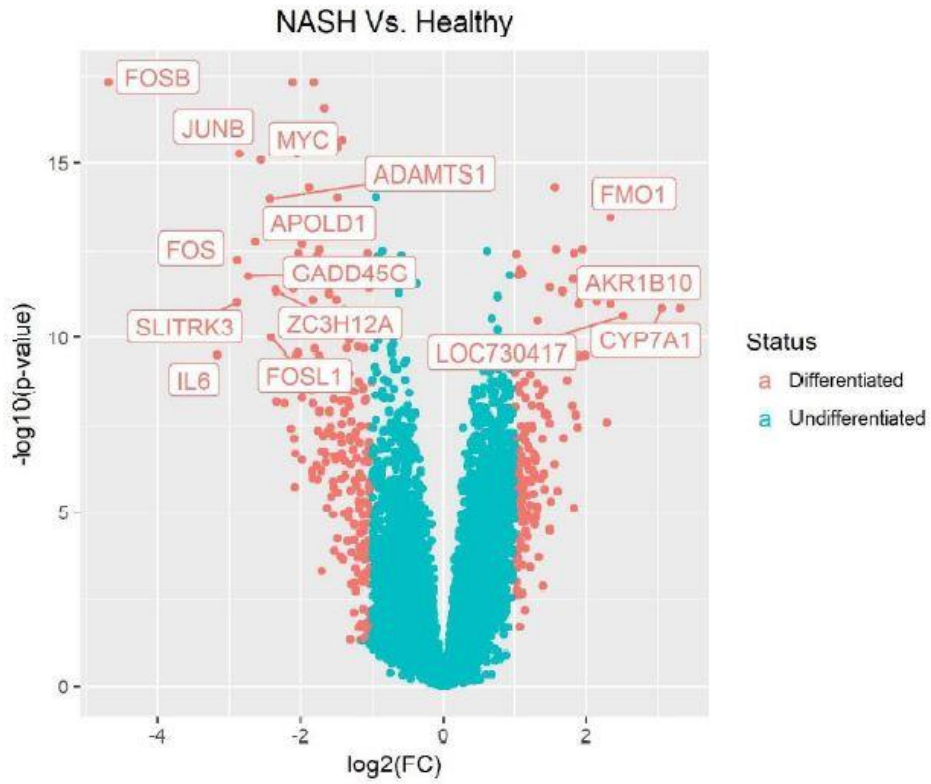


Figure 3.1.3.3: NASH vs Healthy | Volcano Plot with marked DEGs, extracted from GSE89632

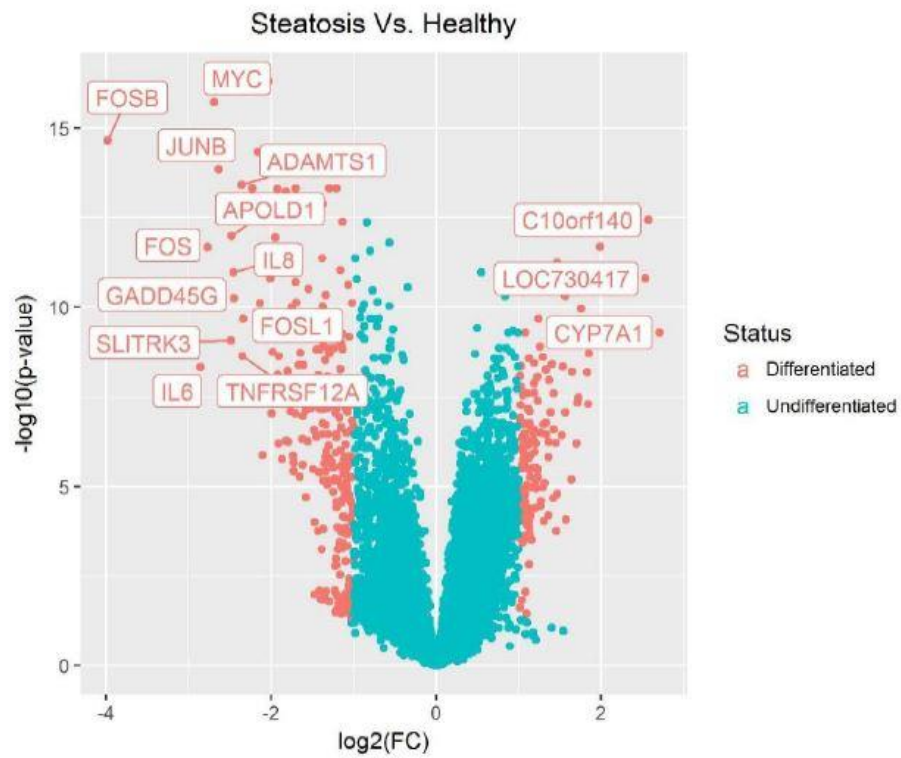


Figure 3.1.3.4: Steatosis vs Healthy | Volcano Plot with marked DEGs, extracted from GSE89632

The names of the top-15 most differentially expressed genes, with regards to either over- or under-expression, are marked on each of the corresponding Volcano Plots.

3.1.4 Gene Set Analysis (GSA)

Gene Set Analysis is then conducted to yield the most significantly triggered pathways, based on the DEGs determined in §3.1.3. The results are extracted in the form of heatmaps. The horizontal axis displays the five categories of differential expression (distinct up/down, mixed up/down and non-directional), while the vertical axis displays the names of the most significant pathways, extracted from MSigDB.

The legend and color axis of the heatmaps regard the values of statistical significance, by use of the p-values, yielded from GSA. Thus, the heatmaps for each of the selected datasets are presented below:

GSE63067

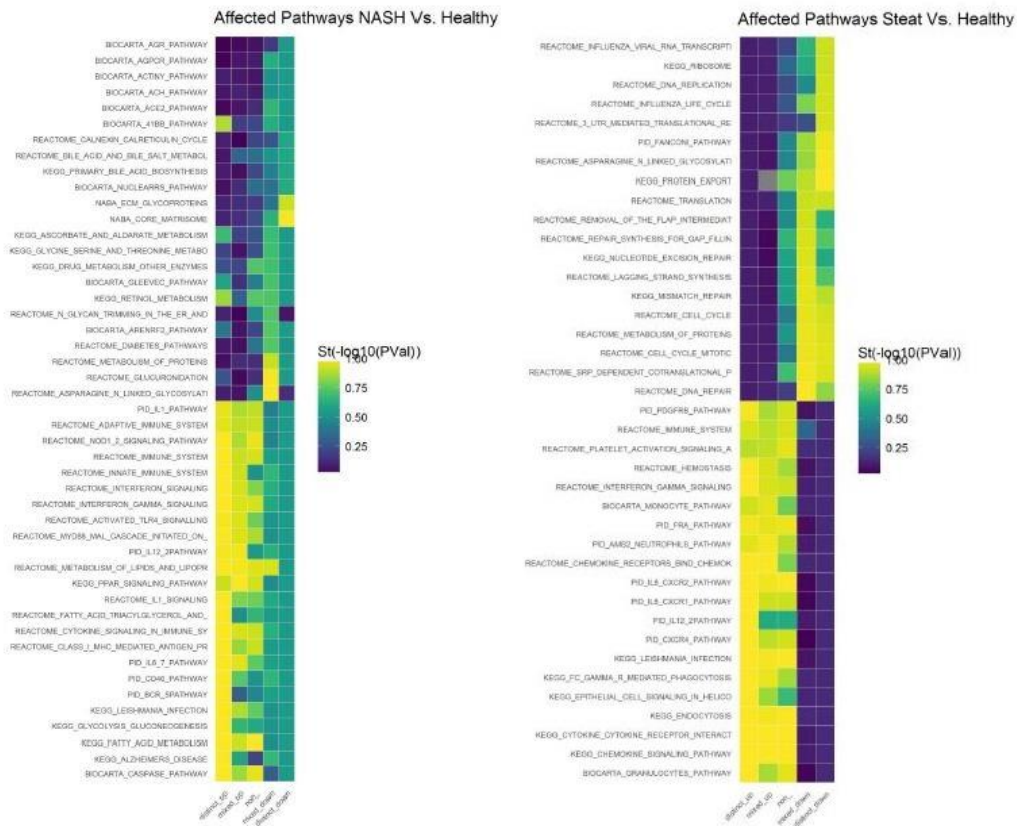


Figure 2.2.3.9.1: Heatmaps extracted from GSE63067 | (a) Affected Pathways of NASH vs Healthy; (b) Affected Pathways of Steatosis vs Healthy

GSE89632

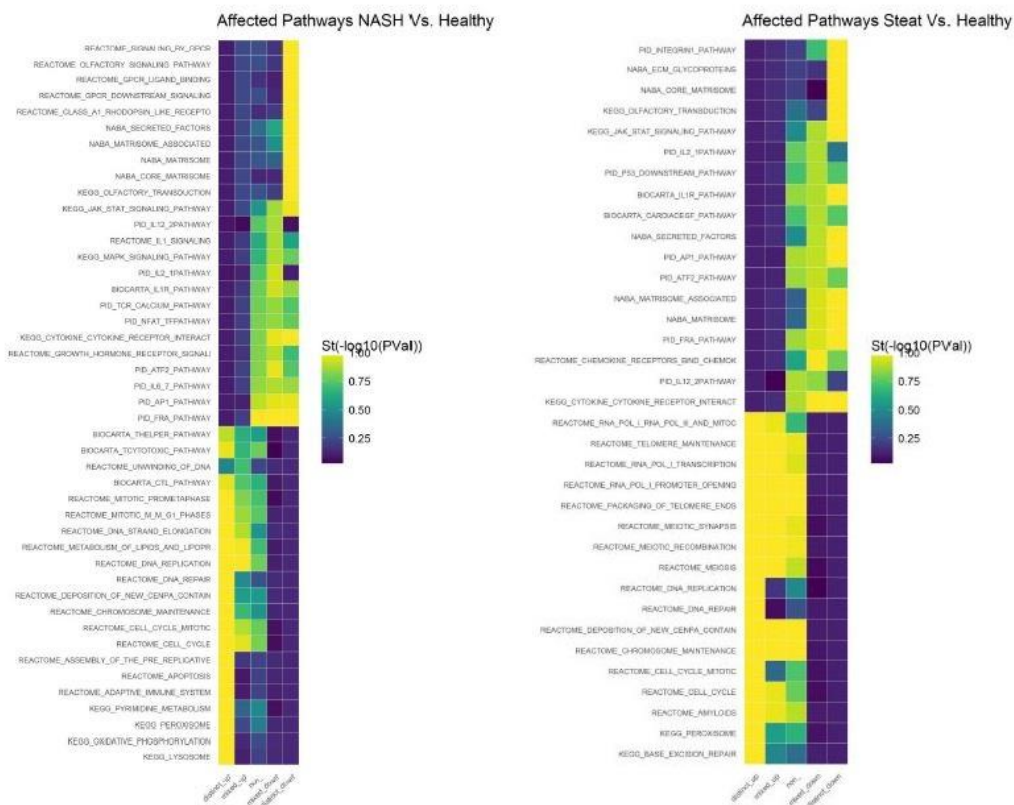


Figure 2.2.3.9.2: Heatmaps extracted from GSE89632 | (a) Affected Pathways of NASH vs Healthy; (b) Affected Pathways of Steatosis vs Healthy

3.1.5 Determination of the Drug-triggered Pathways

MSigDB and DrugBank are used to determine those pathways affected by the known steatogenic compounds (VAP, AMI, TET, TMX, Oleic Acid and Palmitic Acid). In the following tables, pathways derived from the intersection of Groups 1 and 2 (§2.1.7) are presented.

COMPOUND	GENE	PATHWAY
Valproic Acid	ACADSB	KEGG_FATTY_ACID_METABOLISM
		REACTOME_METABOLISM_OF_AMINO_ACIDS_AND_DERIVATIVES
	ODGB	REACTOME_METABOLISM_OF_AMINO_ACIDS_AND_DERIVATIVES
	PPARA	KEGG_PPAR_SIGNALING_PATHWAY
		BIOCARTA_NUCLEARRS_PATHWAY
		REACTOME_METABOLISM_OF_LIPIDS_AND_LIPOPROTEINS
		REACTOME_FATTY_ACID_TRICYLGLYCEROL_AND_KETONE_BODY_METABOLISM
	PPARD	KEGG_PPAR_SIGNALING_PATHWAY
		BIOCARTA_NUCLEARRS_PATHWAY
	PPARG	KEGG_PPAR_SIGNALING_PATHWAY

		BIOCARTA_NUCLEARRRS_PATHWAY	
		PID_NFAT_TFPATHWAY	
		REACTOME_METABOLISM_OF_LIPIDS_AND_LIOPROTEINS	
		REACTOME_FATTY_ACID_TRICYLGLYCEROL_AND_KETONE_BODY_METABOLISM	
Amiodarone	ADRB1	KEGG_ENDOCYTOSIS	
	PPARG	KEGG_PPAR_SIGNALING_PATHWAY	
		BIOCARTA_NUCLEARRRS_PATHWAY	
		PID_NFAT_TFPATHWAY	
		REACTOME_METABOLISM_OF_LIPIDS_AND_LIOPROTEINS	
		REACTOME_FATTY_ACID_TRICYLGLYCEROL_AND_KETONE_BODY_METABOLISM	
Tetracycline	-	-	
Tamoxifen	ESR1	PID_ATF2_PATHWAY	
		PID_AP1_PATHWAY	
	EBP	REACTOME_METABOLISM_OF_LIPIDS_AND_LIOPROTEINS	
Oleic Acid	PPARA	KEGG_PPAR_SIGNALING_PATHWAY	
		BIOCARTA_NUCLEARRRS_PATHWAY	
		REACTOME_METABOLISM_OF_LIPIDS_AND_LIOPROTEINS	
		REACTOME_FATTY_ACID_TRICYLGLYCEROL_AND_KETONE_BODY_METABOLISM	
	PPARD	KEGG_PPAR_SIGNALING_PATHWAY	
		BIOCARTA_NUCLEARRRS_PATHWAY	
	PPARG	KEGG_PPAR_SIGNALING_PATHWAY	
		BIOCARTA_NUCLEARRRS_PATHWAY	
		PID_NFAT_TFPATHWAY	
		REACTOME_METABOLISM_OF_LIPIDS_AND_LIOPROTEINS	
			REACTOME_FATTY_ACID_TRICYLGLYCEROL_AND_KETONE_BODY_METABOLISM
	RXRA	KEGG_PPAR_SIGNALING_PATHWAY	
REACTOME_METABOLISM_OF_LIPIDS_AND_LIOPROTEINS			
REACTOME_FATTY_ACID_TRICYLGLYCEROL_AND_KETONE_BODY_METABOLISM			
Palmitic Acid	PPT1	KEGG_LYSOSOME	
	PPARA	KEGG_PPAR_SIGNALING_PATHWAY	
		BIOCARTA_NUCLEARRRS_PATHWAY	
		REACTOME_METABOLISM_OF_LIPIDS_AND_LIOPROTEINS	
		REACTOME_FATTY_ACID_TRICYLGLYCEROL_AND_KETONE_BODY_METABOLISM	

Table 3.1.5.1: Genes and corresponding pathways that are triggered by known steatogenic compounds (VAP, AMI, TET, TMX, Oleic Acid, Palmitic Acid)

With those pathways, triggered by both the disease's mechanisms and the known steatogenic compounds, being known, other substances of similar/opposite behavior can be determined.

3.1.6 Identification of Relative Compounds via cMap

In the following figures, each of the known steatogens are introduced to cMap's dedicated tool as a signature-question. For each signature-question, two lists of relative compounds are returned. The first contains drugs and substances that exhibit similar expression to the question, while the second contains those that exhibit the opposite expression.

For instance, when Amiodarone is put as the signature-question:

Cmap name	Dose	Cell line	Instance id
Amiodarone	6mM	HL60	2434
Amiodarone	6mM	PC3	4657
Amiodarone	6mM	MCF7	3296

Figure 3.1.6.1: AMI as Signature-Question

Rank	Cmap name	Mean	n	Enrichment	P	Specificity	% non null
11	Timolol	-0.510	4	-0.792	0.00376	0.0224	100
39	Ketoconazole	-0.408	4	-0.689	0.0213	0.0000	75
41	Aminoglutethimide	-0.280	3	-0.781	0.02157	0.0179	66
48	Fusidic acid	-0.406	4	-0.666	0.02801	0.0063	75

Figure 3.1.6.2: Compounds with an opposite expression to AMI

Rank	Cmap name	Mean	n	Enrichment	P	Specificity	% non null
8	Ethisterone	0.432	6	0.698	0.00205	0.0000	8
14	Meclizine	0.412	5	0.709	0.00491	0.0131	80
24	Omeprazole	0.379	4	0.739	0.00889	0.0642	100
28	Trimetazidine	0.338	4	0.720	0.01243	0.0078	100
51	Prednisone	0.282	5	0.607	0.02842	0.0526	80
55	Amiloride	0.340	5	0.597	0.03276	0.0167	80
65	Ursodeoxycholic acid	0.390	3	0.725	0.04054	0.0517	100

Figure 3.1.6.3: Compounds with a similar expression to AMI

Cmap name	Dose	Cell line	Instance id
Tamoxifen	7 μ M	HL60	1366
Tamoxifen	7 μ M	PC3	2050
Tamoxifen	7 μ M	MCF7	2212

Figure 3.1.6.4: TMX as Signature-Question

Rank	Cmap name	Mean	n	Enrichment	P	Specificity	% non null
13	Estropipate	-0.374	4	-0.816	0.00209	0.0000	50
18	Physostigmine	-0.391	4	-0.804	0.00284	0.0000	75
45	Cefmetazole	-0.312	4	-0.708	0.01514	0.0142	50
50	Carbimazole	-0.396	3	-0.792	0.01827	0.0480	66
60	Sulindac	-0.342	7	-0.524	0.02499	0.0388	57
64	Diflorasone	-0.376	4	-0.668	0.02731	0.0186	50

Figure 3.1.6.5: Compounds with an opposite expression to TMX

Rank	Cmap name	Mean	n	Enrichment	P	Specificity	% non null
1	Mefloquine	0.476	5	0.933	0.00000	0.0098	100
5	Sirolimus	0.215	4 4	0.330	0.00012	0.2590	65
16	Acepromazine	0.360	4	0.810	0.00241	0.0074	100
23	Disulfiram	0.357	5	0.709	0.00495	0.0694	80
30	Clomifene	0.415	4	0.748	0.00778	0.0517	100
44	Ivermectin	0.321	5	0.651	0.01442	0.1075	80
46	Clomipramine	0.410	4	0.705	0.01578	0.1105	100
49	Albendazole	0.390	3	0.793	0.01815	0.0116	100
52	Rimexolone	0.333	4	0.689	0.01950	0.0840	100
58	Gallamine triethiodide	0.314	5	0.616	0.02453	0.0081	80
69	Clotrimazole	0.263	5	0.597	0.03258	0.1333	80
73	Pimozide	0.325	4	0.642	0.03995	0.1708	75
76	Fenoterol	0.326	3	0.723	0.04202	0.0692	100
77	Isoetarine	0.230	4	0.637	0.04227	0.0400	75
80	Progesterone	0.282	4	0.632	0.04579	0.0307	75
85	Mifepristone	0.241	4	0.629	0.04768	0.0584	75

Figure 3.1.6.6: Compounds with a similar expression to TMX

Cmap name	Dose	Cell line	Instance id
Tetracycline	8µM	HL60	1397
Tetracycline	8µM	PC3	2080
Tetracycline	8µM	MCF7	2243

Figure 3.1.6.7: TET as Signature-Question

Rank	Cmap name	Mean	n	Enrichment	P	Specificity	% non null
31	Raloxifen	-0.380	7	-0.519	0.02697	0.0520	57
42	Oxprenolol	-0.502	4	-0.650	0.03529	0.0594	75
46	Dipivefrin	-0.519	4	-0.641	0.03965	0.0526	75
54	Metoprolol	-0.417	4	-0.624	0.04953	0.0534	75

Figure 3.1.6.8: Compounds with an opposite expression to TET

Rank	Cmap name	Mean	n	Enrichment	P	Specificity	% non null
16	Aceclofenac	0.720	4	0.727	0.01108	0.0137	75
39	Cefotaxime	0.675	5	0.592	0.03475	0.0136	80
41	Cortisone	0.701	3	0.738	0.03523	0.0826	100

Figure 3.1.6.9: Compounds with a similar expression to TET

Cmap name	Dose	Cell line	Instance id
Valproic acid	1mM	HL60	2669
Valproic acid	1mM	PC3	458
Valproic acid	1mM	MCF7	989

Figure 3.1.6.10: VPA as Signature-Question

Rank	Cmap name	Mean	n	Enrichment	P	Specificity	% non null
42	Naftifine	-0.558	4	-0.698	0.01751	0.0196	75
63	Ketoprofen	-0.370	6	-0.525	0.04660	0.0385	50
66	Pralidoxime	-0.320	4	-0.625	0.04864	0.0526	75

Figure 3.1.6.13.1.61: Compounds with an opposite expression to VPA

Rank	Cmap name	Mean	n	Enrichment	P	Specificity	% non null
8	Resveratrol	0.294	9	0.655	0.00026	0.1226	77
36	Nabumetone	0.267	4	0.722	0.01182	0.0130	100
60	Mepacrine	0.330	2	0.860	0.03941	0.0677	100

Figure 2.2.3.9.12: Compounds with a similar expression to VPA

By repeating the steps described in §3.1.2-3.1.5, via MSigDB and DrugBank, the super-intersection of Groups 1, 2 and 3 yields the following significant pathways that associate NAFLD, known steatogens and candidate steatogenic compounds:

Significant Pathways of Groups 1, 2 and 3 Super-intersection	BIOCARTA_NUCLEARRS_PATHWAY
	KEGG_ENDOCYTOSIS
	KEGG_FATTY_ACID_METABOLISM
	KEGG_PPAR_SIGNALING_PATHWAY
	PID_AP1_PATHWAY
	PID_ATF2_PATHWAY
	PID_NFAT_TFPATHWAY
	REACTOME_FATTY_ACID_TRICYLGLYCEROL_AND_KETONE_BODY_METABOLISM
	REACTOME_METABOLISM_OF_AMINO_ACIDS_AND_DERIVATIVES
	REACTOME_METABOLISM_OF_LIPIDS_AND_LIPOPROTEINS

Table 3.1.6.1: Significant pathways of the Super-intersection between Groups 1, 2 and 3

What needs to be noted, is that, from the relative compounds yielded for each known steatogens, some may be non-steatogenic or known steatogens or even anti-steatogenic.

Thus, we select three of the drugs listed, that will proceed to *in-vitro* verification of their possible steatogenic effects. These are depicted, along with some additional information, in the following figure (Figure 3.1.6.13):

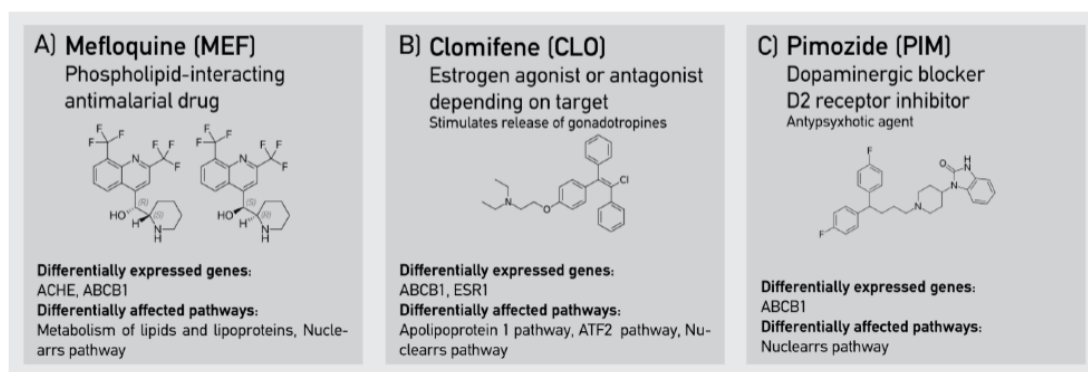


Figure 3.1.6.13 Final selection of candidate steatogenic compounds to proceed to *in-vitro* verification

3.2 IN-VITRO VERIFICATION

3.2.1 FBS Threshold Determination Experiment

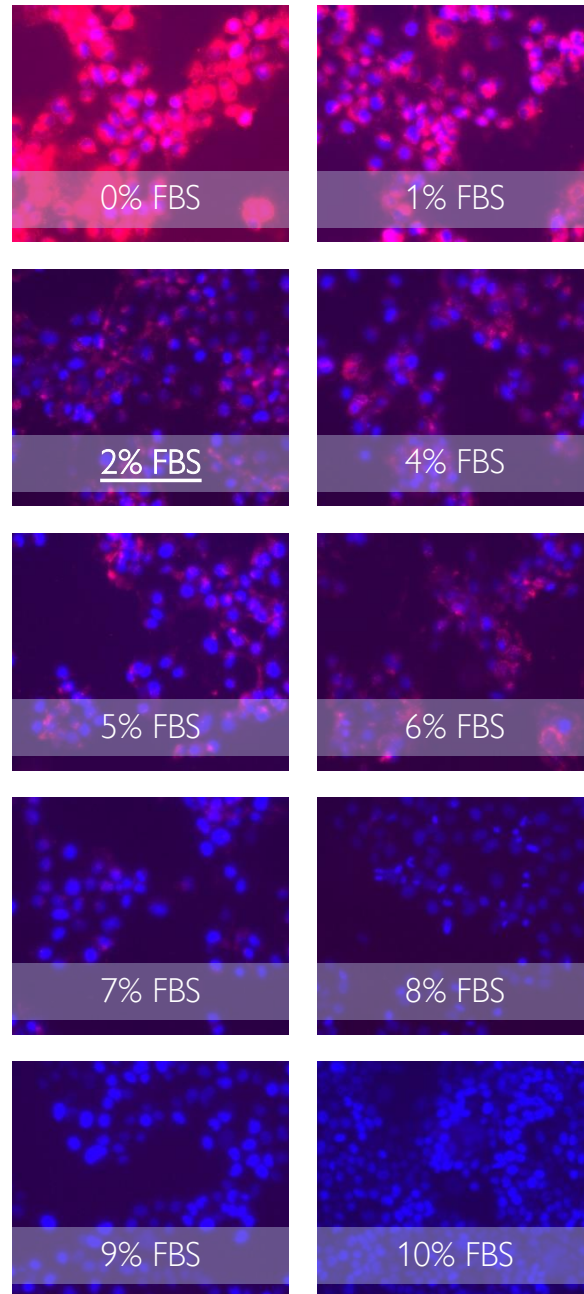


Figure 2.2.3.9.1: HUH7 cell line exposed to different FBS concentrations for 24h

The acquired images support the notion that as fasting increases (lower FBS concentrations in the culture medium), DNL also increases. Thus, and in order to satisfy the two conditions, described thoroughly in §2.2.3.1, the serum concentration is selected to be 2% v/v.

3.2.2 FFA Threshold Determination Experiment

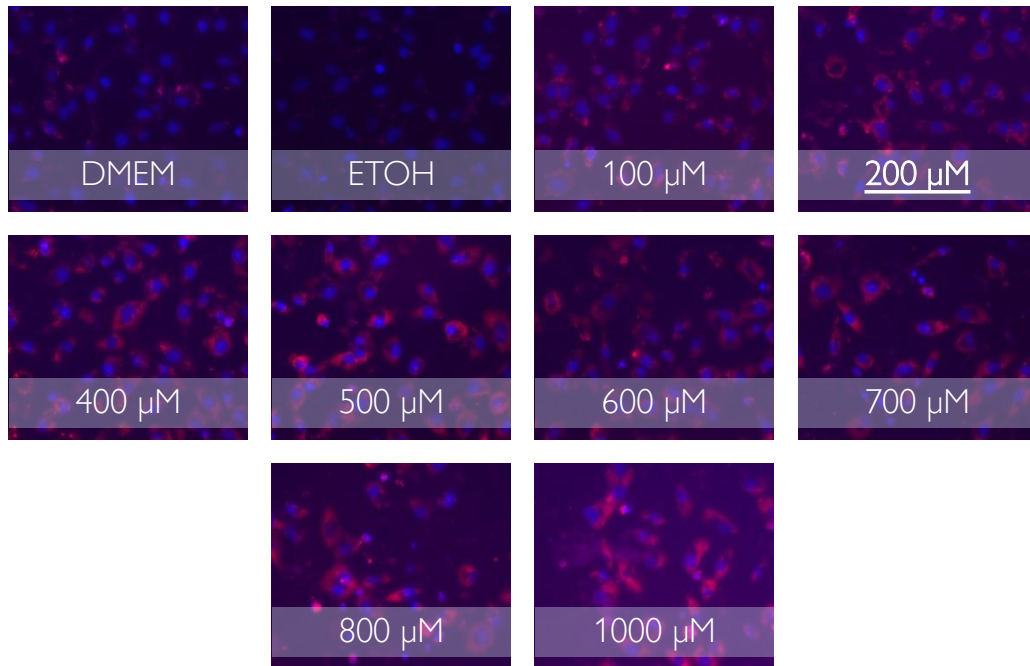


Figure 3.2.2.2: FOCUS cell line exposed to increasing FFA concentrations (in 24h)

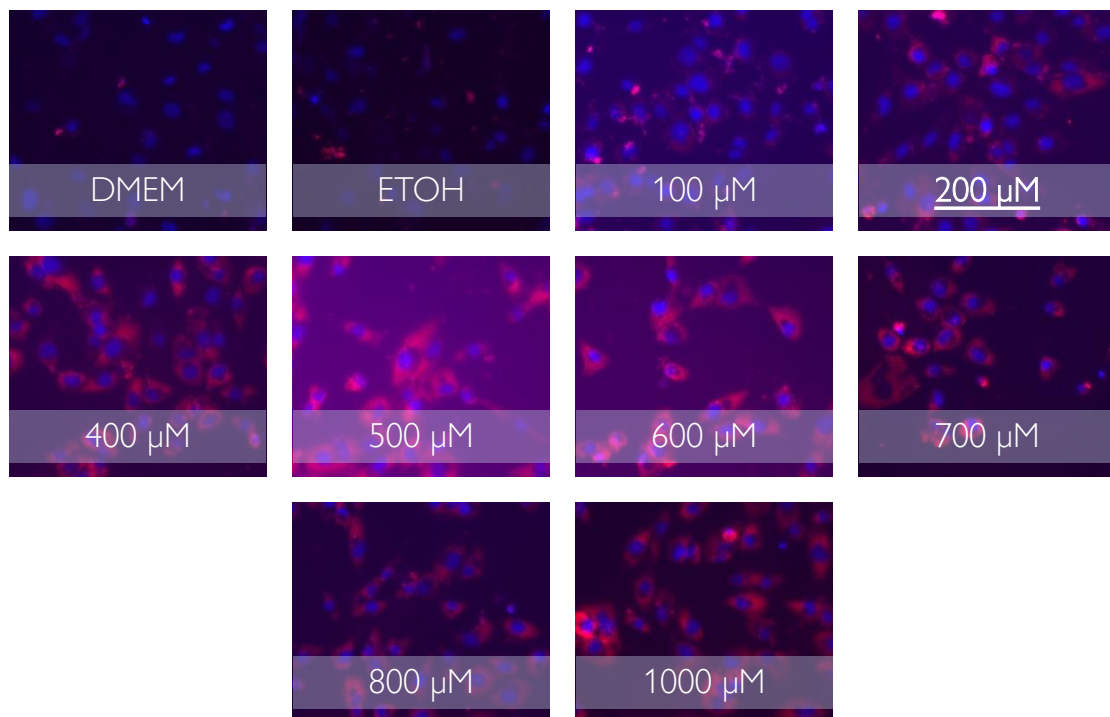


Figure 3.2.2.3: FOCUS cell line exposed to increasing FFA concentrations (in 48h)

An observational overview of the fat levels in 24h and 48h of FFA treatment reveal that at approximately 200μM, FOCUS cells become unable to accommodate the FFA's excess.

3.2.3 Bulk Verification of Steatogenic Effects

As the pathway analysis concludes on an intersection of potentially steatogenic compounds, that may also be known to the scientific community or even anti-steatogenic, a bulk verification of the steatogenic effects is needed for Pimozide (PIM), Clomiphene (CLO) and Mefloquine (MEF).

Hence, Hep3B cells are exposed to 10 μ M of either PIM, CLO or MEF and fat levels are reviewed within 24h of treatment. The acquired images are provided:

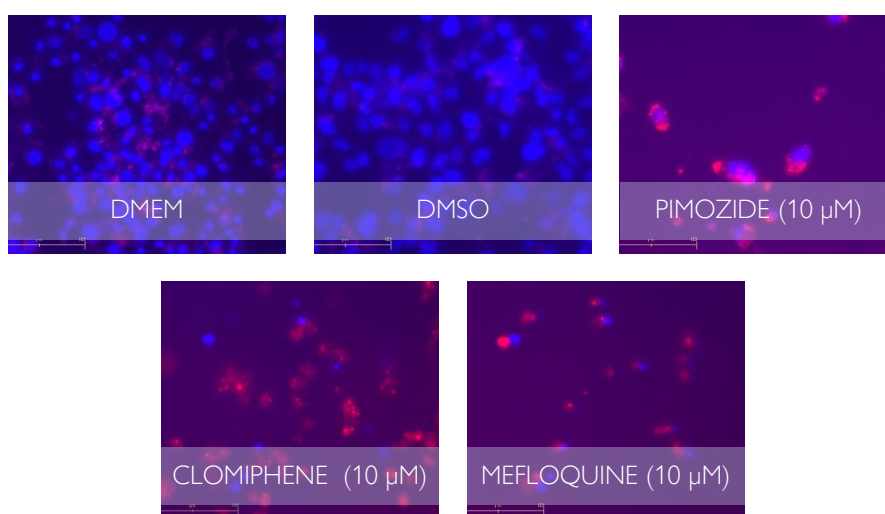


Figure 2.2.3.9.1: Bulk verification of the steatogenic effects on Hep3B cell line

As observed, fat seems elevated in the treated wells, however the used dosing concentrations may be hepatotoxic, as the majority of the controls' cells are eliminated in the treatment wells. Thus, IC₁₀ of PIM, CLO and MEF should be determined.

3.2.4 IC₁₀ Determination

IC₁₀ determination is performed for both FOCUS and Hep3B cell lines, as dosing concentrations are usually cell-dependent. Following Resazurin Viability Assay, a dose-viability plot is created, with the viability points being interpolated through 4PL regression models. The dose-response curves, IC₁₀ and R² are provided for each drug and cell line and can be found in the following page:

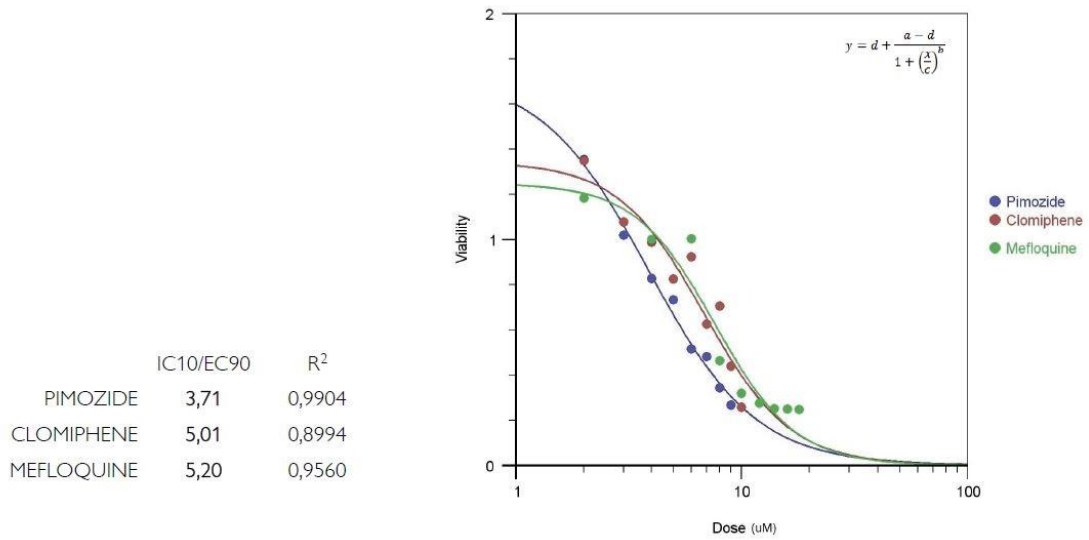


Figure 2.2.3.9.1: Dose-Response curves of PIM, CLO and MEF for FOCUS cell line | IC10 or EC90 | 4PL's R-square values

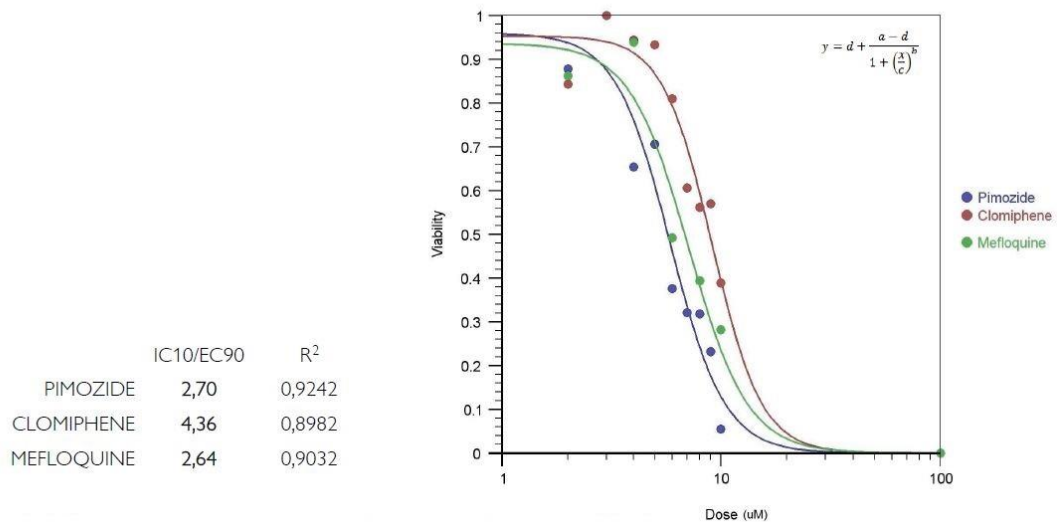


Figure 3.2.4.2: Dose-Response curves of PIM, CLO and MEF for Hep3B cell line | IC10 or EC90 | 4PL's R-square values

In the following pages, ROS production levels and Relative Fat levels will be examined for PIM, CLO and MEF treatments on FOCUS and Hep3B cells that are administered with concentrations as proximal to the corresponding IC10s as possible.

In order to minimize the underlying standard error of the IC10 determination, a windows around IC10 will be used for the treatment of FOCUS and Hep3B cells. Thus, in the following figures 3 concentrations will be examined for each drug: the IC10, one slightly below the IC10 and one slightly above the IC10.

3.2.5 Intracellular Lipid Accumulation

The data are presented as Mean±SEM of 3 independent experiments, while the statistical analysis is performed with ANOVA. The (*) correspond to statistical significance.

3.2.5.1 Pimozide (PIM)

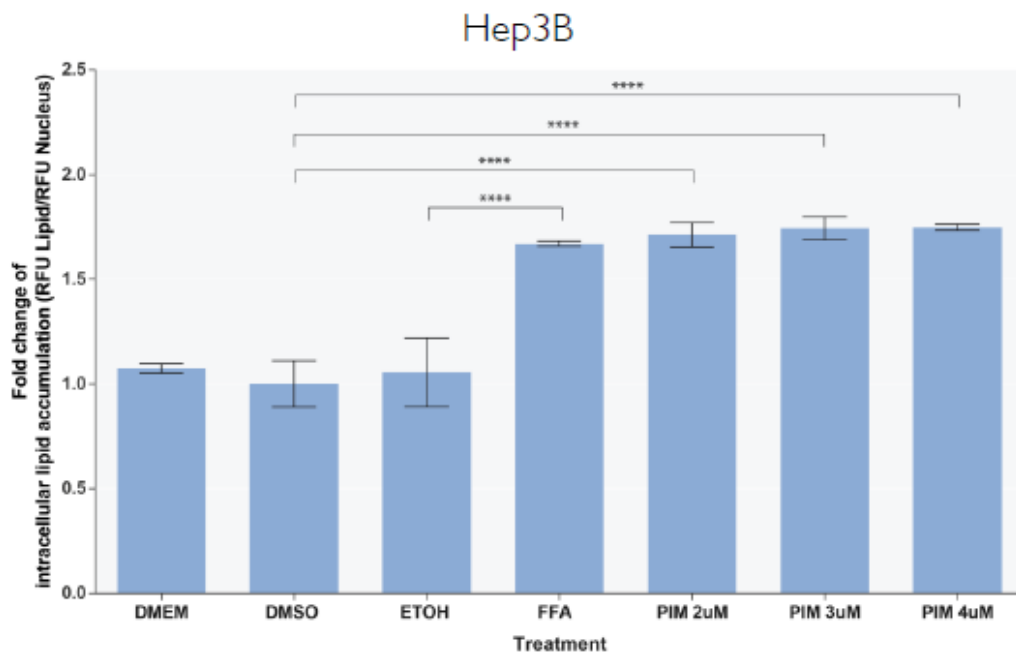


Figure 3.2.5.1.1: Intracellular lipid accumulation of PIM-treated Hep3B hepatocytes

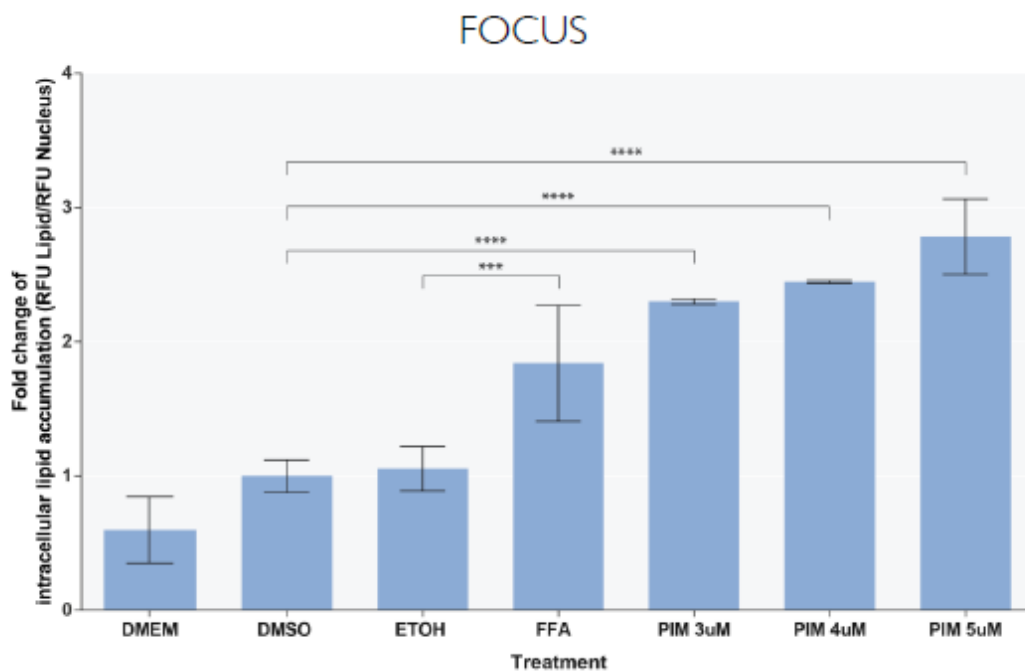


Figure 3.2.5.1.2: Intracellular lipid accumulation of PIM-treated FOCUS hepatocytes

3.2.5.2 Clomiphene (CLO)

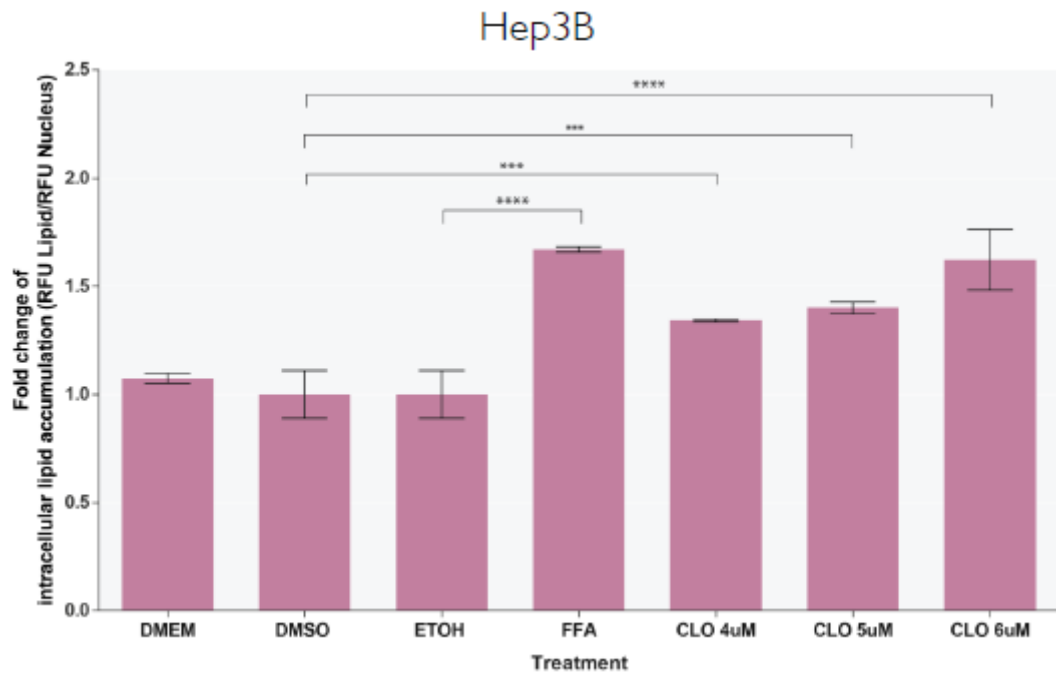


Figure 3.2.5.2.1: Intracellular lipid accumulation of CLO-treated Hep3B hepatocytes

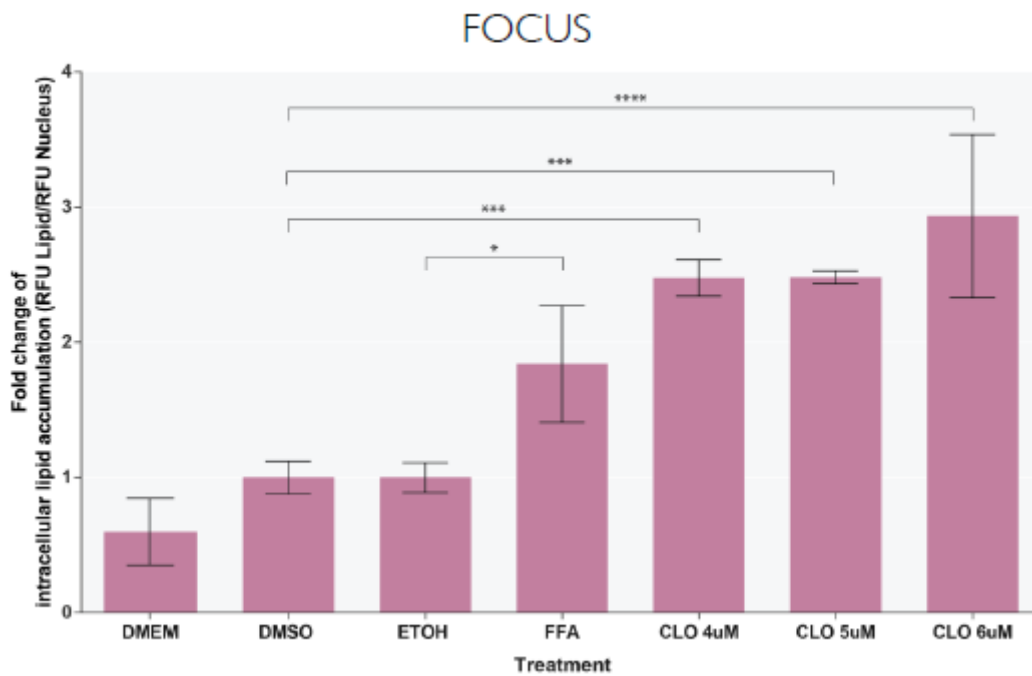


Figure 3.2.5.2.2: Intracellular lipid accumulation of CLO-treated FOCUS hepatocytes

3.2.5.3 Mefloquine (MEF)

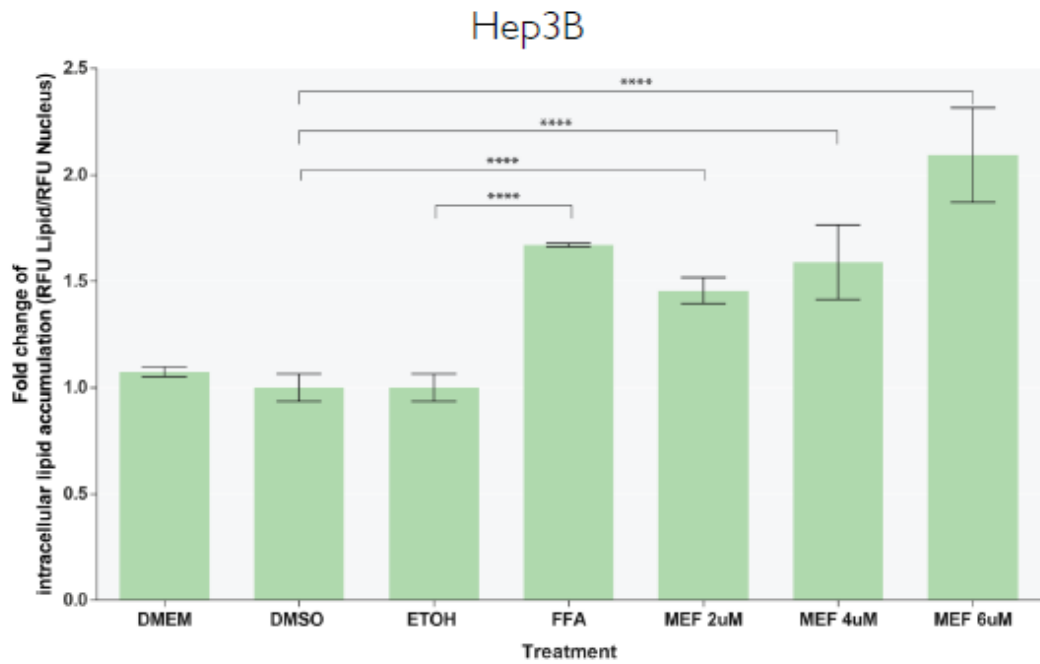


Figure 3.2.5.3.1: Intracellular lipid accumulation of MEF-treated Hep3B hepatocytes

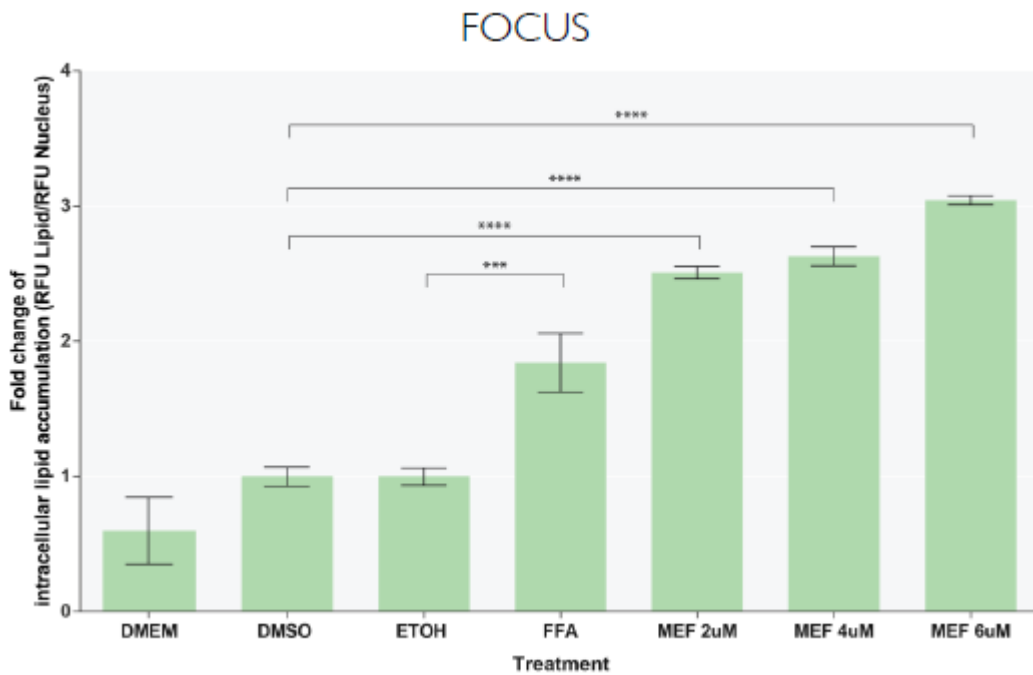


Figure 3.2.5.2.2: Intracellular lipid accumulation of MEF-treated FOCUS hepatocytes

3.2.6 Intracellular ROS Production

3.2.6.1 Pimozide (PIM)

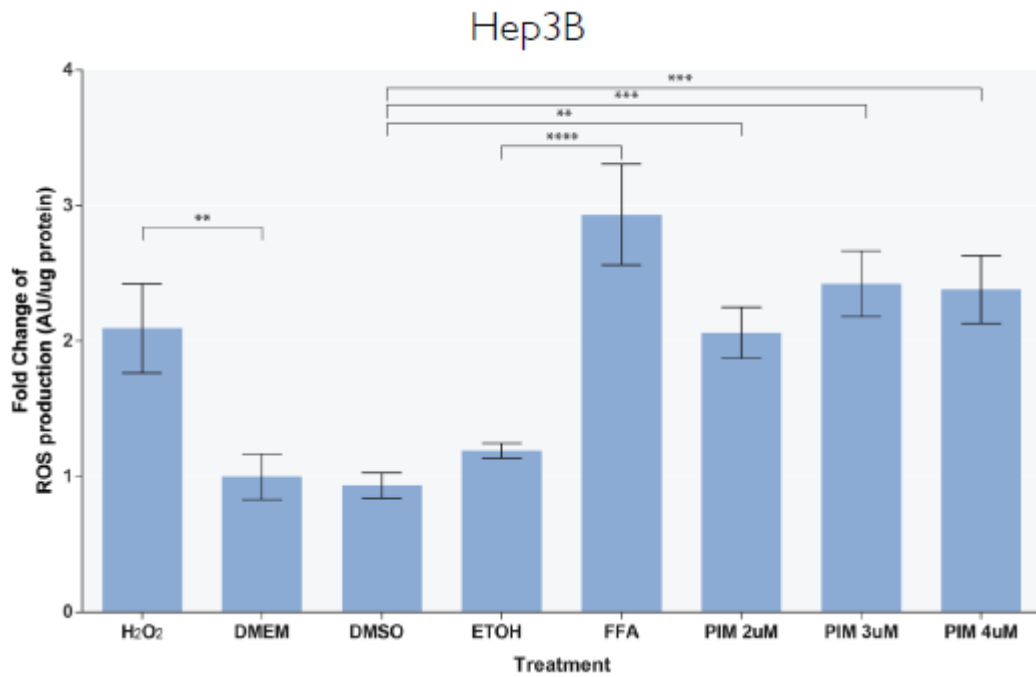


Figure 3.2.6.1.1: Intracellular ROS production of PIM-treated Hep3B hepatocytes

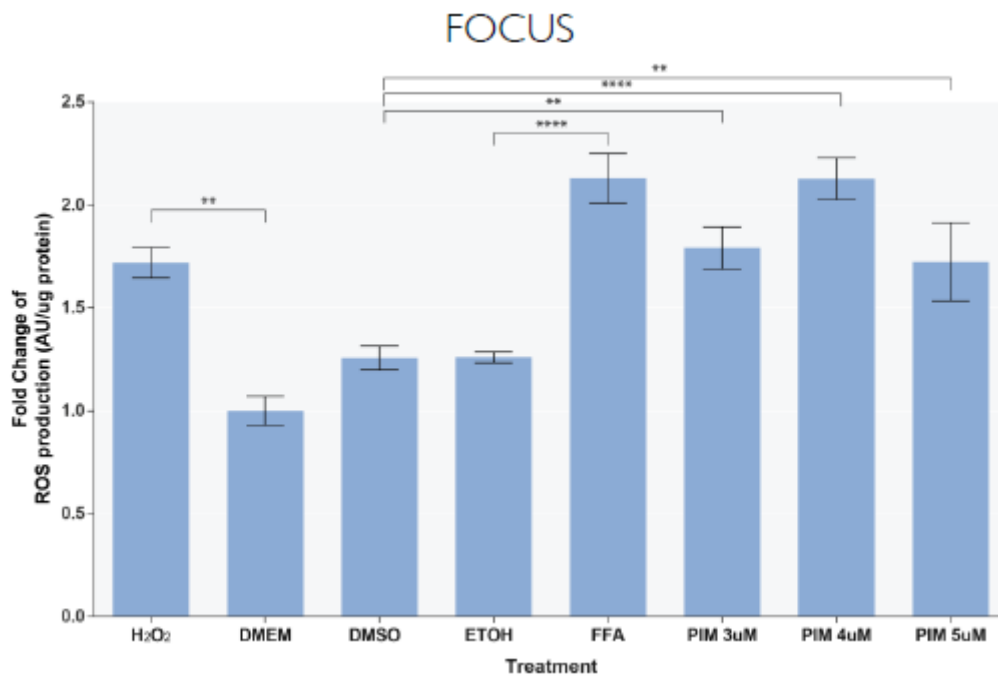


Figure 3.2.5.3.2: Intracellular ROS production of PIM-treated FOCUS hepatocytes

3.2.6.2 Clomiphene (CLO)

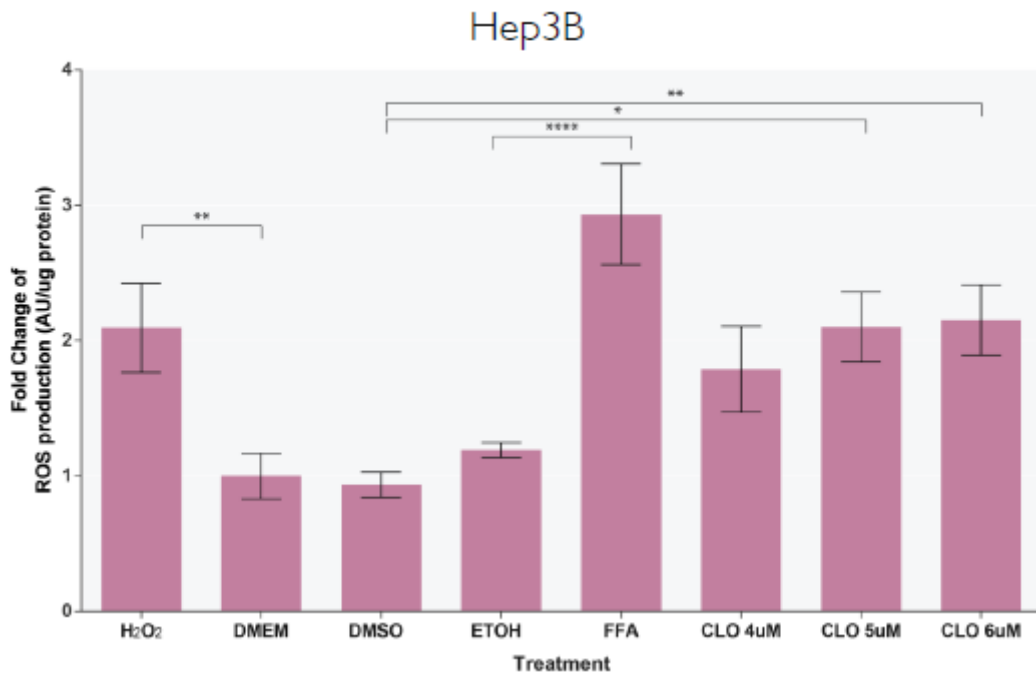


Figure 3.2.6.2.1: Intracellular ROS production of CLO-treated Hep3B hepatocytes

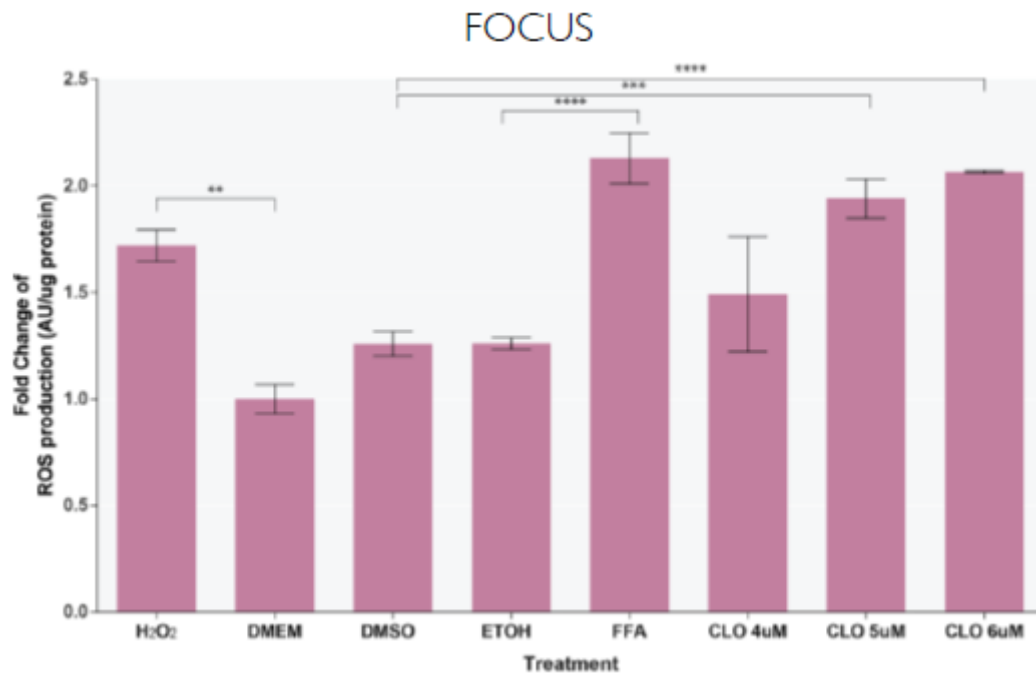


Figure 3.2.6.2.2: Intracellular ROS production of CLO-treated FOCUS hepatocytes

3.2.6.3 Mefloquine (MEF)

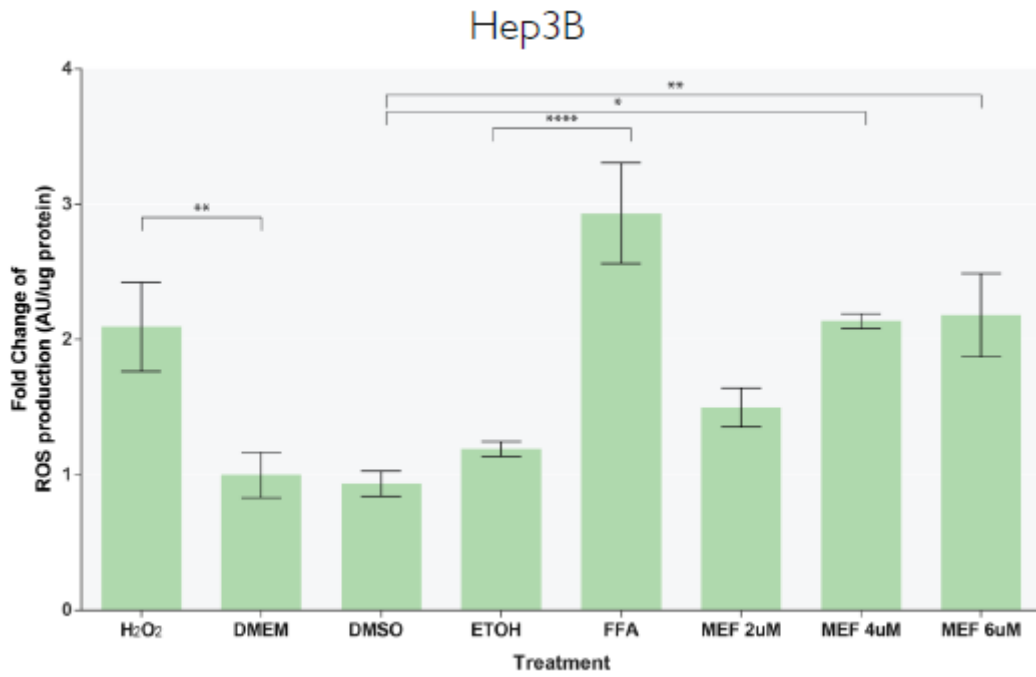


Figure 3.2.6.2.1: Intracellular ROS production of MEF-treated Hep3B hepatocytes

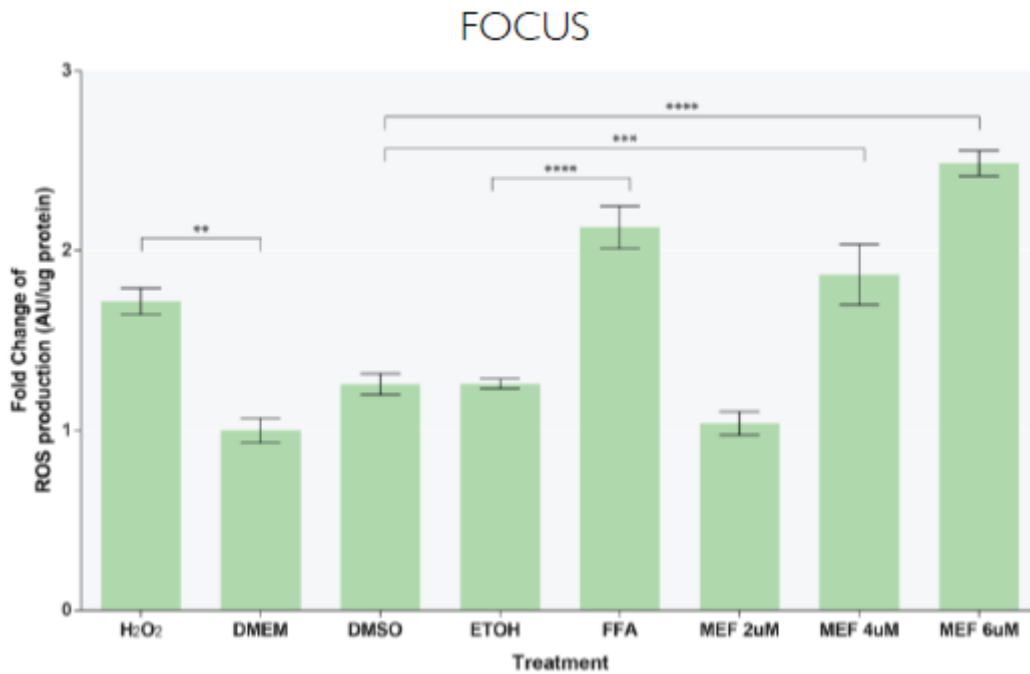


Figure 3.2.6.3.2: Intracellular ROS production of MEF-treated FOCUS hepatocytes

4 CONCLUSIONS

In summary, the present study is aiming to the identification and *in-vitro* verification of potential steatogenic compounds, that derive from a network-based pathway analysis of NAFLD's underlying molecular mechanisms.

First, in order to determine the candidate steatogenic compounds, a prioritization of several sets of pathways is performed towards the construction of the respective networks. To do so, a network-based computational platform that utilize gene expression datasets, derived from NAFLD/NASH liver biopsies (GEO-NCBI), and datasets from compound-treated lines (cMap), is constructed. Via computational comparisons between networks of NAFLD's underlying mechanisms and networks of literally known steatogenic compounds (VPA, AMI, TET, TMX), an intersection is deduced. This intersection delivers networks that are significantly involved in NAFLD/NASH steatogenesis. These networks, in turn, correspond to differentially expressed genes and thus, to significantly differentiated pathways, that are concurrently triggered by NAFLD's pathogenesis and by the known steatogens. From these networks, several compounds are yielded out of their sharing targets to the known NAFLD-inducers. The compounds may include novel steatogenic compounds, known steatogenic compounds and potential drug-repositioning substances for NAFLD's treatment. After eliminating the known steatogens and other literally promising drug-repositioning substances, a final selection of three -potentially steatogenic-compounds is made.

Thus, Pimozide, Clomiphene and Mefloquine proceed to *in-vitro* verification of their potential steatogenic effects on human hepatocytes. Complementary *in-vitro* NAFLD/NASH assays are developed to validate the *in-silico* predictions and identify PIM, CLO and MEF's steatogenic effects. For that purpose, Hep3B and FOCUS hepatocellular lines are seeded on 96-well plates and exposed, for 24h, to PIM, CLO and MEF treatments of experimentally determined dosing concentrations; their corresponding IC10. Intracellular lipid droplets are then verified via high-content screening that employs Nile Red fluorescent probe and Hoechst 33342 for nuclei counterstaining. JuLI™Stage (NanoEntek) automatically acquires images of the droplets. Compounds found to induce droplet accumulation, are also examined for producing intracellular ROS with CM-H2DCFDA fluorescent substrate.

All PIM-, CLO- and MEF-treated cell lines exhibit significantly elevated levels of intracellular lipid accumulation that is significantly higher than the accumulation demonstrated in the control wells of DMEM (culture medium) and DMSO (drug solvent). Hep3B and FOCUS hepatocytes also exhibit lipid accumulation levels that are significantly correlated to the corresponding positive controls, the FFA-treated wells. These results suggest that PIM, CLO and MEF induce steatosis to Hep3B and FOCUS hepatocytes, although the mechanism by which they do so is yet to be examined.

Furthermore, all PIM-, CLO- and MEF-treated cell lines seem to produce significantly elevated levels of intracellular Reactive Oxygen Species (ROS) that is significantly higher than the levels of the control wells of DMEM (culture medium), DMSO (drug solvent) and ETOH (FFA solvent). Hep3B and FOCUS hepatocytes also exhibit lipid accumulation levels that are significantly correlated to the corresponding positive controls, the FFA-treated and H₂O₂-treated cells. These results suggest that PIM, CLO and MEF induce the production of ROS to Hep3B and FOCUS hepatocytes, leading to an increase of their oxidative stress; a major key-feature of NAFLD's pathogenesis.

Finally, these results conclude on adequate evidence that Pimozide, Clomiphene and Mefloquine can be considered to have a steatogenic tendency, successfully predicted by the computational platform used. However, 2D cell cultures cannot fully imitate the actual hepatic environment while the cell-line dependency of the steatogenic effects do not allow for conclusive deductions.

In conclusion, the *in-silico* approach deduces a network similarity, thus identifies both compounds reducing and inducing steatosis *in-vitro*. A high-throughput setup for NAFLD/NASH drug-screening is successfully developed. Further experiments are necessary to decipher the mechanisms that the identified compounds facilitate, and to assess their *in-vivo* effects. ELISA for protein and cytokine measurement needs to be conducted in order to establish the experimentally verified tendency of PIM, CLO and MEF to induce steatosis at the protein level, while also a clustering among PIM, CLO, MEF and the known NAFLD-inducing compounds needs to be performed in order to classify relative compounds and predict their sharing features of action. Moreover, 3D cell cultures can also be used to better mimic the actual hepatic environment, while also analysis at the level of Single cell may provide substantial information on the exact pathogenic mechanisms.

5 REFERENCES

1. Angulo P., Non-Alcoholic Fatty Liver Disease, *N Eng J Med*, 2002, 346:1221-1236
2. J.K. Dowman, J.W. Tomlinson, P.N. Newsome, Pathogenesis of non-alcoholic fatty liver disease, *Qjm*, 2010, 71-83
3. B.M. Attar K., Van Thiel D.H., Current concepts and management approaches in non-alcoholic fatty liver disease, *Sci. World J*, 2013, 481893
4. Bambha K. et al., Ethnicity and non-alcoholic fatty liver disease, *Hepatology*, 2012, 55:865-873
5. Eksdtedt et. Al., Long-term follow up of patients with NAFLD and elevated liver enzymes, *Hepatology*, 2006, 44:865-873
6. Argo CK., Al-Osaimi AM, Cardwell SH, Systematic review of risk factors for fibrosis progression in non-alcoholic fatty liver disease, *J. Hepatology*, 2009, 51:371-379
7. Hamabe A. et al., Impact of cigarette smoking on onset of nonalcoholic fatty liver disease over a 10-year period, *J. Gastroenterology*, 2011, 46:769-778
8. Dunn W., Xu R., Schwimmer J.B., Modest wine drinking and decreased prevalence of suspected nonalcoholic fatty liver disease, *Hepatology*, 2008, 47:7947-1954
9. Than N.N., Newsome P.N., A concise review of non-alcoholic fatty liver disease, *Atherosclerosis*, 2015, 219:192-202
10. C.P. Day, O.F. James, Steatohepatitis: a tale of "two hits"?, *Gastroenterology*, 1998, 114:842-845
11. Jeremy M Berg, John L Tymoczko, and Lubert Stryer, *Biochemistry*, New York: W H Freeman; 2002, ISBN-10: 0-7167-3051-0
12. Neuschwander-Tetri BA, Hepatic lipotoxicity and the pathogenesis of nonalcoholic steatohepatitis: the central role of nontriglyceride fatty acid metabolites, *Hepatology*, 2010, 52:774-788
13. Alba Berlanga, Esther Guiu-Jurado, José Antonio Porras, Teresa Auguet, Molecular pathways in non-alcoholic fatty liver disease, *Clinical and Experimental Gastroenterology*, 2014, 7;221-239
14. Lambert JE, Ramos Roman MA, Browning JD, et al. Increased de novo lipogenesis is a distinct characteristic of individuals with non-alcoholic fatty liver disease, *Gastroenterology*, 2014, 14:726-735
15. Stefan N., Kantartzis K., Haring HU, Causes and metabolic consequences of fatty liver, *Endocr Rev*, 2008, 29:939-960
16. Buzzeti E, Pinzani M, Tsohatzis E.A., The multiple-hit pathogenesis of non-alcoholic fatty liver disease (NAFLD), *Metabolism*, 2016, 65:1038-1048
17. Sabio G, Das M, Mora A, et al., A stress signaling pathway in adipose tissue regulates hepatic insulin resistance, *Science*, 2008, 322:1539-1543

18. Begriche K, Igougil A, Pessayre E, et al., Mitochondrial dysfunction in NASH: causes, consequences and possible outcomes, *Mitochondrion*, 2006, 6:1-28
19. Paradies G, Paradies V, Ruggieto FM et al., Oxidative stress, cardiolipin and mitochondrial dysfunction in non-alcoholic fatty liver disease, *World J Gastroenterology*, 2014, 14:581-597
20. Kapoor A, Sanyal AJ, Endoplasmic reticulum stress and the unfolded protein response, *Clin Liver Disease*, 2009, 13:581-590
21. Park SW, Zhou Y, Lee J, et al., The regulatory subunits of P13K, p85alpha and p85beta, interact with XBP-1 and increases its nuclear translocation, *Nature Medicine*, 2010, 16:429-437
22. Tilg H, Moschen AR, Evolution of inflammation in nonalcoholic fatty liver disease: the multiple parallel hits hypothesis, *Hepatology*, 2010, 52:1836-1846
23. Ribeiro PS, Cortez-Pinto H, Sola S et al., Hepatocyte apoptosis, expression of death receptors and activation of NF-kappaB in the liver of alcoholic and nonalcoholic steatohepatitis patients, *American Journal of Gastroenterology*, 2004, 99:1708-1717
24. J.K. Dowman, J.W. Tomlinson, P.N. Newsome, Systematic Review: the diagnosis and staging of non-alcoholic fatty liver disease and non-alcoholic steatohepatitis, *Alimentary Pharmacology Ther.*, 2011, 33:525-540
25. Veronica Martin-Dominguez, R.G-C.J. Mendoza-Jimenes-Ridruejo, Luisa Garcia-Buey, Ricardo Moreno-Otero, Pathogenesis, diagnosis and treatment of non-alcoholic fatty liver disease, *Rev. Esp. Enferm. Dig.*, 2013, 105:409-420
26. J.K. Dowman et al., Current therapeutic strategies in non-alcoholic fatty liver disease, *Diabetes Obesity Metabolism*, 2013, 13:692-702
27. J.K. Dowman et al., Current therapeutic strategies in non-alcoholic fatty liver disease, *Diabetes Obesity Metabolism*, 2013, 13:692-702
28. N.C. Chavez-Tapia, N. Rosso and C. Tiribelli, In Vitro Models for the Study of Non-Alcoholic Fatty Liver Disease, *Current Medicinal Chemistry*, 2011, 18, 1079-1084
29. Tirosch, O.; Ilan, E.; Anavi, S.; Ramadori, G.; Madar, Z. Nutritional lipid- induced oxidative stress leads to mitochondrial dysfunction followed by necrotic death in FaO hepatocytes. *Nutrition (Burbank, Los Angeles County, Calif)*, 2009, 25(2), 200-208.
30. Janorkar, A.V.; King, K.R.; Megeed, Z.; Yarmush, M.L. Development of an in vitro cell culture model of hepatic steatosis using hepatocyte-derived reporter cells. *Biotechnol. Bioeng.*, 2009, 102(5), 1466-1474.
31. Gentile, C.L.; Pagliassotti, M.J. The role of fatty acids in the development and progression of nonalcoholic fatty liver disease. *J. Nut r. Biochem.*, 2008, 19(9), 567-576
32. Liane Rabinowich and Oren Shibolet, Drug Induced Steatohepatitis: An Uncommon Culprit of a Common Disease, 2015, *BioMed Research International*, Volume 2015
33. Nanau RM, Neuman MG. Adverse drug reactions induced by valproic acid. *Clin Biochem* 2013; 46: 1323-1338 [PMID: 23792104 DOI: 10.1016/j.clinbiochem.2013.06.012]
34. Powell-Jackson PR, Tredger JM, Williams R. Hepatotoxicity to sodium valproate: a review. *Gut* 1984; 25: 673-681

35. Verrotti A, D'Egidio C, Mohn A, Coppola G, Chiarelli F. Weight gain following treatment with valproic acid: pathogenetic mechanisms and clinical implications. *Obes Rev* 2011; 12: e32-e43
36. Pylvänen V, Knip M, Pakarinen A, Kotila M, Turkka J, Isojärvi JI. Serum insulin and leptin levels in valproate-associated obesity. *Epilepsia* 2002; 43: 514-517
37. Luef GJ, Lechleitner M, Bauer G, Trinka E, Hengster P. Valproic acid modulates islet cell insulin secretion: a possible mechanism of weight gain in epilepsy patients. *Epilepsy Res* 2003; 55: 53-58
38. Evans JL, Goldfine ID, Maddux BA, Grodsky GM. Are oxidative stress-activated signaling pathways mediators of insulin resistance and beta-cell dysfunction? *Diabetes* 2003; 52: 1-8
39. Meeker RB, Myers RD. GABA and glutamate: possible metabolic intermediaries involved in the hypothalamic regulation of food intake. *Brain Res* 1980; 5: 253-259
40. McGarry JD. Banting lecture 2001: dysregulation of fatty acid metabolism in the etiology of type 2 diabetes. *Diabetes* 2002; 51:7-18
41. Wong HY, Chu TS, Lai JC, Fung KP, Fok TF, Fujii T, Ho YY. Sodium valproate inhibits glucose transport and exacerbates Glut1 deficiency in vitro. *J Cell Biochem* 2005; 96: 775-785
42. Edoardo Farinelli, David Giampaoli, Anja Cenciarini, Ephraim Cercado, Alberto Verrotti, Valproic acid and nonalcoholic fatty liver disease: A possible association?, *World J Hepatol* 2015 May 28; 7(9): 1251-1257
43. Turnbull DM, Bone AJ, Bartlett K, Koundakjian PP, Sherratt HS. The effects of valproate on intermediary metabolism in isolated rat hepatocytes and intact rats. *Biochem. Pharmacol.* 1983;32:1887-92
44. Ponchaut S, van Hoof F, Veitch K. In vitro effects of valproate and valproate metabolites on mitochondrial oxidations. Relevance of CoA sequestration to the observed inhibitions. *Biochem. Pharmacol.* 1992;43:2435-42
45. Kassahun K, Farrell K, Abbott F. Identification and characterization of the glutathione and N-acetylcysteine conjugates of (E)-2-propyl-2,4-pentadienoic acid, a toxic metabolite of valproic acid, in rats and humans. *Drug Metab. Dispos.* 1991;19:525-35
46. Sadeque AJ, Fisher MB, Korzekwa KR, Gonzalez FJ, Rettie AE. Human CYP2C9 and CYP2A6 mediate formation of the hepatotoxin 4-ene-valproic acid. *J. Pharmacol. Exp. Ther.* 1997;283:698-703
47. Lemasters JJ, Nieminen AL, Qian T, Trost LC, Elmore SP, Nishimura Y, et al. The mitochondrial permeability transition in cell death: a common mechanism in necrosis, apoptosis and autophagy. *Biochim. Biophys. Acta* 1998;1366:177-96
48. Aires CC, Ijst L, Stet F, Prip-Buus C, de Almeida IT, Duran M, et al. Inhibition of hepatic carnitine palmitoyl-transferase I (CPT IA) by valproyl-CoA as a possible mechanism of valproate-induced steatosis. *Biochem. Pharmacol.* 2010;79:792-9
49. J. Willebrords et al., Strategies, models and biomarkers in experimental non-alcoholic fatty liver disease research, *Progress in Lipid Research* 59 (2015) 106-125
50. Varbiro G, Toth A, Tapodi A, Veres B, Sumegi B, Gallyas F. Concentration dependent mitochondrial effect of amiodarone. *Biochem. Pharmacol.* 2003;65:1115-28

51. Liane Rabinowich and Oren Shibolet, Drug Induced Steatohepatitis: An Uncommon Culprit of a Common Disease, 2015, BioMed Research International, Volume 2015
52. S. Antherieu, A. Rogue, B. Fromenty, A. Guillouzo, and M.A. Robin, "Induction of vesicular steatosis by amiodarone and tetracycline is associated with up-regulation of lipogenic genes in heparg cells," *Hepatology*, 53;1895–1905,2011
53. A. Berson, V. de Beco, P. Letteron et al., "Steatohepatitisinducing drugs cause mitochondrial dysfunction and lipid peroxidation in rat hepatocytes," *Gastroenterology*,vol.114,no. 4 I, pp. 764–774, 1998
54. Felser A, Blum K, Lindinger PW, Bouitbir J, Krähenbühl S. Mechanisms of hepatocellular toxicity associated with dronedarone—a comparison to amiodarone. *Toxicol. Sci.* 2013;131:480–90
55. Chopra I, Roberts M. Tetracycline antibiotics: mode of action, applications, molecular biology, and epidemiology of bacterial resistance. *Microbiol. Mol. Biol. Rev.* 2001;65:232–60
56. Lepper, M. H., Wolfe, C. K., Zimmerman, H. J., Caldwell, E. R., Spies, H. W., and Dowling, H. F. (1951). Effects of high doses of Aureomycin on human liver. *Arch. Intern. Med.* 88, 271–283
57. Deboyser, D.; Goethals, F.; Krack, G.; Roberfroid, M. Investigation into the mechanism of tetracycline-induced steatosis: study in isolated hepatocytes. *Toxicol. Appl. Pharmacol.*, 1989, 97(3), 473-479
58. Fromenty, B., Fisch, C, Labbe, G., Degott, C, Deschamps, D., Berson, A., Letteron, P., and Pessayre, D. (1990). Amiodarone inhibits mitochondrial beta-oxidation of fatty acids and produces microvesicular steatosis in the liver of mice. *J. Pharmacol. Exp. Ther.* 255, 1371-1376
59. You-Jin Choi, Chae-Hyeon Lee, Kang-Yo Lee, Seung-Hwan Jung, and Byung-Hoon Lee, Increased Hepatic Fatty Acid Uptake and Esterification Contribute to Tetracycline-Induced Steatosis in Mice, *TOXICOLOGICAL SCIENCES*, 145(2), 2015, 273–282
60. Tuquet C, Dupont J, Mesneau A, Roussaux J. Effects of tamoxifen on the electron transport chain of isolated rat liver mitochondria. *Cell Biol. Toxicol.* 2000;16:207–19
61. F.Zhao,P.Xie,J.Jiang,L.Zhang,W.An,andY.Zhan,"The effect and mechanism of tamoxifen-induced hepatocyte steatosis in vitro," *International Journal of Molecular Sciences*,vol.15,no.3, pp.4019–4030,2014
62. I. Larosche, P. Letteron, B. Fromenty et al., "Tamoxifen inhibits topoisomerases, depletes mitochondrial DNA, and triggers steatosis in mouse liver," *Journal of Pharmacology and Experimental Therapeutics*,vol.321,no.2,pp.526–535,2007
63. L. K. Cole, R. L. Jacobs, and D. E. Vance, "Tamoxifen induces triacylglycerol accumulation in the mouse liver by activation of fatty acid synthesis," *Hepatology*, vol. 52, no. 4, pp. 1258–1265, 2010
64. G. M. Suddek, "Protective role of thymoquinone against liver damage induced by tamoxifen in female rats," *Canadian Journal of Physiology and Pharmacology*,vol.92,no.8,pp.640–644, 2014
65. Ramachandran R, Kakar S. Histological patterns in drug-induced liver disease. *J. Clin. Pathol.* 2009;62:481–92
66. Vauthey JN, Pawlik TM, Ribero D, Wu TT, Zorzi D, Hoff PM, et al. Chemotherapy regimen predicts steatohepatitis and an increase in 90-day mortality after surgery for hepatic colorectal metastases. *J. Clin. Oncol.* 2006;24:2065–72

67. Lettéron P, Sutton A, Mansouri A, Fromenty B, Pessayre D. Inhibition of microsomal triglyceride transfer protein: another mechanism for drug-induced steatosis in mice. *Hepatology* 2003;38:133–40
68. Igoudjil A, Massart J, Begriche K, Descatoire V, Robin MA, Fromenty B. High concentrations of stavudine impair fatty acid oxidation without depleting mitochondrial DNA in cultured rat hepatocytes. *Toxicol. In Vitro* 2008;22:887–98
69. Kennedy JA, Unger SA, Horowitz JD. Inhibition of carnitine palmitoyltransferase-1 in rat heart and liver by perhexiline and amiodarone. *Biochem. Pharmacol.* 1996;52:273–80
70. Jazcilevich S, Villa-Treviño S. Induction of fatty liver in the rat after cycloheximide administration. *Lab. Invest.* 1970;23:590–4
71. Simon Bucher, Sophie Martinais, Pegah Jalili, Daniel Zalko, Dounia Le Guillou, Anne Corlu, Karima Begriche, Marie-Anne Robin, Karine Rondel, Bernard Fromenty, Bisphenol A Induces Steatosis in HepaRG Cells Using a Model of Perinatal Exposure, 2016 Wiley Periodicals
72. De Gottardi A, Vinciguerra M, Sgroi A, Moukil M, Ravier-Dall'Antonia F, Paziienza V, et al. Microarray analyses and molecular profiling of steatosis induction in immortalized human hepatocytes. *Lab. Invest.* 2007;87:792–806
73. Cui W, Chen SL, Hu KQ. Quantification and mechanisms of oleic acid-induced steatosis in HepG2 cells. *Am. J. Transl. Res.* 2010;2:95–104
74. Chavez-Tapia NC, Rosso N, Tiribelli C. Effect of intracellular lipid accumulation in a new model of non-alcoholic fatty liver disease. *BMC Gastroenterol.* 2012;12:20
75. Robim M, Rodrigues, Steven Branson, Veerle De Boe, Agapios Sachinidis, Vera Rogiers, Joery De Kock, Tamara Vanhaecke, In vitro assessment of drug-induced liver steatosis based on human dermal stem cell-derived hepatic cells, *Arch Toxicol* (2016) 90:677–689
76. Bhatia SN, Balis UJ, Yarmush ML, Toner M. Effect of cell-cell interactions in preservation of cellular phenotype: cocultivation of hepatocytes and nonparenchymal cells. *FASEB J.* 1999;13:1883–900
77. Krause P, Saghatolislam F, Koenig S, Unthan-Fechner K, Probst I. Maintaining hepatocyte differentiation in vitro through co-culture with hepatic stellate cells. *In Vitro Cell Dev. Biol. Anim.* 2009;45:205–12
78. Khetani SR, Bhatia SN. Microscale culture of human liver cells for drug development. *Nat. Biotechnol.* 2008;26:120–6
79. Giraudi PJ, Barbero Becerra VJ, Marin V, Chavez-Tapia NC, Tiribelli C, Rosso N. The importance of the interaction between hepatocyte and hepatic stellate cells in fibrogenesis induced by fatty accumulation. *Exp. Mol. Pathol.* 2014;98:85–92
80. Bhatia SN, Yarmush ML, Toner M. Controlling cell interactions by micropatterning in co-cultures: hepatocytes and 3T3 fibroblasts. *J. Biomed. Mater. Res.* 1997;34:189–99
81. Godoy P, Hewitt NJ, Albrecht U, Andersen ME, Ansari N, Bhattacharya S, et al. Recent advances in 2D and 3D in vitro systems using primary hepatocytes, alternative hepatocyte sources and non-parenchymal liver cells and their use in investigating mechanisms of hepatotoxicity, cell signaling and ADME. *Arch. Toxicol.* 2013;87:1315–530

82. Nativ NI, Yarmush G, Chen A, Dong D, Henry SD, Guarrera JV, et al. Rat hepatocyte culture model of macrosteatosis: effect of macrosteatosis induction and reversal on viability and liver-specific function. *J. Hepatol.* 2013;59:1307–14
83. Parmentier C, Truisci GL, Moenks K, Stanzel S, Lukas A, Kopp-Schneider A, et al. Transcriptomic hepatotoxicity signature of chlorpromazine after short- and long-term exposure in primary human sandwich cultures. *Drug Metab. Dispos.* 2013;41:1835–42
84. Surendradoss J, Chang TK, Abbott FS. Evaluation of in situ generated valproyl 1-O-b-acyl glucuronide in valproic acid toxicity in sandwich-cultured rat hepatocytes. *Drug Metab. Dispos.* 2014
85. Janorkar AV, Harris LM, Murphey BS, Sowell BL. Use of three-dimensional spheroids of hepatocyte-derived reporter cells to study the effects of intracellular fat accumulation and subsequent cytokine exposure. *Biotechnol. Bioeng.* 2011;108:1171–80
86. Damelin LH, Coward S, Kirwan M, Collins P, Selden C, Hodgson HJ. Fat-loaded HepG2 spheroids exhibit enhanced protection from Pro-oxidant and cytokine induced damage. *J. Cell. Biochem.* 2007;101:723–34
87. Lu Y, Zhang G, Shen C, Uygun K, Yarmush ML, Meng Q. A novel 3D liver organoid system for elucidation of hepatic glucose metabolism. *Biotechnol. Bioeng.* 2012;109:595–604
88. Szalowska E, van der Burg B, Man HY, Hendriksen PJ, Peijnenburg AA. Model steatogenic compounds (amiodarone, valproic acid, and tetracycline) alter lipid metabolism by different mechanisms in mouse liver slices. *PLoS One* 2014;9:e86795
89. Nassir F, Adewole OL, Brunt EM, Abumrad NA. CD36 deletion reduces VLDL secretion, modulates liver prostaglandins, and exacerbates hepatic steatosis in ob/ob mice. *J. Lipid Res.* 2013;54:2988–97
90. Joka D, Wahl K, Moeller S, et al. Prospective biopsy-controlled evaluation of cell death biomarkers for prediction of liver fibrosis and nonalcoholic steatohepatitis. *Hepatology* 2012;55:455-64.
91. Page S, Birerdinc A, Estep M, et al. Knowledge-based identification of soluble biomarkers: hepatic fibrosis in NAFLD as an example. *PLoS One* 2013;8:e56009.
92. Guy CD, Suzuki A, Burchette JL, et al. Costaining for keratins 8/18 plus ubiquitin improves detection of hepatocyte injury in nonalcoholic fatty liver disease. *Hum Pathol* 2012;43:790-800.
93. Skoien R, Richardson MM, Jonsson JR, et al. Heterogeneity of fibrosis patterns in non-alcoholic fatty liver disease supports the presence of multiple fibrogenic pathways. *Liver Int* 2013;33:624-32.
94. Canbakan B, Senturk H, Canbakan M, et al. Is alanine aminotransferase level a surrogate biomarker of hepatic apoptosis in nonalcoholic fatty liver disease? *Biomark Med* 2010;4:205-14.
95. Polyzos SA, Toulis KA, Goulis DG, Zavos C, Kountouras J. Serum total adiponectin in nonalcoholic fatty liver disease: A systematic review and meta-analysis. *Metabolism* 2011;60:313-26.
96. Carazo A, León J, Casado J, et al. Hepatic expression of adiponectin receptors increases with non-alcoholic fatty liver disease progression in morbid obesity in correlation with glutathione peroxidase 1. *Obes Surg* 2011;21:492-500.

97. Montague CT, Farooqi IS, Whitehead JP, et al. Congenital leptin deficiency is associated with severe early-onset obesity in humans. *Nature* 1997;387:903-8
98. Zelber-Sagi S, Ratziu V, Zvibel I, et al. The association between adipocytokines and biomarkers for nonalcoholic fatty liver disease-induced liver injury: A study in the general population. *Eur J Gastroenterol Hepatol* 2012;24:262-9
99. Soriano-Guillen L, Barrios V, Lechuga-Sancho A, Chowen JA, Argente J. Response of circulating ghrelin levels to insulin therapy in children with newly diagnosed type 1 diabetes mellitus. *Pediatr Res* 2004;55:830-5.
100. Boyraz M, Cekmez F, Karaoglu A, Cinaz P, Durak M, Bideci A. Serum adiponectin, leptin, resistin and RBP4 levels in obese and metabolic syndrome children with nonalcoholic fatty liver disease. *Biomark Med* 2013;7:737-45.
101. MG Neuman, LB Cohen, RM Nanau. Biomarkers in nonalcoholic fatty liver disease. *Can J Gastroenterol Hepatol* 2014;28(11):607-618.
102. Wieckowska A, Papouchado BG, Li Z, Lopez R, Zein NN, Feldstein AE. Increased hepatic and circulating interleukin-6 levels in human nonalcoholic steatohepatitis. *Am J Gastroenterol* 2008; 103: 1372-1379
103. Abiru S, Migita K, Maeda Y, Daikoku M, Ito M, Ohata K, Nagaoka S, Matsumoto T, Takii Y, Kusumoto K, Nakamura M, Komori A, Yano K, Yatsuhashi H, Eguchi K, Ishibashi H: Serum cytokine and soluble cytokine receptor levels in patients with non-alcoholic steatohepatitis. *Liver Int* 2006, 26:39–45
104. Garcia-Galiano D, Sanchez-Garrido MA, Espejo I, Montero JL, Costan G, Marchal T, Membrives A, Gallardo-Valverde JM, Munoz-Castaneda JR, Arevalo De la Mata M, Muntane J: IL-6 and IGF-1 are independent prognostic factors of liver steatosis and non-alcoholic steatohepatitis in morbidly obese patients. *Obes Surg* 2007, 17:493–503.
105. Alaaeddine N, Sidaoui J, Hilal G, Serhal R, Abedelrahman A, Khoury S: TNFalpha messenger ribonucleic acid (mRNA) in patients with nonalcoholic steatohepatitis. *Eur Cytokine Netw* 2012, 23:107–111
106. Satapathy SK, Sakhuja P, Malhotra V, Sharmma BC, Sarin SK: Beneficial effects of pentoxifylline on hepatic steatosis, fibrosis and necroinflammation in patients with non-alcoholic steatohepatitis. *J Gastroenterol Hepatol* 2007, 22:634–638.
107. Park SH, Kim BI, Yun JW, Kim JW, Park DI, Cho YK, Sung IK, Park CY, Sohn CI, Jeon WK, Kim H, Rhee EJ, Lee WY, Kim SW: Insulin resistance and c-reactive protein as independent risk factors for non-alcoholic fatty liver disease in non-obese Asian men. *J Gastroenterol Hepatol* 2004, 19:694–698
108. Yoneda M, Mawatari H, Fujita K, Iida H, Yonemitsu K, Kato S, Takahashi H, Kirikoshi H, Inamori M, Nozaki Y, Abe Y, Kubota K, Saito S, Iwasaki T, Terauchi Y, Togo S, Maeyama S, Nakajima A: High-sensitivity c-reactive protein is an independent clinical feature of nonalcoholic steatohepatitis (NASH) and also of the severity of fibrosis in NASH. *J Gastroenterol* 2007, 42:573–582.
109. Yoneda M, Uchiyama T, Kato S, Endo H, Fujita K, Yoneda K, Mawatari H, Iida H, Takahashi H, Kirikoshi H, Inamori M, Nozaki Y, Kobayashi N, Kubota K, Saito S, Maeyama S, Saraga M, Aburatani H, Kodama T, Nakajima A: Plasma pentraxin3 is a novel marker for nonalcoholic steatohepatitis. *BMC Gastroenterol* 2008, 8:53.

110. Fargion S, Mattioli M, Fracanzani AL, Sampietro M, Tavazzi D, Fociani P, Taioli E, Valenti L, Fiorelli G: Hyperferritinemia, iron overload, and multiple metabolic alterations identify patients at risk for nonalcoholic steatohepatitis. *Am J Gastroenterol* 2001, 96:2448–2455.
111. Kowdley KV, Belt P, Wilson LA, Yeh MM, Neuschwander-Tetri BA, Chalasani N, Sanyal AJ, Nelson JE: Serum ferritin is an independent predictor of histologic severity and advanced fibrosis in patients with nonalcoholic fatty liver disease. *Hepatology* 2012, 55:77–85
112. Sakugawa H, Nakayoshi T, Kobashigawa K, Yamashiro T, Maeshiro T, Miyagi S, Shiroma J, Toyama A, Nakayoshi T, Kinjo F, Saito A: Clinical usefulness of biochemical markers of liver fibrosis in patients with nonalcoholic fatty liver disease. *World J Gastroenterol* 2005, 11:255–259
113. Lydatakis H, Hager IP, Kostadelou E, Mpousmpoulas S, Pappas S, Diamantis I: Non-invasive markers to predict the liver fibrosis in non-alcoholic fatty liver disease. *Liver Int* 2006, 26:864–871
114. Tanwar S, Trembling PM, Guha IN, Parkes J, Kaye P, Burt AD, Ryder SD, Aithal GP, Day CP, Rosenberg WM: Validation of PIIINP for the detection and assessment of non-alcoholic steatohepatitis in patients with nonalcoholic fatty liver disease. *Hepatology* 2012
115. Neuman M, Hilzenrat N, Cohen L, Winkler RE, Nanau R. Multiple factors involved in nonalcoholic hepatitis pathogenesis. *Int J Hepatol* 2012;2012:429805
116. Rotman Y, Koh C, Zmuda JM, Kleiner DE, Liang TJ, CRN N. The association of genetic variability in patatin-like phospholipase domain-containing protein 3 (PNPLA3) with histological severity of nonalcoholic fatty liver disease. *Hepatology* 2010;52:894–903
117. Liu YL, Reeves HL, Burt AD, Tiniakos D, McPherson S, Leathart JB, et al. TM6SF2 rs58542926 influences hepatic fibrosis progression in patients with non-alcoholic fatty liver disease. *Nat. Commun.* 2014;5:4309
118. Kiziltas S, Ata P, Colak Y, Mesçi B, Senates E, Enc F, et al. TLR4 gene polymorphism in patients with nonalcoholic fatty liver disease in comparison to healthy controls. *Metab. Syndr. Relat. Disord.* 2014;12:165–70
119. Musso G, Bo S, Cassader M, De Michieli F, Gambino R. Impact of sterol regulatory element-binding factor-1c polymorphism on incidence of nonalcoholic fatty liver disease and on the severity of liver disease and of glucose and lipid dysmetabolism. *Am. J. Clin. Nutr.* 2013;98:895–906
120. Zheng W, Wang L, Su X, Hu XF. MTP-493G>T polymorphism and susceptibility to nonalcoholic fatty liver disease: a meta-analysis. *DNA Cell Biol.* 2014;33:361–9
121. Li MR, Zhang SH, Chao K, Liao XH, Yao JY, Chen MH, et al. Apolipoprotein C3 (-455T>C) polymorphism confers susceptibility to nonalcoholic fatty liver disease in the Southern Han Chinese population. *World J. Gastroenterol.* 2014;20:14010–7
122. Lee MH, Hong I, Kim M, Lee BH, Kim JH, Kang KS, et al. Gene expression profiles of murine fatty liver induced by the administration of valproic acid. *Toxicol. Appl. Pharmacol.* 2007;220:45–59
123. Lee MH, Kim JW, Kim JH, Kang KS, Kong G, Lee MO. Gene expression profiling of murine hepatic steatosis induced by tamoxifen. *Toxicol. Lett.* 2010;199:416–24

124. Yin HQ, Kim M, Kim JH, Kong G, Lee MO, Kang KS, et al. Hepatic gene expression profiling and lipid homeostasis in mice exposed to steatogenic drug, tetracycline. *Toxicol. Sci.* 2006;94:206–16
125. Guillén N, Navarro MA, Arnal C, Noone E, Arbonés-Mainar JM, Acín S, et al. Microarray analysis of hepatic gene expression identifies new genes involved in steatotic liver. *Physiol. Genomics* 2009;37:187–98
126. Hennig EE, Mikula M, Goryca K, Paziewska A, Ledwon J, Nesteruk M, et al. Extracellular matrix and cytochrome P450 gene expression can distinguish steatohepatitis from steatosis in mice. *J. Cell. Mol. Med.* 2014;18:1762–72
127. Xu E, Forest MP, Schwab M, Avramoglu RK, St-Amand E, Caron AZ, et al. Hepatocyte-specific Ptpn6 deletion promotes hepatic lipid accretion, but reduces NAFLD in diet-induced obesity: potential role of PPAR c. *Hepatology* 2014;59:1803–15
128. Chiappini F, Barrier A, Saffroy R, Domart MC, Dagues N, Azoulay D, et al. Exploration of global gene expression in human liver steatosis by highdensity oligonucleotide microarray. *Lab. Invest.* 2006;86:154–65
129. Starmann J, Fälth M, Spindelböck W, Lanz KL, Lackner C, Zatloukal K, et al. Gene expression profiling unravels cancer-related hepatic molecular signatures in steatohepatitis but not in steatosis. *PLoS One* 2012;7:e46584
130. Barr J, Caballería J, Martínez-Arranz I, et al. Obesity-dependent metabolic signatures associated with nonalcoholic fatty liver disease progression. *J Proteome Res* 2012;11:2521–32.
131. Yu C, Xu C, Xu L, Yu J, Miao M, Li Y. Serum proteomic analysis revealed diagnostic value of hemoglobin for nonalcoholic fatty liver disease. *J Hepatol* 2012;56:241-7.
132. Miller M, Walsh S, Atirh A, Huang JT, Ferguson MA, Dillon JF. The serum proteome of non-alcoholic fatty liver disease – a multimodal approach to discovery of biomarkers of non-alcoholic steatohepatitis. *J Gastroenterol Hepatol* 2014, 29:1839-1847
133. Kalhan SC, Guo L, Edmison J, et al. Plasma metabolomic profile in nonalcoholic fatty liver disease. *Metabolism* 2011;60:404-13.
134. Li H, Wang L, Yan X, et al. A proton nuclear magnetic resonance metabonomics approach for biomarker discovery in nonalcoholic fatty liver disease. *J Proteome Res* 2011;10:2797-806.
135. Terry L Riss, PhD, Richard A Moravec, BS, Andrew L Niles, MS, Sarah Duellman, PhD, Hélène A Benink, PhD, Tracy J Worzella, MS, and Lisa Minor, Cell Viability Assays, 2004-, Assay Guidance Manual [Internet], Eli Lilly & Company and the National Center for Advancing Translational Sciences
136. Alexopoulos, L, Αλεξόπουλος, Λ. Συστημική Βιολογία. Εμβιομηχανική – Βιολογική Τεχνολογία. <https://ocw.aoc.ntua.gr/modules/document/file.php/MECH114/%CE%A3%CE%B7%CE%BC%CE%B5%CE%B9%CF%8E%CF%83%CE%B5%CE%B9%CF%82/6o.pdf>
137. Theodoridis, G., Girousi, S., Zachariadis, G., Zotou, A. S., Samanidou, V., Θεοδωρίδης, Γ., ... & Σαμανίδου, Β. (2015). Βιοαναλυτική χημεία. Αθήνα: Σύνδεσμος Ελληνικών Ακαδημαϊκών Βιβλιοθηκών. Διαθέσιμο στο: <http://hdl.handle.net/11419/3667>

138. Nikolaou, C., Chouvardas, P., Νικολάου, Χ., & Χουβαρδός, Π. (2015). Εισαγωγή. Τι είναι η Υπολογιστική Βιολογία. Αθήνα: Σύνδεσμος Ελληνικών Ακαδημαϊκών Βιβλιοθηκών. Διαθέσιμο στο: <http://hdl.handle.net/11419/1578>
139. Λεφέβρ, Ν. (2016). Σύνθετα δίκτυα: μελέτη και ανάλυση βιολογικών δικτύων-εφαρμογή στην διάδοση ασθενειών. (Πτυχιακή εργασία, ΤΕΙ Ηπείρου).
140. Davidson, E. H. (2010). The regulatory genome: gene regulatory networks in development and evolution. Academic press.
141. Stelling, J., Klamt, S., Bettenbrock, K., Schuster, S., & Gilles, E. D. (2002). Metabolic network structure determines key aspects of functionality and regulation. *Nature*, 420(6912), 190.
142. Eissmann, P., Evans, J. H., Mehrabi, M., Rose, E. L., Nedvetzki, S., & Davis, D. M. (2010). Multiple mechanisms downstream of TLR-4 stimulation allow expression of NKG2D ligands to facilitate macrophage/NK cell crosstalk. *The Journal of Immunology*, 184(12), 6901-6909.
143. Meyers, R. A. (2009). *Encyclopedia of complexity and systems science*. Springer. (pp.719-741).
144. Wilson, N. S., Dixit, V., & Ashkenazi, A. (2009). Death receptor signal transducers: nodes of coordination in immune signaling networks. *Nature immunology*, 10(4), 348-355.
145. Bhalla, U. S., & Iyengar, R. (1999). Emergent properties of networks of biological signaling pathways. *Science*, 283(5400), 381-387.
146. Johnson, D. S., Mortazavi, A., Myers, R. M., & Wold, B. (2007). Genome-wide mapping of in vivo protein-DNA interactions. *Science*, 316(5830), 1497-1502.
147. Emmert-Streib, F., & Glazko, G. V. (2011). Pathway analysis of expression data: deciphering functional building blocks of complex diseases. *PLoS computational biology*, 7(5), e1002053.
148. Mootha, V. K., Lindgren, C. M., Eriksson, K. F., Subramanian, A., Sihag, S., Lehar, J., ... & Houstis, N. (2003). PGC-1 [alpha]-responsive genes involved in oxidative phosphorylation are coordinately downregulated in human diabetes. *Nature genetics*, 34(3), 267.
149. Khatri, P., Sirota, M., & Butte, A. J. (2012). Ten years of pathway analysis: current approaches and outstanding challenges. *PLoS computational biology*, 8(2), e1002375.
150. PhRMA. (n.d.). [Brochure]. Author. Retrieved October 10, 2017, from http://cmidd.northwestern.edu/files/2015/10/Drug_RD_Brochure-12e7vs6.pdf
151. Modernizing Drug Discovery, Development & Approval. (n.d.). Retrieved October 4, 2017, from <http://www.phrma.org/report/modernizing-drug-discovery-development-and-approval1>.
152. Sirota, M., Dudley, J. T., Kim, J., Chiang, A. P., Morgan, A. A., Sweet-Cordero, A., ... & Butte, A. J. (2011). Discovery and preclinical validation of drug indications using compendia of public gene expression data. *Science translational medicine*, 3(96), 96ra77-96ra77.
153. Deotarse, P. P., Jain, A. S., Baile, M. B., Kolhe, N. S., & Kulkarni, A. A. (2015). Drug repositioning: a review. *International Journal of Pharma Research & Review*, 4(8), 51-58.
154. Ashburn, T. T., & Thor, K. B. (2004). Drug repositioning: identifying and developing new uses for existing drugs. *Nature reviews Drug discovery*, 3(8)

155. Ζαρείφη, Δ. Σ. (2017). Πρωτεομική ανάλυση της μη-αλκοολικής λιπώδους νόσου του ήπατος σε in vitro μοντέλα πρωτογενών ανθρώπινων ηπατοκυττάρων. (Μεταπτυχιακή Μελέτη, Γεωπονικό Πανεπιστήμιο Αθηνών). Αθήνα.
156. Edgar, R., Domrachev, M., & Lash, A. E. (2002). Gene Expression Omnibus: NCBI gene expression and hybridization array data repository. *Nucleic acids research*, 30(1), 207-210.
157. Lee, M. L. T., Kuo, F. C., Whitmore, G. A., & Sklar, J. (2000). Importance of replication in microarray gene expression studies: statistical methods and evidence from repetitive cDNA hybridizations. *Proceedings of the National Academy of Sciences*, 97(18), 9834-9839.
158. Gillespie, C. (2011). Volcano plots of microarray data. *The Bioinformatics Knowledgeblog*.
159. Ritchie, M. E., Phipson, B., Wu, D., Hu, Y., Law, C. W., Shi, W., & Smyth, G. K. (2015). limma powers differential expression analyses for RNA-sequencing and microarray studies. *Nucleic acids research*, 43(7), e47-e47.
160. Våremo, L., Nielsen, J., & Nookaew, I. (2013). Enriching the gene set analysis of genome-wide data by incorporating directionality of gene expression and combining statistical hypotheses and methods. *Nucleic acids research*, 41(8), 4378-4391.
161. Molecular Signatures Database v6.1. (n.d.). Retrieved May 26, 2017, from <http://software.broadinstitute.org/gsea/msigdb>
162. Fisher, R. A. (1932). *Statistical methods for research workers*. Edinburgh: Oliver and Boyd, 1925. Google Scholar.
163. Stouffer, S. A., Suchman, E. A., DeVinney, L. C., Star, S. A., & Williams Jr, R. M. (1949). *The American soldier: Adjustment during army life*. (Studies in social psychology in World War II), Vol. 1.
164. Oliveira, A. P., Patil, K. R., & Nielsen, J. (2008). Architecture of transcriptional regulatory circuits is knitted over the topology of bio-molecular interaction networks. *BMC systems biology*, 2(1), 17.
165. Taylor, J., & Tibshirani, R. (2005). A tail strength measure for assessing the overall univariate significance in a dataset. *Biostatistics*, 7(2), 167-181.
166. Kim, S. Y., & Volsky, D. J. (2005). PAGE: parametric analysis of gene set enrichment. *BMC bioinformatics*, 6(1), 144. [36] [Efron, B., & Tibshirani, R. (2007). On testing the significance of sets of genes. *The annals of applied statistics*, 107-129.
167. Law, V., Knox, C., Djoumbou, Y., Jewison, T., Guo, A. C., Liu, Y., ... & Tang, A. (2013). DrugBank 4.0: shedding new light on drug metabolism. *Nucleic acids research*, 42(D1), D1091-D1097.
168. Toutenburg, H. (1975). Hollander, M., *DA Wolfe: Nonparametric statistical methods*. John Wiley & Sons, New York-Sydney-Tokyo-Mexico City 1973. 503 S., \$9.50. *Biometrical Journal*, 17(8), 526-526.
169. Qu, X. A., & Rajpal, D. K. (2012). Applications of Connectivity Map in drug discovery and development. *Drug discovery today*, 17(23), 1289-1298.
170. Lamb, J., Crawford, E. D., Peck, D., Modell, J. W., Blat, I. C., Wrobel, M. J., ... & Reich, M. (2006). The Connectivity Map: using gene-expression signatures to connect small molecules, genes, and disease. *science*, 313(5795), 1929-1935.

171. Σιαβέλης, Ι. (2015). Μέθοδοι βιοπληροφορικής για τον επαναπροσδιορισμό φαρμάκων στη νόσο Αλτσχάιμερ (Μεταπτυχιακή διπλωματική εργασία, Πανεπιστήμιο Πατρών , ΕΜΠ). Αθήνα.
172. Hardt, C., Beber, M. E., Rasche, A., Kamburov, A., Hebels, D. G., Kleinjans, J. C., & Herwig, R. (2016). ToxDB: pathway-level interpretation of drug-treatment data. Database, 2016.